INFORMATION TO USERS

The most advanced technology has been used to photograph and reproduce this manuscript from the microfilm master. UMI films the text directly from the original or copy submitted. Thus, some thesis and dissertation copies are in typewriter face, while others may be from any type of computer printer.

The quality of this reproduction is dependent upon the quality of the copy submitted. Broken or indistinct print, colored or poor quality illustrations and photographs, print bleedthrough, substandard margins, and improper alignment can adversely affect reproduction.

In the unlikely event that the author did not send UMI a complete manuscript and there are missing pages, these will be noted. Also, if unauthorized copyright material had to be removed, a note will indicate the deletion.

Oversize materials (e.g., maps, drawings, charts) are reproduced by sectioning the original, beginning at the upper left-hand corner and continuing from left to right in equal sections with small overlaps. Each original is also photographed in one exposure and is included in reduced form at the back of the book.

Photographs included in the original manuscript have been reproduced xerographically in this copy. Higher quality 6" x 9" black and white photographic prints are available for any photographs or illustrations appearing in this copy for an additional charge. Contact UMI directly to order.

U·M·I

University Microfilms International
A Bell & Howell Information Company
300 North Zeeb Road, Ann Arbor, MI 48106-1346 USA
313 761-4700 800 521-0600

Order Number 9020768

Dynamic surface tension of aqueous surfactant solutions

Hua, Xi Yuan, Ph.D.

City University of New York, 1990

Copyright ©1990 by Hua, Xi Yuan. All rights reserved.

U·M·I
300 N. Zeeb Rd.
Ann Arbor, MI 48106

Dynamic Surface Tension of Aqueous Surfactant Solutions

by

Xi Yuan Hua

A dissertation submitted to the Graduate Faculty in Chemistry in partial fulfillment of the requirements for the degree of Doctor of Philosophy, The City University of New York.

1990

COPYRIGHT BY

XI YUAN HUA

All Rights Reserved

1990

This manuscript has been read and accepted for the Graduate Faculty in Chemistry in satisfaction of the dissertation requirement for the degree of Doctor of Philosophy.

10/31/95	
Date	Chair of Examining Committee
11/1/95	
Date	Executive Officer
	Supervisory Committee

The City University of New York

Abstract

Dynamic Surface Tension of Aqueous Surfactant Solutions

by

Xi Yuan Hua

Advisor: Professor Milton J. Rosen

The contributions of this work are as follows:

(1) The technique of dynamic surface tension measurments by the maximum bubble pressure has been improved.

(2) The dynamic behavior in surface adsorption for 15 highly purified surfactants and one partially purified commercial surfactant has been investigated. A general conclusion has been drawn: the greater the surface activity of the surfactant, the more will its dynamic behavior deviate from its equilibrium behavior.

(3) Methodology has been developed for presenting dynamic surface tension data. Various parameters characterizing dynamic surface tension have been defined and various factors affecting these parameters have been discussed. A new term, meso-equilibrium surface tension, which is useful both in applications and in discussing the mechanism, is suggested.

(4) A fairly good correlation between the wetting time on cotton skeins and the surface tension at 1 second has been found for 20 commonly used industrial and 3 purified surfactants, each at three different concentrations.

(5) Theoretical advances have been made, which might be further developed: (a) the relation between dynamic surface tension data measured by the maximum bubble pressure method to surface elasticity, which is another important area in dynamic processes; (b) a semi-quantitative criterion for the mechanism of surface tension change with time; (c) a new concept, dynamic critical micelle concentration, based on non-equilibrium thermodynamics.

Dedication

To my family: my mother, Jing Feng Qiao; my husband, Zhen Huo Zhu; and my lovely daughter, Hua Zhu, for their love, support, and encouragement throughout my studies.

Acknowledgements

I would like to express my sincere thanks:

to Professor Milton J. Rosen for his intellectual guidance, constant encouragement, accessibility, understanding and friendship throughout this work. The thanks here cannot fully show my deep appreciation for all of his kindness, which will be remembered forever;

to Professor Seymour Aronson and Dr. Jan Bock, the members of my examining and advisory commitee, for their advice and time;

to Professor Avigdor M. Ronn and Mrs. Stokes in the Department of Chemistry of The Graduate Center of CUNY for their advice, encouragement, and help.

to Mr. William Knoop in the Chemistry Office of Brooklyn College for his help in using the computer and to personnel of the Electronics Shop, Glass-blowing, Machine Shop, and Stock Rooms for their cooperation.

Contents

List of Table

Abbreviation for Surfactants Studied

No.	Surfactant [a]	Abbreviation
1	$C_{12}H_{25}(OC_2H_4)_4OH$	$C_{12}EO4$
2	$C_{12}H_{25}(OC_2H_4)_7OH$	$C_{12}EO7$
3	$C_{12}H_{25}(OC_2H_4)_8OH$	$C_{12}EO8$
4	$C_{12}H_{25}(OC_2H_4)_{10}OH$	$C_{12}EO10$
5	$C_{12}H_{25}(OC_2H_4)SO_4Na$	$C_{12}EOSNa$
6	$C_{12}H_{25}(OC_2H_4)_2SO_4Na$	$C_{12}EO_2SNa$
7	$C_{12}H_{25}\ SO_4Na$	$C_{12}SO_4Na$
8	$C_{10}H_{21}\ SO_3Na$	$C_{10}SNa$
9	$C_{12}H_{25}\ SO_3Na$	$C_{12}SNa$
10	$C_{10}H_{21}N^+(CH_3)(CH_2C_6H_5)CH_2COO^-$	$C_{10}BMG$
11	$C_{12}H_{25}N^+(CH_3)(CH_2C_6H_5)CH_2COO^-$	$C_{12}BMG$
12	$C_{14}H_{25}N^+(CH_3)(CH_2C_6H_5)CH_2COO^-$	$C_{14}BMG$
13	N-dodecyl-2-pyrrolidone	$C_{12}PY$
14	N-decyl-2-pyrrolidone	$C_{10}PY$
15	N-octyl-2-pyrrolidone	n-C_8PY
16	Di(2-ethylhexyl)sulfosuccinate, sodium salt	DESS
17	Sulfated oxyethylenated (2-hexyl) decyl alcohol with 5 oxyethylene units, sodium salt	$C_{16}LGSO_4Na$
18	Compound 17 with more branching in the hydrocarbon group	$C_{16}BGSO_4Na$
19	Sodium secondary dodecane sulfonate	$C_{12}SAS$

20	Sodium secondary tetradecane sulfonate	C_{14}SAS
21	Sodium secondary hexadecane sulfonate	C_{16}SAS
22	$C_8H_{17}(C_6H_4)(OC_2H_4)_7OH$	CA-620
23	$C_8H_{17}(C_6H_4)(OC_2H_4)_9OH$	CA-630
24	$C_8H_{17}(C_6H_4)(OC_2H_4)_{12.5}OH$	CA-720
25	$C_9H_{19}(C_6H_4)(OC_2H_4))_9OH$	CO-630
26	$C_9H_{19}(C_6H_4)(OC_2H_4)_{12.5}OH$	CO-720
27	Oxyethylenated C_{12-14} alcohol with 9 oxyethylenated units	C_{14}EO9
28	Sulfated oxyethylenated C_{12-14} alcohol with 2 oxyethylene units, sodium salt	N25
29	Linear C_{10-14} alkylbenzene sulfonate	LAS
30	N-"coco"alkyl betaine	CDMB
31	t-$C_{12}H_{25}S(OC_2H_4)_6OH$	S-260
32	t-$C_{12}H_{25}S(OC_2H_4)_8OH$	S-SK
33	t-$C_{12}H_{25}S(OC_2H_4)_{10}OH$	S-218
34	Methoxy terminated ethoxylenated silicone, molecular weight 1000	L7607
35	Methoxy terminated ethoxylenated silicone, molecular weight 4000	L7600
36	Oxyethylenated trimethylnonanol alcohol with 6 oxyethylene units	TMN-6

[a] No. 16 - 36 are commercial materials.

Chapter I: Introduction

A. History

It has been known for long time that the surface tension of a freshly formed soap solution falls steadily with time, and may require anywhere from a few second to several days before reaching its final equilibrium value. This effect was first demonstrated by Lord Rayleigh in 1890, who showed that the dynamic surface tension of a sodium oleate solution, measured by a vibrating jet technique, is only slightly lower than water. However, the equilibrium surface tension, measured by the capillary rise method, is about 25 mN/m. Moilliet and Collie[1] divided this phenomenon into two types: (i) a rapid ageing, which usually appears to be complete in a few seconds at most; (ii) a slow ageing which may last for several days or weeks. (According to our investigation, the rapid ageing for commonly used surfactants appears to be complete in several tens of seconds).

The first comprehensive and systemetic experimental work in the area of "rapid surface ageing" is Addison's study [2-9] of the dynamic surface tensions of aqueous solutions of a series of aliphatic alcohols by means of the oscillating jet method. Although most of the alcohols which he studied are not to be considered as very effective surface-active agents, his work is of considerable interest in that it reveals the general nature of the time dependence of the surface tension of solutions during rapid surface ageing phenomena.

Addison studied aqueous solutions of methyl, ethyl, n-propyl, n-butyl,

n-amyl, iso-amyl, n-hexyl, tert-hexyl, n-heptyl, n-octyl, and iso-octyl alcohols. He found that equilibrium was established so rapidly with the alcohols up to and including the butyl, that no ageing could be detected by the experimental method used. A measurable time-lag was found with the other members of the series, the surface tensions falling continuously from that pure water to the final equilibrium values. The column 4 in Table I gives some typical figures for the time, t, required for the surface tension to reach the final equilibrium values. The rate at which equilibrium was attained with a given alcohol was also found by Addison to be greater the greater the concentration.

Now the question is why surface tension changes with time. There are many possibilities, for example, the rate-determining process is a simple diffusion of surface-active solute from the interior of solution to the interface, or the velocity of attainment of equilibrium is determined by processes involving activation at energy barriers in adsorption from sub-surface to surface, or in orientation. Ward[10] suggested the following possibilities for the time effect: (i) A barrier in the chain of processes leading to adsorption, for example, slow diffusion to the surface, followed by immediate adsorption; or rapid diffusion to the surface with the barrier immmediately before adsorption; or barrier in the bulk solution to supply of adsorbed species, such as the existence of dimers in solution; (ii) rapid diffusion and adsorption, followed by a slow molecular rearrangement or reorientation in the surface; (iii) A time effect caused by slow changes in bulk, as in complicated colloid systems.

Table I

Mean Migrational Velocity

Alcohol	C, %	d x 10^5, cm	t, sec	v x 10^4 cm/sec
n-Amyl	0.10	2.35	0.023	10.2
	0.20	1.62	0.016	10.1
	0.40	1.15	0.012	9.6
n-Hexyl	0.03	8.63	0.055	15.7
	0.06	6.43	0.041	15.7
	0.09	5.02	0.034	15.0
	0.12	4.17	0.026	15.9
	0.18	3.35	0.023	14.6
n-Heptyl	0.02	24.7	0.074	33.5
	0.04	16.2	0.048	32.8
	0.06	11.4	0.037	31.1
	0.08	8.95	0.029	30.6
n-Octyl	0.0224	42.7	0.068	62.8
	0.030	34.7	0.052	66.7
tert-Hexyl	0.06	4.10	0.035	11.6
	0.09	3.14	0.028	11.2
	0.14	2.26	0.019	12.0

B. Measuring Techniques

(1) Oscillating Jet Method

This method belonges to the category of "liquid flow methods". If a jet of the liquid to be examined is forced through a small elliptical orifice under constant pressure, stationary waves are produced in the stream. These waves oscillate about their equilibrium circular form, the restoring force being the surface tension.

Determination of the outflow rate, the mean radius of the jet, and the wavelength are sufficient for the calculation of the surface tensions along the jet, for surface ages varying between 0.1 and 0.001 second. Rayleigh[11] in 1879 gave the first mathematical treatment to it. Pederson[12], Bohr[13], and Stocker[14] further improved the experimental technique. Bohr[13], in 1908, derived a complete hydrodynamical treatment of the problem. He suggested an equation giving surface tension (γ_t) along the jet in terms of the wavelengths (λ), the outflow rate (Q), and the maximum and minimum radii of the jet (r_x and r_i). Sutherland[15] has shown that, for dilute aqueous solutions the viscosity of which is not greater than 0.01 poise, correction factors in the Bohr equation can be neglected. The equation then becomes

$$\gamma_t = \frac{4\rho Q^2}{6r\lambda^2} \cdot \frac{1 + (37/24)\,(b / r)^2}{1 + (5/3)\,(\pi r^2 / \lambda^2)} \qquad [I-1]$$

where ρ is the density of solution, Q, the volume flow quantity, and r is the equivalent radius of the cross section of jet, shown as in equation I-2

$$r = (r_x + r_i) / 2 [1 - (1/6) [(r_x - r_i) / (r_x + r_i)]^2 \qquad [I-2]$$

where r_x and r_i are the maximum and minimum radii of jet, respectively. The term (b/r) denotes the ellipticity degree of the jet cross-section,

$$\frac{b}{r} = \frac{(r_x - r_i)}{(r_x + r_i)} \qquad [I-3]$$

The method of measuring the wavelength is essentially due to Stocker[14]. The jet is illuminated with a parallel beam of light. A pinhole in a tinfoil screen forms a point source of light. The hole is illuminated by projecting on the screen the image of the filament of a lamp, using a lens. The point source is placed at the focus of another lens, and the resultant parallel beam of light is narrowed by a horizontal slit in the screen to illuminate only the jet. Each wave of the jet acts as a cylindrical convergent lens, producing well-defined line images, which can be observed on a focusing screen or recorded on a photographic plate.

Another liquid flow technique[16] for the measurement of dynamic surface tension depends on the relationship between surface tension and the shape of a falling column of liquid. Surface tension opposes the elongation produced by accelerated motion and consequential cross-sectional area constriction. The control of the column is diffucult and precise measurement is elusive.

(2) Inclined Plate Method[17]

This method bears some analogy to the oscillating jet method. It consists of flowing a thin layer of a surfactant solution over an inclined plate. At the inlet, a fresh surface is formed and gradually surfactant molecules adsorb with increasing distance from it. In this way the surface tension decreases at increasing distance from the inlet. This surface tension is measured as a function of the distance by means of a Wilhelmy plate connected to a transducer. This method was designed to measure dynamic surface tensions in a time scale between a tenth of a second and a few seconds, as a supplement to the oscillating jet method.

(3) Maximum Bubble Pressure Method

The maximum bubble pressure method is based on the idea that a bubble of gas growing at the tip of an immersed capillary is stable as the pressure of the gas increases until the bubble becomes hemispherical. At this point its radius of curvature is minimum. Beyond it, the bubble is unstable and grows explosively until it detaches itself. A maximum pressure difference, ΔP_{max}, which equals the difference between the maximum pressure in the bubble and the atmospheric pressure, is measured when the radius of the bubble (r) just equals that of the capillary, and from this the surface tension of the liquid (γ_t) at that instant can be directly calculated by Laplace's relation:

$$\Delta P_{max} - \rho gh = 2\gamma_t / r \qquad [I-4]$$

where the term (ρgh) is a correction for the hydrostatic pressure due to the immersion of the capillary. Since Simon[18] first used this method in 1851, it has

been refined and adapted in many ways[19-50]. Mysels[51] has suggested a number of modifications and improvements in the measuring technique. As a result, the surface tension can be measured with a sensitivity of 0.01 dyne/cm and an accuracy of some 0.1 dyne/cm over bubble intervals from 0.1 second to several hours. Miller and Meyer[52] have described an instrument for dynamic surface tension measurement by this method.

(3) Wilhelmy Plate Method

This arrangement determines surface tension from the force required to pull a plate vertically from the test solution surface. The Cahn Instrument Company[53] offers a device for dynamic surface tensiometry capable of comparatively low rates of surface formation[54].

(4) Drop Volume Method

The principle of the drop volume method for equilibrium surface tension measurements has been described by many investigators. For measurements of time-dependent surface tension a modified procedure is necessary. Tornberg[55] has suggested a procedure in which a drop of a certain volume is expelled rapidly and the time necessary for surface tension to fall to such a value that the drop becomes detached is measured. Due to the surface tension decay from the time of formation until detachment of drop, the surface of the drop expands. This technique is limited to slow adsorption processes, as in the case of protein adsorption. The surface age in this techinique is up to 40 min.

(5) Surface Potential Method

This method employs an air electrode. This is a metal electrode tipped with a small amount of radioactivity, which ionises the air in its neighbourhood. This electrode is used to measure changes in the contact potential at an air-liquid interface caused by adsorption of surface-active ions or molecules. The change in potential is caused by the dipoles or ions of the film molecules. The magnitude of the change depends on the vertical component of the dipoles or molecules in the film, and on the extent to which the water molecules and ions in the solution are re-arranged near the surface under the influence of these dipoles. This technique was first devised by Guyot[56] and Frumkin[57] and later developed and extended by Schulman and Rideal[58] for the study of insoluble monolayers at the air-water interface. It has been applied since by Posner and Alexander[59] to measure the potential along a steady jet of liquid; the surface age is a function of flow rate and the distance along the jet, and the surface potential gives a measure of the surface tension. Surface potential measurements are translated into surface tensions by comparing the dynamic potentials with similar measurements made on static surfaces of the same compound at different concentrations.

Table II lists the range of surface age for some methods of dynamic surface tension measurements. We can see from table II that the maximum bubble pressure method covers a relatively large range of surface ages.

Table II

The Range of Surface Age for Dynamic Surface Tension Mesurements

Method	Range of Surface Age	Reference
Oscillating Jet	0.6 ms - 90 ms	60
Surface Potential	0.6 ms -90 ms	59
Maximum Bubble Pressure	50 ms - 1000 s	23, 61, 51
Inclined Plate	50 ms - 2 s	17
Drop Weight	0.1 s -30 s	62
Drop Volume	up to 40 min	55
Falling Meniscus	1s- 1 min	63
Wilhelmy Plate	min - hour	53

C. Previous Work in Dynamic Surface Tension

There are two directions of research in this field: studies of the adsorption mechanism and kinetics, and phenomenological studies. The Ward and Tordai treatment, Joos treatment, Hansen and Bendure treatment, "diffusion-kinetic model", and Addison's mean migrational velocity belong to the former.

If it is assumed that the orientation of surfactant molecules at the surface does not affect dynamic surface tension, then the dynamic surface tension can be attributed to the changing concentration of surfactant at the surface due to rate of adsorption. Adsorption may be considered as a two-step process involving: (i) diffusion of solute molecules from the bulk to the sub-surface (which is the layer a few molecules thick immediately below the surface); (ii) adsorption of the solute molecules from the sub-surface onto the surface.

(1) Ward and Tordai Treatment

Ward and Tordai[64] have given the general formulation and complete mathematical solution to the problem of diffusion-controlled adsorption. They have assumed that (i) the adsorption from the bulk to the sub-surface is instantaneous, hence the rate of approaching the equilibrium surface tension is determined only by the diffusion of the surface-active material from the bulk of the solution onto the surface; (ii) the formation of the diffusional layer is not disturbed by convective currents.

(a) The Ward and Tordai Equation [64]

The Ward and Tordai equation is

$$\Gamma_t = 2\,(D_{ap} / \pi)^{1/2} \{ Ct^{1/2} - \int_0^{t^{1/2}} C_s\,(z)\, d[(t - z)^{1/2}]\} \qquad [\,I\text{-}5\,]$$

where Γ_t is the surface concentration at time t; D_{ap}, the apparent diffusion coefficient; C, the concentration in the bulk phase of the solution; C_s, the concentration in the subsurface; z, a time variable from zero to t, and π equals 3.1416.

The sub-surface concentration (C_s) can be obtained from the equilibrium surface tension versus concentration curve, assuming that sub-surface and adsorbed layer are in equilibrium. The integral term on the right-hand side of equation I-5 is a correction for back-diffusion, which can be evaluated graphically. Thus, either Γ_t or D_{ap} may be calculated by use of equation I-5 if one of them is known.

The Ward and Tordai equation makes it possible to obtain apparent diffusion coefficient (D_{ap}) from measurements of surface tension which vary with time. If there is nothing in the nature of the physical system to invalidate the assumption of instantaneous equilibrium between the surface and the sub-surface, D_{ap} should be equivalent to the actual diffusion coefficient (D). If the assumption is not true, and there an activation barrier between the surface and sub-surface, the value of D_{ap} will depend on which is the controlling step. For a calculated value of D_{ap} which is of the same order of magnitude as D, the normal diffusion process is the slower of the two; for a calculated value of D_{ap} which is smaller than the value of D, it is evidently the barrier at the surface which has the controlling role. Quantitative conclusions cannot, however, be drawn.

(b) Simplified Equation

The calculation procedure by the Ward and Tordai equation is time consuming because of the back-diffusion term in equation I-5. Besides, the value of this calculation depends on the accuracy with which C_s and Γ_t are known.

A simplification is to restrict the analysis to surface ages where the surface tension has not decreased appreciably from the value of pure solvent. Under this condition, the back-diffusion term in equation I-5 can be neglected. Equation I-5 then reduces to

$$\Gamma_t = 2 (D_{ap} / \pi)^{1/2} (C t^{1/2}) \qquad [I-6]$$

Taking logarithms, we obtain

$$\log t = 2 \log (\Gamma_t / C D_{ap}^{1/2}) + \log (\pi / 4) \qquad [I-6']$$

Using the actual diffusion coefficient (D), a plot of log t vs. log (Γ^t / C $D^{1/2}$) should be a straight line with a slope of two, if diffusion is the controlling step.

Defay and Hommelen[65] reported that the plot of log t vs. log (Γ_t / C $D^{1/2}$) for some aliphatic alcohols and acids with D = 5 x 10^{-6} cm^2/s and Γ_t = 2 x 10^{-10} $mole/cm^2$, which was calculated from the static surface tension, shows a straight line with a slope of two.

(2) Joos Treatment[66]

Joos and Bleys[66] discussed the relationships in the dynamic surface tension measurements by the oscillating jet method. In an oscillating jet experiment the surface tension is measured with increasing distance from the orifice of the jet. The distance is usually related to a diffusion time t through the equation

$$t = x / V_s \qquad [I-7]$$

where V_s is the surface velocity at x, x is the distance from the orifice of the jet. Instead of using the Ward and Tordai equation, Joos and Bleys considered the whole system to be in a steady state and the surface is gradually stretched. This stretching is expressed by the surface dilatation, θ

$$\theta = dV_s / dx \qquad [I-8]$$

This dilatation is largest at the orifice of the jet and is zero when the surface tension has attained the equilibrium value. Such a stretching experiment is described by the theory of Van Voorst Vader[67]. For small dilatation and assuming a linear relation between the variation of the surface tension with concentration in a limited interval, the resulting variation of surface tension is

$$\Delta\gamma = \gamma_t - \gamma_{eq} = -\Gamma_{eq} (d\gamma_t / dC) (\pi \theta /2 D)^{1/2} \qquad [I-9]$$

where γ_t and γ_{eq} are the surface tension at time, t, and the equilibrium surface tension, respectively; D is the diffusion coefficient and Γ_{eq} is the equilibrium surface excess concentration. From equation I-9, log $\Delta\gamma$ plotted vs. log θ should give, at least for small deviation from equilibrium, a straight line with slope 0.5. For higher dilatations, however, the the $\Delta\gamma - \theta^{1/2}$ curve flattens out as predicted by Van Voorst Vader's theory[67], and the results plotted on a log - log scale yield a slope between zero and 0.5. Hence diffusion theory requires a slope between zero and 0.5.

Since $\theta = 1/2\ t$ in the oscillating jet experiment, equation I-9 becomes

$$\Delta\gamma = \gamma_t - \gamma_{eq} = -\Gamma_{eq} (d\gamma_t / dC) (\pi /4\ t\ D)^{1/2} \qquad [I-10]$$

This equation indicates that log $\Delta\gamma$ plotted vs. log t should give a straight line with

slope equal to -0.5 when diffusion is the controlling mechanism.

Of course equation I-10 is only an approximation, since both Γ_{eq} and $d\gamma_t / dC$ depend on concentration. Hence equation I-10 remains valid at low values for $\Delta\gamma$. This restriction is not serious since the product, $\Gamma_{eq}(d\gamma_t / dC)$, does not change much with concentration.

Examples given by Joos and Bleys are as following:

The curve of log $\Delta\gamma$ vs. log t for octanol ($C = 2.7 \times 10^{-3}$ mole/ dm^3) is a line with a slope of -0.5, whereas the curve for 1,9-nonanediol ($C = 3.8 \times 10^{-3}$ mole/ dm^3) is approximately a line with a slope of -1. This indicates that diffusion is the rate-controlling step for the system of octanol, and a relaxation mechanism other than diffusion operates for the system of 1,9-nonanediol.

(3) Hansen and Bendure Treatment

Hansen[68] suggested a theory for diffusion-controlled adsorption kinetics in systems obeying the Langmuir adsorption isotherm. The general solution has two limiting cases which can be compared to experiment corresponding to the initial (short-time) adsorption and the final (long-time) adsorption. For the limiting case of diffusion at long adsorption times Hansen obtained equation I-11

$$\gamma_t - \gamma_{eq} = \frac{(\Gamma_{eq})^2 RT}{(\pi D)^{1/2}(C)(t)^{1/2}} \qquad [I-11]$$

where C is the bulk phase concentration, Γ_{eq} is the equilibrium limiting surface excess, and the other symbols are as defined above. This equation predicts that a

plot of dynamic surface tension as a function of the reciprocal of the square root of the adsorption time should be linear with a slope depending on the surface excess, the bulk phase concentration, and the diffusion coefficient. Note that the right side of this equation is π times smaller than that in equation I-10, Hansen's result is only qualitatively in agreement with Joos', i.e. the curve of log $\Delta\gamma$ vs. log t has a slope of -0.5 when diffusion is the controlling mechanism.

For the short time limitation, Bendure[69], according to Hansen's theory, suggested equation I-12

$$\frac{(\gamma_0 - \gamma_t)}{C} = 2\,RT\,(D/\pi)^{1/2}\,t^{1/2} \qquad [I-12]$$

where the term $(\gamma_0 - \gamma_t) / C$ is defined as the reduced surface pressure (γ_0 is the surface tension of pure solvent). This equation predicts that a plot of reduced surface pressure as a function of the square root of the adsorption time should be linear with a slope depending on the diffusion coefficient, if diffusion is the controlling step. Bendure reported the diffusion coefficients calculated from the slope of the reduced surface pressure vs. the square root of t (measured by the maximum bubble pressure method) by use of equation I-12: 1.0×10^{-6} cm^2/s for dimethyldecylphosphine oxide, 0.4×10^{-6} cm^2/s for dimethyldodecyl amine oxide, 1.5×10^{-6} cm^2/s for dimethyldodecylphosphine oxide, and 1.3×10^{-6} cm^2/s for n-dodecyl hexaoxyethylene glycol ether. These values are within a factor of five of typical bulk phase diffusion coefficients (5×10^{-6} cm^2/s).

(4) Addison's Mean Migrational Velocity

Addison[3] introduced the concept of migrational velocity of a solute molecule, i.e. the mean velocity at which it travels to the surface. By applying the Gibbs equation to the equilibrium surface vs. concentration curve, Addison calculated the total excesses, Γ_{eq}, at various concentrations. He then supposed that these excesses were drawn from a disc of unit cross-sectional area placed with one face in the surface. With this assumption, he then calculated the thickness d of this disc from the values of Γ_{eq} and the bulk concentrations, using the equation $d = \Gamma_{eq} / C$, where C is the bulk concentration in mole/ml. Adison then assumed that surface equilibrium was established when the last of the molecules initially in the disc had reached the surface, and obtained the migrational velocity by dividing d by the time required for the attainment of equilibrium. The value of the mean migrational velocity thus calculated was found to be characteristic of each aliphatic alcohol studied, and to be independent, within the experimental error, of the concentration. A further interesting characteristic of Addison's "migration velocity" is that, in a homologous series of straight chain alcohols, it increases with increasing chain length and decreases if the aliphatic chain is branched. This leads to the suggestion that the driving force behind the transport of solute to the interface is what Addison calls the "free energy of the surface", $(\gamma_t - \gamma_{eq})$, where γ_t is the surface tension at time t, and γ_{eq} is the equilibrium surface tension, and he considered that migration is at least the major (if not the only) factor determining surface tension changes over the experimental range of surface ages. Table I lists Addison's mean migrational

velocity for short-chain alcohols[5], where t is the time for establishment of equilibrium, d is the thickness of the disc as defined above, and v is the mean migrational velocity.

Ward and Tordai[64] calculated diffusion coefficients of some normal alcohols using the experimental data of Addison[2-8]. The value obtained deviated considerably from those generally accepted, hence they also considered that diffusion is not the rate-determining process, and a activation barrier exists.

Some investigators, in the other hand, considered that the discrepancies of the apparent diffusion coefficients for those alcohols from the nomal values of bulk phase diffusion were due to the experimental procedure developed by Addison (oscillating jet method). Sutherland[15], using the oscillating jet method, and Alexander and Posner[70], using surface potential measurment, failed to reproduce Addison's data for dynamic surface tension of aqueous solution of some aliphatic alcohols. Defey and Hommelen[65], using their own dynamic and equilibrium surface tension data, calculated the diffusion coefficients for some aliphatic alcohols and acids by use of the Ward and Tordai equation. The values of the apparent diffusion coefficient (see Table III) are very close to the normal value for bulk phase diffusion (5×10^{-6} cm^2/s). Hence, Defey and Hommelen suggested that the mono alcohols and mono acids listed in Table III follow a mechanism of adsorption governed mostly by diffusion.

Table III

Diffusion Coefficients from Defay and Hommelen's Work[65]

Compound	t, sec.	C x 10^6 mole/ cm^3	Γ_{eq} x 10^{10} mole/ cm^2	D x 10^6 cm^2/s
n- hexyl alcohol	10^{-2}	3.44	3.6	5.7
n- heptyl alcohol	10^{-2}	3.44	4.9	5.2
n- heptyl alcohol	10^{-2}	2.43	3.8	5.3
n-octyl alcohol	10^{-2}	3.44	5.8	4.9
Methylhexyl carbinol	10^{-2}	1.96	4.7	7.0
2-Ethyl hexanol	10^{-2}	2.10	4.2	5.6
n-decyl alcohol	60	0.076	4.9	1.7
n-decyl alcohol	60	0.114	5.7	2.7
Capric acid	60	0.076	4.9	4.5
Capric acid	60	0.114	5.7	4.2

(5) Diffusion-Kinetic Model

Several workers have examined the problem of mixed adsorption kinetics of surfactant solutions where both transfer from the sub-surface to the surface and diffusion from the bulk phase to the sub-surface operate. For example, Kimizuka et al.[71] suggested an approach wherein the surfactant adsorption is assumed to be determined by its concentration gradient as well as by the gradient of the potential field at the interface. This approach, though fundamentally more correct, admits random selection of the gradient of potential and hence has limited usefulness as a model. In most cases, the transfer from the sub-surface to the surface is described by a kinetic expression[72-81]. This model is called a "diffusion-kinetic model" as suggested by Miller and Kretzschmar[77], or "barrier-limited" or "adsorption-limited mechanism" used by Hansen[73] and Tsonopoulos et al.[74]. Despite several attempts, there is no single treatment of the problem which achieves a general numerical scheme for solving the non-linear set of equations for a general isotherm without making any simplifying assumptions.

For the mixed adsorption kinetics, the thermodynamic relation between adsorption and sub-surface concentration is replaced by a kinetic one. The most simple situation is to assume that equilibrium between the sub-surface and bulk is established and the transfer of surfactant from the sub-surface to the surface is the rate-controlling step. Joos et al.[80] derived equation I-13 for this case, based on the Frumkin equation and the Langmuir equation for adsorption kinetics.

$$\Pi = -RT\,\Gamma_{max}\,\ln\left\{1 - \left[1 - \exp\left(\frac{-\Pi_0}{RT\,\Gamma_{max}}\right)\right]\left(1 - e^{-kt}\right)\right\} \qquad [I - 13]$$

where Π_0 is the surface pressure at equilibrium, Γ_{max} is the saturated surface excess concentration, k is an adjustable parameter

$$k = \frac{k_1 C + k_2}{\Gamma_{max}} \qquad [I-14]$$

where C is the bulk phase concentration, k_1 the rate constant for adsorption (cm / s), k_2 the rate constant for desorption (mole / cm^2. s). The parameter k depends on the concentration of the surfactant. Fitting the dynamic surface tension data into equation I-13 for a set of concentrations, one obtains the values of k, changing with C. Plotting k vs. C the adsorption and desorption rate constants, k_1 and k_2 are obtained. The ratio k_2/k_1 should be equal to the Langmuir constant a.

Bleys et al.[81] defined a characteristic time, τ_k, for pure transfer-controlled adsorption

$$\tau_k = k^{-1} = \frac{\Gamma_{max}}{k_2\,(1 + C/a)} \qquad [I-15]$$

For a diffusion-controlled adsorption the characteristic time τ_D[82] is

$$\tau_D = \frac{1}{D}\left[\frac{d\Gamma}{dC}\right]^2 \qquad [I-16]$$

Assuming a Langmuir adsorption isotherm, it follows that

$$\tau_D = \left(\frac{\Gamma_{max}}{a}\right)^2 \left[\frac{1}{D\,(1 + C/a)^4}\right] \qquad [I-17]$$

where a is the Langmuir constant, D is the diffusion coefficient, Γ_{max} is the saturated surface excess concentration. The ratio of these two characteristic times is

$$R = \frac{\tau_D}{\tau_k} = \frac{\Gamma_{max}\, k_2}{a^2\, D\, (1 + C/a)^3} \qquad [I-18]$$

For a given surfactant, Bleys et. al.[81] define this ratio at zero concentration

$$R_0 = \frac{\Gamma_{max}\, k_2}{a^2\, D} \qquad [I-19]$$

R_0 tends to be large for diffusion-controlled adsorption and small for kinetic-controlled adsorption. Table IV lists some examples from reference 81.

Table IV

Parameters in e Mixed Adsorption Kinetics[81]

Component	k_1, cm/s	k_2, mol/cm^2.s	R_o
1-octanol	---	---	131
2-octanol	10^{-1}	6.2×10^{-8}	18.7
3-octanol	10^{-1}	6.9×10^{-8}	15.1
4-octanol	9×10^{-2}	6.6×10^{-8}	12.7
1,2-octanediol	3×10^{-2}	5.4×10^{-8}	1.2
1,8-octanediol	6×10^{-3}	2.1×10^{-8}	8×10^{-2}
1,11-undecanediol	3×10^{-1}	2.5 x 1	142
1,12-dodecanediol	---	---	1.6×10^{3}
dodecanedioic acid	---	---	657
dodecanedioic Na salt	7×10^{-4}	1.8×10^{-8}	0.15

(6) Miscellaneous Ideas

Fordham[83] criticized using equilibrium relationships in the Ward and Tordai treatment. He considered that it was this over-simplified method caused considerable error in the apparent diffusion coefficient, and that if it had been corrected the values of the apparent diffusion coefficients for most of the systems in the literature may be closer to the diffusion coefficients of the normal bulk phase diffusion. He suggested an equation based on the thermodynamic condsiderations of free energy, which took care of the effects of the concentration gradient in the bulk phase and the progressive surface adsorption. His main idea is that "even in systems not in equilibrium the surface tension must equal the change in the free energy of the system caused by forming unit area of new surface, with its associated surface adsorption and consequent concentration gradients in the bulk solution". Though the final equation was too complicated to use and no satisfactory results were obtained by Fordham, his approach suggested an alternative way to view the problem.

Until now we have assumed that the orientation of surfactant molecules at the surface does not effect dynamic surface tension. A typical statment made by Hansen and Wallace[84] is that "The surface tension depends only on the surface excess whether the system is in equilibrium or not.". Now the question is whether this assunption is valid. Hansen[73] discussed two possibilities which might cause the spreading pressure in dynamic systems to differ from that in equilibrium systems: (i) If the rate of orientation of adsorbed molecules were markedly slower than the rate of entry and the surface tension depended strongly

on orientation; (ii) the existence of a diffusional concentration gradient in dynamic systems.

The surface potential studies of Posner and Alexander[59] indicate that the rate of orientation is indeed considerably less than the rate of entry, but also indicate that surface tension does not change much during the orientation process. Further, at sufficiently low surface concentrations the spreading pressure should be approximately nRT regardless of orientation. From this consideration, Hansen[84] neglected the first possibility. He suggested a conceptual picture of the spreading pressure which took care of the second possibility: the spreading pressure measurment sums the difference in spreading pressure due to a slab of liquid of thickness dx and concentration C (x,t) and a correponding slab of liquid of bulk concentration C over all x. For the cases of interest, C (x, t) and C are always small; the spreading pressure due to these slabs should therefore be those for ideal films. The total spreading pressure should therfore be

$$\Pi_{dyn} = \Pi\ (n) + RT \int_0^{\infty} [\ C(x,t) - C]\ dx \qquad [I-20]$$

where $\Pi(n)$ is the spreading pressure due to a surface concentration at equilibrium as given by the surface equation of state, Π_{dyn} is the spreading pressure at time t. The material balance requires that

$$\int_0^{\infty} [C(x,t) - C]\ dx + n(t) = 0\ , \qquad [I-21]$$

where n (t) is the surface excess at time t. Substituting equation I-21 to equation I-20, Hansen obtained

$$\Pi_{dyn} = \Pi (n) - nRT, \qquad [I-22]$$

Π (n) can be expanded in virial form

$$\Pi (n) = nRT + a_2 n^2 + a_3 n^3 + ... \qquad [I-23]$$

and therefore

$$\Pi_{dyn} = a_2 n^2 + a_3 n^3 + ... \qquad [I-24]$$

where n is the surface concentration at time t. Equation I-24 shows that the effect of the concentration gradient has been to cancel the leading term in Π (n). If n varies as $Ct^{1/2}$ for short time, as required by diffusion theory, Π_{dyn} will vary as C^2 t at short time, as observed by Hansen and Wallace[84]. Equation I-22 may overestimate the difference of the spreading pressures between dynamic and equilibrium cases, nevertheless it qualitatively elucidates the effect due to the concentration gradient.

(7) Phenomenological Studies

Burcik's work

Burcik[85-88] in the1950s published a series of papers on the dynamic surface tension of surfactants. He simply measured the surface tension versus time at various conditions, concentration, temperature, added salt, organic additives, pH, over a time range of about 0.003 to 0.03 second by use of the oscillating jet method. The compounds Burcik investigated were sodium laurate, sodium dodecyl sulfate, sodium oleate, sodium myristate, dodecylpyridium chloride, and Tween 20 (commercial polyoxyethylene sorbitan monolaurate).

Burcik's main results were (i) The addition of 1-dodecanol or

dodecanoic acid decreased the rate of surface tension lowering of aqueous solutions of sodium dodecyl sulfate; however, adding decane to the surfactant solution had no effect on the rate of surface tension lowering. (ii) Surfactants whose surface-active components are charged show an increase in rate of surface tension lowering on the addition of electrolyte, the effectiveness increases with the charge of the added counterion, but the nature of the added similion is of little consequence; surfactants whose surface-active components are uncharged have rates of surface tension lowering that are not influenced by the addition of electrolytes; (iii) The rate of surface tension lowering for 0.015 N sodium laurate solution increases with increase in temperature over the range 9.2 ^{0}C to 29.4 ^{0}C; (iv) There is no pH effect on the rate of surface tension lowering of 0.005 N sodium dodecyl sulfate, which is not readily susceptible to hydrolysis; for 0.005 N sodium myristate an increase in pH over the range of 8.3 to 10.0 (pH was changed by the addition of sodium hydroxide or myristic acid) resulted in an increase in the rate of surface tension lowering; for 0.01 N dodecylamine hydrochloride an increase in pH by the addition of dodecylamine resulted in a decrease in the rate of lowering, and addition of hydrochloric acid increased the rate.

Netzel et. al and Austin et al.'s Work

Netzel[89] investigated the dynamic surface tension for Triton X-100 (commercial polyoxyethylenated t-octylphenol with 9-10 moles of ethylene oxide) by the oscillating jet method, and suggested a "first-order rate equation"

(equation I-25) to fit their dynamic surface tension data.

$$\log (\gamma_t - \gamma_{eq}) = \log (\gamma_0 - \gamma_{eq}) - kt \qquad [I-25]$$

where γ_t , γ_0 , and γ_{eq} are the surface tension at time t, the surface tension of pure solution, and the equilibrium surface tension, respectively, k is a rate constant and t is time in second.

Austin et al.[23] investigated the dynamic surface tension of Manoxol OT (containing 98.8 % Na salt of 2(ethylhexyl) sulfosuccinate and about 0.2 % sodium sulfate) by the maximum bubble pressure method over the time range of 0.01 to 0.2 second, and also used equation I-25 fitted to the initial part of their dynamic surface tension - time curve. They found that the value of k gave a straight line when plotted against bulk phase concentration.

Work on Sodium Dodecyl Sulfate Solutions

Mysels[90] measured the surface tension of sodium dodecyl sulfate solutions as a function of time at different stage of purification. He reported that the relatively rapid adsorption of surfactant is accompanied by the relatively slow adsorption of traces highly surface-active impurities which affect the results, especialy at long times. He suggested to use dynamic surface tension as a working criterion of surface purity for surface tension measurements.

Mysels compared his result with the work[91] of Adison and Hutchinson, published in 1948. They reported the "static" and "disturbed" surface tensions of sodium dodecyl sulfate solutions. Their "static" measurements were made with a Wilhelmy plate, whereas the surface tension of "disturbed" surfaces was

measurad by the drop volume method with the drops formed at several constant flow rates, which correspond to approximate surface ages of 25 s, 6 min, and 12 min. Addison and Hutchinson found that with increasing flow rate the surface tension increases and there was an apparent increase in the CMC, where they designated the intersection of two linear portions of the dynamic surface tension versus log C curve above and below it as CMC. The surface tension data at 25 seconds were close to the surface tension data measured by Mysels with highly purified sample over the range of surface age 30 s to 1000 s.

Woolfrey et. al.[92] reported the plots of dynamic surface tension versus log of surfactant molar concentration for sodium dodecyl sulfate solutions in the absence and presence of 0.5 M sodium chloride at surface ages 0.3 s, 0.5 s, and 10 s, using a Sensadyne 5000 Bubble Tensiometer (Chem Dyne Research Corporation, Wisconsin) based on the principle of maximum bubble pressure. They found that the CMCs in the dynamic cases, as designated by the intersection of two linear portions of the dynamic surface tension versus log C curve above and below it, for the salt-free surfactant was between 8.67 and 8.88 mM, within 4 % of the equilibrium value in the literature, whereas, the CMC values in the dynamic cases for the system with salt were between 0.95 and 1.99 mM, and at least 45% greater than the equilibrium value in the literature.

Dynamic Surface Tension and Performance

Burcik[87] measured the rate of attainment of surface tension equilibrium for detergent systems under varying conditions and compared these

rates with results of detergency studies on an oily soil. Table V lists his results. Such a close relationship between detergency and rates of adsorption at the air-water interface is surprising. It is possible that because only oily soil was used, the important process is an alteration of the contact angle, and since contact angle depends on surface and interfacial tension, a high rate of adsorption might mean a rapid decrease in contact angle, and consquently good detergent action. However, in general we can hardly expect a correlation between rate of adsorption at the air-water interface and the complex process of detergency involving the removal and suspension of particulate and oily soil.

Petrova et al.[93] tried to relate the washing action on a glass surface, soiled by a standard procedure, with the dynamic surface tension, measured by the maximum bubble pressure method. The compounds which they investigated were commercial sulfosuccinates of nonylphenolpolyglycolether with 4, 8, and 10 oxyethylene units and laurylether sulfate. They tried to find a correlation between the total washing time, t_w, and the surface tension at the concentrations at which the washing experiments were carried out. No correlation existed with the equilibrium value, whereas t_w was found to increase with increase in the dynamic surface tension. They also found systematic variations both of t_w and of the maximum slope, $-d\gamma_t$ / dlog C, with the number of oxyethylene groups. Again, no correlation was found between t_w and the maximum slope of the equilibrium curves. Their conclusion is that washing ability is determined by the dynamic, rather than by the equilibrium surface tension.

Earnshaw[94] related the rate of adsorption to the wetting-out time of

pieces of fabric. He used the surface potential method to study rates of adsorption for a series of surfactants at several concentrations and empolyed a novel method of measuring wetting time. He reported that the surfactant with higher rate of adsorption has shorter time of half wetting, and there is a definite correlation between the rate of adsorption and the wetting time.

Table V

The Relationship Between the Effect on Detergency and The Rate of γ Equilibrium Attainment[87]

Variations in Detergent System	Effect on Detergency	Effect on Rate of Attaining γ equ.
1. Increasing temp.	Increases	Increases
2. Increase in conc.	Increases	Increases
3. Increase in pH with non-hydrolysable surfactant	No effect	No effect
4. Increase in pH with surfactant that is a salt of strong base and weak acid	Increases for moderate increase in pH	Increases
5. Addition of electrolyte to an ionic detergent	Increases for low electrolyte concen.	Increases
6. Increasing valence of cation of electrolyte with anionic detergents	Increases	Increases
7. Increasing anionic valence of electrolyte with anionic detergents	No effect, or increases	No effect

(8) Surface Dilational Modulus

As long ago as 1878 Gibbs gave an explanation for the fact that liquid soap films behave as elastic membranes, whereas pure liquids do not. He assumed that as a result of adsorption on the surfaces, the solution becomes depleted in surface-active solute, and therefore the surface tension increases with extension of the lamella. The modulus of elasticity, E, of a lamella is defined by

$$E = 2A \frac{d\gamma}{dA} \qquad [I-25]$$

where γ is the surface tension of the lamella at an area A. The names suggested for E as defined in Equation I-25 include "Gibbs elasticity," "areal elasticity," "compressional modulus," and "film elasticity" [95-100] and have been used in cases where E is a pure elasticity. The term "surface dilational modulus" has been used for the more general case where surface behavior has both an elastic and viscous component[100-101]. The modulus E is a measure of the resistance against the creation of surface tension gradients, and of the rate at which such gradients disappear once the system is again left itself.

The Gibbs elasticity forces can be induced only in thin liquid lamella. The thickness of such lamella must be so small that the amount of surface active molecules in its bulk is not high enough to restore equilibrium coverage after deformations. Moreover, the frequency of film deformation must be lower than the frequency of the diffusional exchange between the bulk and surface of the

locally deformed film element.

On the other hand, the Marangoni elasticity[102], ϵ, is defined as

$$\epsilon = \frac{d\gamma}{d\ln A} \qquad [I-26]$$

where $d\ln A$ denotes the relative surface area change and $d\gamma$ denotes the corresponding surface tension change. Values of the Marangoni elasticity are dynamic, non-equilibrium values. Marangoni elasticity forces can be induced not only in liquid lemella but also in surface layers of semi-infinitive solutions. The value of the Marangoni elasticity depends on the frequency of deformation and for sufficiently high frequencies each surface layer can behave as an insoluble monolayer.

There are several methods for investigating surface rheology: (i) Surface Waves[103]. For small deformations, the elasticity modulus defined in Equation I-26 is commonly determined by subjecting the surface to oscillations from a barrier moving either parallel or normal to the surface, or from a thermal origin. (ii) Steady-state experiments[103]. The surface of a surfactant solution is extended by means of two movable barriers on a trough. The barriers are kept moving apart at such velocity that the relative rate of surface expansion ($d\ln A/dt$) is constant. When a steady state is reached, in which the measured value of dynamic surface tension no longer changes with time, the value of $\Delta\gamma$ and $\Delta A/A$ can be used to obtain $|\epsilon|$. The increase in surface tension is measured by means of a Wilhelmy plate located between the two barriers where no liquid

motion occurs. (ii') Pulsating Bubble Method[104-106]. The method is based on the following principle. A bubble of definite size is formed at the tip of a small capillary, dipped into a liquid. The bubble is forced by a special electromechanical system to radical harmonic pulsations of definite amplitude. The force nececessary for obtaining the required pulsations is measured as a function of pulsation frequency and concentration of solution. The magnitude of this force depends on the elasticity force arising on the bubble surface.The Marangoni surface elasticity modulus is calculated from these mesurements.

The "trough techniques" as described in (i) and (ii) have a number of disadvantages, as Clint[107] has pointed out: (a) Measurements are reliable only at fairly low frequencies, where the wavelength of the longitudinal waves is long compared with the distance between oscillating barrier and Wilhelmy plate. (b) Good results depend on the rapid response of the Wilhelmy plate and maintenance of a well defined contact angle. (c) The method uses a large amount of test material. Consequently, some investigators[107-108] have made some preliminary studies of the relationship between the dilational modulus and the formation of a bubble or an oil drop in a surfactant solution.

Chapter II: Experimental

A. Materials

The polyoxyethylenated n-dodecyl alcohols with homogeneous head group ($C_{12}EO4$, $C_{12}EO7$, $C_{12}EO8$) were purchased from Nikko Chemical Co., Tokyo, Japan as compounds of >98% purity as indicated by gas chromatography. The polyoxyethylenated n-dodecyl alcohol with homogeneous head group of 10 oxyethylene units ($C_{12}EO10$), the structure of which was quantitatively proved by NMR, was a research sample, kindly given by Chemische Werke Huls Co., Germany. The sodium salts of sulfated polyoxyethylenated n-dodecyl alcohols ($C_{12}EOSNa$ and $C_{12}EO_2SNa$), where the oxyethylene units are 1 and 2, respectively, were synthesized and purified in our laboratory[109] (The purity of $C_{12}EOSNa$ and $C_{12}EO_2SNa$ was 99.2 and 99.0%, respectively.). The sodium decanesulfonate ($C_{10}SNa$), sodium dodecanesulfonate ($C_{12}SNa$), and sodium dodecyl sulfate ($C_{12}SO_4Na$) of >98% purity were purchased from Research Plus, Bayonne, NJ. The N-decyl-N-benzyl-N-methylglycine ($C_{10}BMG$), N-dodecyl -N-benzy-N-methylglycine ($C_{12}BMG$) and N-tetradecyl-N-benzyl-N-methylglycine ($C_{14}BMG$) of >99.0% purity were synthesized in our laboratory and purified by the method[110] previously described. The N-alkyl-2-pyrrolidones, N-octyl(C_8PY), N-decyl ($C_{10}PY$), and N-dodecyl ($C_{12}PY$), were research samples of >99.0%, supplied by GAF Chemicals Corporation. The sodium di-(2-ethylhexyl) sulfosuccinate (DESS) was supplied by American Cyanamid as Aerosol OT-100, purified by the procedure[111,112] previously described.

Before being used for surface tension measurements, aqueous solutions of the above surfactants (in water that had been first deionized and then distilled twice, the last time from alkaline permanganate solution through 3-ft-high Vigreaux column with quartz condenser and receiver) were further purified by passage four times through minicolumns of octadecylsilanized silica gel to remove any traces of impurities more surface active than the parent compound.

The concentration of ionic surfactant in the effluent from these columns was determined by two-phase titration[113,114] with Hyamine 1622; the concentration of the polyoxyethylenated n-dodecyl alcohols was determined by surface tension versus log C curve previously published[115] and by two-phase titration[116]; the concentration of N-alkyl-2-pyrrolidones[117] and zwitterionics [118] was determined by UV spectral analysis (C_{10}BMG: ε_{208} = 8220, ε_{263} = 366; C_{12}BMG: ε_{208} = 7580, ε_{263} = 334; C_{14}BMG: ε_{208} = 8020).

Sodium chloride used to increase the ionic strength of solutions was analytical grade material, which was then baked for several hours in a porcelain casserole at red heat to remove traces of organic compounds.

The materials used in the wetting test were mostly commercial. The t-octylphenol oxyethylenated with 7, 9, and 12.5 moles of ethylene oxide, and t-nonyl-phenol oxyethylenated with 9 and 12.5 moles of ethylene oxide, were supplied by the GAF Chemicals Corporation as Igepal CA-620, CA-630, CA-720, CO-630, and CO-720, respectively. C_{12-14} alcohol oxyethylenated with 9 moles of ethylene oxide and the sodium salt of sulfated oxyethylenated C_{12-14} alcohol with 2 moles of ethylene oxide were supplied by Henkel KGaA Corporation

as Dehydol 100 and Texapon N25, respectively, courtesy of Dr. M. J. Schwuger. The linear alkyl benzene sulfonate (C-550 LAS) and the sodium secondary C_{12} and C_{14} alkanesulfonates were supplied by Vista Chemicals, courtesy of Dr. Michael Cox. The zwitterionic, N-"coco" alkyl betaine (Mirataine CDMB) was supplied by the Miranol Chemical Company. Two sodium salts of sulfated oxyethylenated branched C_{16} alcohols with 5 oxyethylene units were supplied by the Exxon Research and Engineering. Three polyoxyethylenated dodecyl mercaptans were supplied by Alcolac Corporation as Siponic 260, Siponic SK, and Siponic 218, respectively. Two methoxy terminated ethenoxylated silicones (L7600 and L7607) were supplied by Union Carbide Corporation.

B. Maximum Bubble Pressure Method

The maximum bubble pressure apparatus (Figure 1a) consists of a gas feeding system and a pressure and bubble rate measuring system. The gas feeding system consists of a pressure regulator, a capillary, and a flow control meter with filter to further purify the gas. The gas used is nitrogen. The pressure variation in the capillary during bubble formation is monitored by a pressure transducer. The output from the pressure transducer is fed into an IBM personal computer. With "Notebook" software, both bubble frequency and maximum bubble pressure are measured. The bubble break time (so called "dead time") can also be estimated. Figure 1 b shows a graph of the computer output, with the x-axis being time in seconds and the y-axis the voltage, V. The digital output of the computer also shows the time and voltage from which the maximum voltage,

bubble frequency, and dead time are obtained.

In principle, as gas flows through a capillary tube immersed at a depth, h, under the surface of a liquid, the radius of the liquid / gas interface formed at the tip of the capillary is related to the gas pressure by the Laplace equation. The pressure reaches a maximum, P_{max}, when the radius of the bubble reaches the radius of the capillary.

$$\Delta P_{max} = P_{max} - P_o = 2\gamma / r + pgh \qquad [II-1]$$

where P_o is the atmospheric pressure, γ the surface tension, r the radius of the capillary, p the density of the liquid, and g the acceleration of gravity.

In the present work, the voltage from the output of the transducer linearly changes with the pressure difference between the capillary and the atmospheric pressure (Figure 2), denoted as ΔP. The calibration coefficients from voltage to surface tension depend on transducer constant and the effective radius of the capillary. Hence, instead of the theoretical equation II-1, an empirical equation was used to calculate the surface tension from the voltage of the computer output. To obtain the calibration equation, we made several capillaries of different radius by pulling out glass tubing. For each capillary we used several pure compounds of known surface tension. Figure 3 shows the calibration lines for 4 capillaries with different radii, and Table VI lists the data for the compounds used in the calibration. The slope for the plot of voltage vs. surface tension depends on the capillary radius. All of the lines show a common intercept of -0.021 v ± 0.003, which was used as the instrumental zero correction factor. The general form of the calibration equation is:

$$\gamma = K \text{ (voltage)} + 0.021\ K \qquad [II-2]$$

The values of K are 32.3, 49.9, 86.8, 113.5 for capillaries with the radius 0.0875 mm, 0.135 mm, 0.238 mm, 0.318 mm, respectively. The factor K for a given capillary was checked each day by measuring the response of pure water.

The radius of the capillary was determined in two ways: (i) by microscope, (ii) by measuring the response of the transducer for a certain capillary in pure water, and then using the Laplace equation to calculate the radius of the capillary (see Appendix 2). The measured results by the two different methods were in agreement each other.

The voltage change caused by the immersion of the capillary under the surface of the liquid was measured with a small ruler, which could be read to 0.05 cm, and the reading converted to voltage by the following equation:

$$\frac{\text{(the depth of immersion in cm)}}{\text{2.54 (cm/inch)}} \times 0.33 \text{ (voltage/inch)} \qquad [II-3]$$

The correction for immersion is small. For example, when the depth of immersion is 0.4 cm, the corresponding voltage is 0.052 v. Usually, three measurements were made, and the average value was subtracted from the total computer output.

Table VI

Data for Calibration Curves

Compound	γ^a mN/m	voltage Cap. 1 (0.088 mm)	Cap. 2 (0.135 mm)	Cap. 3 (0.238 mm)	Cap. 4 (0.318 mm)
Water	72.0	2.202	1.425	0.809	0.613
Nitrobenzene	43.9	1.339	0.855	0.486	0.367
		1.326	0.867		
Acetonitrile	29.3	0.879	0.563		
Benzene	28.85	0.867	0.573		
		0.865	0.560		
1-Octanol	27.53	0.820	0.530		
Acetone	23.70	0.704	0.452		
Methyl alcohol	22.61	0.678	0.442	0.240	0.178
		0.670	0.433		

[a] Literature value at 20°C except water at 25°C.

We used water as a test sample to check the output of signal with change in bubble frequency. Table VII lists the data for two different capillaries. Variation of bubble frequency over more than two orders of magnitude showed that voltage was independent of bubble frequency, particularly when the radius of the capillary was small (< 1% variation for a capillary of 0.135 mm).

Reproducibility of the dynamic surface tension data was checked by measuring the same compound, at the same concentration, on different days. Figure 4 (a) shows the dynamic surface tension vs. log t of DESS in aqueous solution (5.844×10^{-4} mole/dm^3), measured at three days. The reproducibility is about 1%. Figure 4 (b) shows the plots of dynamic surface tension vs. log t of $C_{12}SNa$ in aqueous solutions (3.012×10^{-3} mole/dm^3 and 6.024×10^{-3} mole/dm^3). The reproducibility is about 0.5% for duplicate measurements at both concentrations. Figure 4 (c) shows the dynamic surface tension of $C_{14}BMG$ in aqueous solution (pH = 9.3) at 6.85×10^{-5} mole/dm^3 concentration, measured by two capillaries with the radius 0.24 mm and 0.32 mm, respectively. The data points from two sets of measurements can be fitted on same curve.

The dynamic surface tension data, measured by the maximum bubble pressure method, were also checked against equilibrium data obtained by use of the Wilhelmy plate method. For very dilute surfactant solutions, at short times, the surface tension should approach that of the solvent. Figure 5 shows this convergence of dynamic surface tension values to that of the solvent for 5

systems included $C_{12}EO4$ in water (1.94×10^{-5} mole/dm^3), $C_{12}EO4$ in water (3.24×10^{-5} mole/dm^3), $C_{12}PY$ in water (9.59×10^{-5} mole/dm^3), $C_{12}EOSNa$ in 0.5 N NaCl (5.99×10^{-5} mole/dm^3), and $C_{12}EO_2SNa$ in 0.5 N NaCl (4.11×10^{-5} mole/dm^3). The surface tension for solutions in pure water at 25 ^{o}C measured by the Wilhelmy plate method is 72.0 mN/m, and for solutions in 0.5 N NaCl is 72.9 mN/m.

Table VII

The Effect of Bubble Frequency on the Output[a]

Capillary Radius	Bubble Frequency	Voltage
mm	sec^{-1}	v
0.135	10.0	1.4436
	6.7	1.4414
	5.0	1.4388
	4.0	1.4355
	3.3	1.4452
	< 0.23	1.4355
0.312	3.6	0.6299
	2.4	0.6251
	1.8	0.6202
	1.1	0.6180
	0.09	0.6153
	0.025	0.6153

[a] Water was used as testing sample.

On the other hand, for more concentrated solutions of low molecular weight materials (that diffuse rapidly to the surface), the dynamic values measured by the maximum bubble pressure method should approach the equilibrium values measured by the Wilhelmy plate technique. Figure 6 (a) shows the plots of γ_t vs. log t for the aqueous solution of C_8PY (6.53×10^{-3} mole/dm^3), and the 0.1N NaCl solutions of $C_{10}SNa$ (6.35×10^{-3} mole/dm^3 and 1.60×10^{-2} mole/dm^3). The concentrations in Figure 6 (a) are below their cmcs except for C_8PY, which is at the limit of its solubility. Figure 6(b) shows the plots of γ_t vs. log t for 4 systems included DESS in 0.1 N NaCl (1.15×10^{-2} mole/dm^3), $C_{12}BMG$ in aqueous solution of pH = 9 (3.23×10^{-3} mole/dm^3), $C_{12}SO_4Na$ in water (5.06×10^{-2} mole/dm^3), and $C_{12}EO_2SNa$ in 0.5 N NaCl (9.00×10^{-3} mole/dm^3). The concentrations in Figure 6 (b) are all above their cmcs. The equilibrium surface tensions, measured by the Wilhelmy plate method, are shown in the parentheses, following the corresponing curves. The close agreement between the two methods attests to the reliability of our dynamic data.

In calculatiing surface age from the bubble interval, the "dead time" must be considered. There are two periods in the process of bubble separation: (i) the time in which the surfactant is adsorbed on the surface and the radius of the bubble varies accordingly. This first period is finished when pressure becomes infinitesimally larger than $2\gamma/R$. In that instant the pressure in the capillary becomes unbalanced and the bubble starts to grow very fast; (ii) the time in which the bubble grows rapidly and thereupon separates from the capillary. The second period is called "dead time". For evaluation of the surface age the dead time

must be subtracted from the interval measured between two subsequent bubbles. Austin[23] suggested a relation for very short intervals:

"dead time" in milli-second = 31.9 - 0.0042 S [III-4]

where S is the number of bubbles per minute. In the present work, the "dead time" can be read directly from the digital computer output. Table VIII lists two examples of data for "dead time". Generally speaking, it changes slightly with the radius of the capillary.

C. Equilibrium Surface Tension Measurements

Equilibrium surface tension measurements were made by the Wilhelmy vertical plate technique, using a sandblasted platinium blade of ca. 5-cm perimeter. The instrument was calibrated against quartz-condensed water (specific conductivity 1.1×10^{-6} mho cm^{-1} at 25 ^{0}C) each day that measurement was made. Sets of measurements were taken at 15-min. intervals until no significant change occured.

Table VIII

Surface Age and "Dead Time"[a]

Bubble Interval, second	Dead Time, second	Surface Age, second
60.20	0.50	59.70
24.75	0.50	24.25
11.75	0.50	11.25
8.90	0.50	8.40
4.00	0.15	3.85
2.14	0.10	2.04
1.80	0.075	1.725
0.771	0.075	0.696
0.327	0.050	0.277
0.217	0.050	0.167
0.126	0.050	0.076
0.093	0.040	0.053
0.075	0.040	0.035

[a] The capillary with 0.238 mm radius was used in this example. Generally speaking, "dead time" changes slightly with capillary radius.

D. Draves-Clarkson Skein Wetting Test

The Draves-Clarkson sinking test[119] was used in this work. Standard cotton skeins of gray, unboiled, 2-ply yard, folded to form 13 inch loops, each skein weighing 5.00 g were purchased from Testfabrics, Inc., Middlesex, NJ. Wetting times were done in triplicate. Wetting-out times (WOT) were measured on the cotton skeins that were weighted with a 3g stainless steel hook. Test solutions were prepared from deionized, distilled water. All measurements were made at room temperature (27.5 ± 2.5^{o}C).

Chapter III: Methodology

The study of dynamic surface tension adds another variable, time, to the two variables, surface tension and surfactant concentration, that are usually studied under equilibrium conditions. As a result, there are different ways of presenting the data in simple (2-dimensional) form. For example, we can hold surfactant concentration constant and plot surface tension as a function of time or we can hold the time constant and plot surface tension as a function of surfactant concentration in the aqueous phase (for example, at surface age = 1 second).

A. Analysis of a generalized surface tension vs. log time curve

In our published work[112], we divided a typical curve of the change in dynamic surface tension with time into four regions - region I: induction region; region II: rapid fall region; region III: meso-equilibrium region; region IV: equilibrium region (Figure 7). It should be apparent that the surface tension value at time, t, rather the equilibrium value, is an important factor in determining the surface energy requirement in dynamic surface processes. For example, in a process where the surface area is being increased by a value, ΔA, in a short period of time, t, the minimum work required to achieve that surface area expansion is the product of the surface tension at time, t, and the interfacial area increase. The first three regions are important in high speed dynamic processes. As a result, in the present work, we discuss only regions I - III. We also define t_i as the time at the end of induction region, t_m as the time at the beginning of meso-equilibrium, and t^* as the time for the surface pressure, Π

(= $\gamma_0 - \gamma_t$, where γ_0 is the surface tension of pure solvent and γ_t the surface tension at time, t), to reach one-half its value at meso-equilibrium.

The dynamic surface tension data for the first three regions fit the equation

$$\gamma_t - \gamma_m = \frac{\gamma_0 - \gamma_m}{1 + (t/t^*)^n} \qquad [III-1]$$

where γ_m is the meso-equilibrium surface tension and t* and n are constants, with t* having the dimensions of time in the same units as t, and n being dimensionless. Eq. III-1 is in a form similar to the Fourier transform of a correlation function, often used in relaxation theory [120]. This equation can also be put in form

$$(\gamma_0 - \gamma_t) / (\gamma_t - \gamma_m) = (t / t^*)^n . \qquad [III-2]$$

Since $(\gamma_0 - \gamma_m)$ is the depression of the surface tension (or the surface pressure, Π_m) at meso-equilibrium, $(\gamma_0 - \gamma_t) / (\gamma_t - \gamma_m)$ is the ratio of the depression of the surface tensdion at time t (or surface pressure at time t, Π_t), to that remaining before meso-equilibrium is reached (Figure 8). We consider region I (the induction region) to end when the ratiio $(\gamma_0 - \gamma_t) / (\gamma_t - \gamma_m)$ equals 1/10 and the rapid fall region to end when that ratio equals 10. The midpoint between γ_0 and γ_m is when the ratio equals 1. From Equation III-2

$$\log t_i = \log t^* - 1/n \qquad [III-3]$$

$$\log t_m = \log t^* + 1/n \qquad [III-4]$$

$$n = \log [(\gamma_0 - \gamma_t) / (\gamma_t - \gamma_m)] / \log (t/t^*) \qquad [III-5]$$

By putting eqation III-2 in logarithmic form, it can be converted to linear form:

$$\log [(\gamma_0 - \gamma_t) / (\gamma_t - \gamma_m)] = n \log t - n \log t^* \qquad [III-6]$$

This provides a convenient method of evaluating the constants n and t^*, by plotting $\log [(\gamma_0 - \gamma_t) / (\gamma_t - \gamma_m)]$ versus log t. However, when the ratio $(\gamma_0 - \gamma_t) / (\gamma_t - \gamma_m)$ is close to 0 or to ∞, the values of n and t^* calculated in this manner show large errors and fitting values of these constant by computer to equation III-1 gives more accurate values.

Figures 9(a), 9(b), and 9(c) show three sets of model curves for equation III-1. In Figure 9(a), n and t^* are constant, and $(\gamma_0 - \gamma_m)$ is changed. We observe that (i) changing $(\gamma_0 - \gamma_m)$ does not change the induction time and other characteristic times, (ii) the absolute value of the slope in the linear portion of the curve γ_t vs. log t increases with increase in $(\gamma_0 - \gamma_m)$. In Figure 9(b), n and $(\gamma_0 - \gamma_m)$ are constant, and t^* is changed. We observe that (i) changing t^* does not change the absolute value of the slope in the linear portion of the curve, (ii) the induction time and other characteristic times become longer with increase in t^*. In Figure 9(C), $(\gamma_0 - \gamma_m)$ is constant and t^* and n are changed. Since change in t^* does not change the absolute value of the slope in the linear portion of the curve, we observe that the absolute value of the slope becomes large with an increase in the value of n. In the Theory part, we shall see that the absolue value of the slope in the linear portion of curve γ_t vs. log t is related to the maximum surface elasticity.

As an example, Figures 10(a) and 10(b) show the relationship between dynamic surface tension and log t for C_{12}BMG at different bulk concentrations (C, mole / dm^3) in water at 25 ^{0}C. In Figure10(a) the solid curves were

calculated from equation III-1 with constants n and t^* fitted to the data by computer; in Figure 10(b) equation III-6 is plotted, with solid lines drawn using least-squares constants obtained by computer. The values of the parameters used are listed in Table IX.

Table IX

Dynamic Surface Tension Parameters for C_{12}BMG at Various Concentrations in Water (25 ^{0}C)

Log C	γ (mN/m)	$\gamma_0 - \gamma_m$ (mN/m)	Fit to Eq. III-1 n	Fit to Eq. III-1 t* (s)	Fit to Eq. III-6 n	Fit to Eq. III-6 t* (s)
-2.992	34.6	37.4	1.19	0.082	1.17	0.085
-3.224	34.8	37.2	1.31	0.153	1.18	0.155
-3.410	37.3	34.7	1.37	0.340	1.13	0.345
-3.525	39.9	32.1	1.49	0.509	1.39	0.526
-3.701	41.9	30.1	1.53	1.19	1.32	1.24
-3.826	44.8	27.2	1.56	1.86	1.39	1.89
-4.108	48.4	23.6	2.24	3.61	1.75	3.90

The physical meaning of the parameters used in the analysis of dynamic surface tension is as follows: (i) t_i is the time when the surface tension of a given surfactant solution begins to show a significant surface tension reduction from that of the solvent; (ii) t_m is the time when the meso-equilibrium region starts; (iii) mathematically, t^* is at the middle of the fast falling region in dynamic surface tension curve; physically, it is a measure of the relaxation time of the main dynamic process, such as diffusion from bulk phase to sub-surface or transfer from sub-surface to surface (see Theory); (iv) n determines the ratio of the relaxation time of the main and subordinate processes (see Theory).

B. Second Method of Presenting Dynamic Surface Tension Data

A second method of presenting dynamic surface tension data is by holding the time constant and plotting surface tension vs. the surfactant concentration (C) in the aqueous phase. A typical plot of surface tension vs. log C at constant times is shown in Figure 11. For comparison, the plot of equilibrium surface tension vs. log C is included. A degree of parallelism between dynamic and equilibrium surface tension is apparent. Each curve shows a initial gradual decrease in surface tension with increase of surfactant concentration at very low concentrations, followed by a rapid decrease in surface tension with increase in log C over a certain concentration range and then a more gradual decrease with concentration increase as the equilibrium surface tension is approached. This gradual decrease for the dynamic surface tension curve, however, does not occur at the equilibrium critical micelle concentration of the surfactant, but at a

concentration above it. As the time decreases, the concentration at which this slower decrease commences increases. It is notworthy that, for this compound, at 1 second surface age time, there is no apparent change in the slope of the surface tension vs. log C curve at the critical micelle concentration of the surfactant. This means that, at short surface ages, we cannot always expect to find a discontinuity in surface properties at the critical micelle concentration of the surfactant.

Also to be noted, however, is that at sufficiently high surfactant concentrations in the aqueous phase, the dynamic surface tension value approaches the equilibrium value, even at short surface age (e. g. 1 second). We shall see, in a later section, that the surface tension at 1 second surface age, γ_{1s}, is an excellent predictor of wetting speed, as measured by the Draves skein wetting test.

C. Third method of presenting surface tension data

A third method of presenting surface tension data is by plotting the meso-equilibrium surface tension, γ_m, vs. surfactant concentration in the liquid phase. Although neither time nor surfactant concentration is held constant in this type of plot, γ_m changes only gradually with increase in time, as shown in Figure 10 (a), and consequently these plots are similar to a plot of γ_t vs. concentration at constant time (see Figure A1 to A21). If we choose the value of γ_m at the discontinuity in the γ^*_m - log C plot, we have a dynamic surface tension value that changes only gradually both with time and with surfactant concentration.

Hence, γ^*_m and the concentration at the discontinuity in the the γ_m - log C plot, C^*_m, are useful parameters in the discussion of dynamic surface tension behavior.

Chapter IV: Theoretical Development

A. Calculation of Marangoni Elasticity from Dynamic Surface Tension Data

To elucidate the physical meaning of parameters in equation III-1 we have investigated the relationship of dynamic surface tension to Marangoni elasticity.

(1) Theory

The Marangoni elasticity, ε, is defined as

$$\varepsilon = \frac{d\gamma}{dA/A} = \frac{d\gamma}{d\ln A} \qquad [IV-1]$$

where $d\ln A$ denotes the relative surface area change and $d\gamma$ denotes the corresponding surface tension change. Values of the Marangoni surface elasticity are dynamic, non-equilibrium values.

Miller et. al.[108] have related the slope of surface tension with frequency, measured by the maximum bubble pressure method, to a bubble Marangoni surface elasticity. Clint et. al.[107] suggested an equation[a] to calculate the rate of fractional area change at the time the drop detaches, which is based on the assumption that the drop at the tip of a capillary is spherical.

$$\frac{(dA / A)}{dt} = \frac{2f}{3}, \qquad [IV-2]$$

---

[a] For a spherical bubble, $dA / A = 2\, dr / r$ and $dv / v = 3\, dr / r$, then $(dA / A) / dt = (2/3)(dv / v\, dt) = 2f / 3$, where r is the radius of the bubble, v is its volume, and A its area.

where A is the surface area of a bubble, γ is the surface tension, f is the bubble frequency. Equation IV-2 states that the rate of the fractional change of a bubble when it detaches from the tip of a capillary is a function of the bubble frequency. We use this equation to estimate the rate of fractional change at the time the bubble detaches from the tip of a capillary.

On the other hand, the dynamic surface tension measured by the maximum bubble pressure method is also a function of the bubble frequency. From Equation III-1, which describes the surface tension changes with the time at the relatively short surface age (measured by the maximum bubble pressure method), we obtain the rate of surface tension change.

$$\frac{d\gamma}{dt} = (\gamma_0 - \gamma_m)\frac{[-n(t/t^*)^{n-1}/t^*]}{[1+(t/t^*)^n]^2} \qquad \text{[IV-3]}$$

Defining $\Pi_m = (\gamma_0 - \gamma_m)$ and converting equation IV-3 to the frequency domain, using $t = 1/f$ and $t^* = 1/f^*$, we obtain

$$\frac{d\gamma}{dt} = (\Pi_m)\frac{[-n f^*(f^*/f)^{n-1}]}{[1+(f^*/f)^n]^2} \qquad \text{[IV-4]}$$

where f is the frequency in Hz and f^* is a characteristic frequency in Hz for a surfactant system at a certain concentration. In the time range of 1 second to 250 seconds, we can assume that the inverse of the surface age approximately equals the bubble frequency ($f = 1/t$), because the bubble breaking time (dead time) is negligible, compared to surface age (Table VIII).

Equations IV-2 and IV-4 indicate that there is a definite fractional area change rate and a definite surface tension change rate at a certain bubble frequency for a fixed concentration of a surfactant solution. Therefore, the critical fractional surface area change rate at the surface of a bubble, which is formed at the tip of a capillary immersed in the surfactant solution, can be directly related to the surface tension change rate.

Dividing equation IV-4 by equation IV-2 and taking absolute values, we obtain

$$|\varepsilon| = \left| \frac{d\gamma}{dA/A} \right| = (3/2\ \Pi_m)\ \frac{[n\ (\ f^*\ /\ f\ )^n\ ]}{[1\ +\ (f^*/\ f)^n\ ]^2} \qquad [IV-5]$$

In doing this we have neglected the bubble growth time, i.e. we assume that the time when the bubble radius reaches the radius of a capillary approximately equals the time when the bubble detaches. This assumption is reasonable for the range of surface age investigated (1 second to 250 seconds).

The surface elasticity calculated by equation IV-5 should be equivalent to the elasticity on a hypothetical continually expanding bubble surface. Equation IV-5 shows that the Marangoni surface elasticity at such a bubble surface is the function of the bubble frequency, the meso-equilibrium pressure, and the dynamic surface tension parameter n at a fixed surfactant concentration. At low frequency, the value of $|\varepsilon|$ increases with increase in frequency and at high frequency the value of $|\varepsilon|$ decreases with increase in frequency. There is consequently a maximum in the curve of $|\varepsilon|$ vs. f.

Taking the derivative of equation IV-5 and solving for the condition $d|\varepsilon|/df = 0$, we obtain, at maximum $|\varepsilon|$:

$$f = f^*. \qquad [IV-6]$$

Substituting equation IV-6 into equation IV-5 to obtain the maximum value of $|\varepsilon|$,

$$|\varepsilon_{max}| = 3\Pi_m n / 8 . \qquad [IV-7]$$

Equation IV-7 shows that the value of $|\varepsilon_{max}|$ depends on the values of n and Π_m. This derivation elucidates the physical meaning of n.

In spectroscopic terms, we may consider that the system consisting of a surfactant solution has two energy levels: a "surface film level" with lower energy and a "sub-surface level" with higher energy. Expanding a surface film by producing a bubble in a surfactant solution applies an external field to the system and causes transition of molecules between the two levels. When the frequency of the applied field equals the intrinsic frequency of the interfacial region, a resonance occurs. Hence, we designate f^* as the "resonance frequency". $|\varepsilon_{max}|$ should be related to the energy difference of the two levels; in terms of surface chemistry, the Gibbs free energy of adsorption, ΔG_{ad}. However, the motion of a liquid surface is always coupled to that of the adjoining bulk liquid. The "intrinsic" properties of a soluble monolayer are strongly affected by the mass exchange between the sub-surface and the bulk phase. When diffusion between bulk phase and sub-surface is a controlling factor, the parameters $|\varepsilon_{max}|$ and f^* can be related to the diffusion coefficient and to the equilibrium surface adsorption excess, and the inverse of f^*, which equals t^*, is a measure of

the relaxation time of transfer between sub-surface and surface; in terms of surface chemistry, the relaxation time of adsorption and desorption.

As shown above, the surface elasticity reaches a maximum value at the characteristic frequency f*. In surface chemistry terms, as f becomes larger above that frequency and both the rate of area expansion and the absolute value of the fractional area expansion consequently become large, diffusion becomes more and more unable to keep pace with the decrease in surface concentration caused by expansion. Below that frequency, diffusion predominates and, as f becomes smaller, becomes more capable of minimizing the decrease in surface concentration with expansion of the surface.

The surface elasticity obtained by this method is different with that by the classical method, longitudinal surface waves, in which equation IV-1 is replaced by the approximate equation

$$|\varepsilon| = \frac{|\Delta\gamma|}{|\Delta A / A|} \qquad [IV-8]$$

As a result, the experiments are limitted to a small change in area, and the corresponded surface tension variations to between about 0.1 and 4 mN/m. The mathematical expression, equation IV-5, allows us to calculate the surface elasticity both for the surface near equilibrium and far from equilibrium, which is more close to reality.

In addition, in the classical method the frequency of expansion and compression of a surface varies under the condition of a constant fractional area change ($\Delta A/A$), whereas, in our method both fractional area change, dA/A, and

the rate of fractional area change, dA/Adt, vary with the bubble frquency.

Nevertheless, the parameters obtained by this method can, in certain cases, be related to elasticity parameters obtained by the classical method.

(2) Relation to Other Elasticity Parameters

(i) $|\varepsilon_{max}|$ and ε_0

ε_0, "the limiting dilational modulus at high frequency"[121] is an equilibrium surface property of a monolayer, and it is approximately proportional to the equilibrium surface pressure when the surface pressure is not very low and surface mole fraction of surfactant is not very high:

$$\varepsilon_0 \cong 2\Pi, \qquad [IV\text{-}9]$$

where Π is the equilbrium surface pressure. Since equation IV-7 shows that $|\varepsilon_{max}|$ is proportional to Π_m, and our data (see Figure A1-A21) show that Π_m is usually proportional to Π at concentrations below the critical micelle concentration, it follows that, below the critical micelle concentration,

$$|\varepsilon_{max}| = K\,\varepsilon_0, \qquad [IV\text{-}10]$$

where K is a constant.

(ii) f' and ω_0

According to Lucassen et. al.[121], ω_0 is the inverse relaxation time of an interfacial region and the plot of log ω_0 vs. log C has a linear relationship with a slope of 2 for a diffusion-controlled adsorption process. Figure 12 shows the

linear relationships of log f* and log ω_0 to log C. For systems $C_{12}EO7$, $C_{12}EO8$ and $C_{12}EO10$, the plots of log f* vs. log C, which were obtained from our dynamic surface tension data, fall on one line with a slope of 2; for systems $C_{12}EO6$, $C_{14}EO6$, the plots of log ω_0 vs. log C [121] fall on a second line with a slope of 2. The compounds indicated above all belong to the same family and show only a small structural effect. Hence, we can estimate from Figure 12 that for the systems indicated above,

$$\log (f^*/\omega_0) \cong -1 \text{ and } f^* \cong 0.1\ \omega_0. \qquad [IV-11]$$

In general, for these systems, below their critical micelle concentrations, we can write

$$f^* = k\ \omega_0. \qquad [IV-11']$$

We can use the inverse of f*, which equals t*, as a measure of the relaxation time of diffusion from bulk phase to sub-surface, when diffusion is the controlling factor, or as the relaxation time of adsorption and desorption, when transfer from sub-surface to surface is the controlling factor.

(iii) Diffusion Coefficient

When diffusion between bulk phase and sub-surface is the controlling factor, the parameters ε_0 and ω_0 can be related to the diffusion coefficient, D, of the surfactant molecule [115].

$$D = 2\ \omega_0 (RT\Gamma^2 / \varepsilon_0 C)^2 \qquad [IV-12]$$

where Γ is the equilibrium surface excess in mole/cm^2 at a bulk phase concentration, C, (in mole/cm^3). Substituting equations IV-10 and IV-11' into

equation IV-12, we obtain

$$D = 2 (K^{2}/ k) (f^{\circ}) (RT\Gamma^{2} / | \varepsilon_{max}| C)^{2} \qquad [IV-12']$$

Table X lists the diffusion coefficients from dynamic surface tension data, measured by the maximum bubble pressure method, for $C_{12}EO7$, $C_{12}EO8$, and $C_{12}EO10$ calculated by use of equations IV-6, IV-7 and IV-12' with the assumption of $K^{2}/ k = 1$. For comparision, diffusion coefficients for $C_{12}EO6$, $C_{14}EO6$, calculated from ε_0 and ω_0 of reference 115 by use of equation 12 are included. The concentrations in Table X are all below their critical micelle concentrations. The diffusion coefficients for $C_{12}EO7$, $C_{12}EO8$, and $C_{12}EO10$ are of the same order of magnitude as results for the systems $C_{12}EO6$, $C_{14}EO6$ in reference121, obtained by a monolayer expansion and compression method using a Langmuir trough.

Table X

Diffusion Coeffecients Calculated by Use of Eq.12' and Eq. 12

System	C x 10^5 mole/dm^3	f* s^{-1}	ε_{max} mN/m	D x 10^6 cm^2/s
$C_{12}EO7$	2.911	0.041	10.1	3.9
	5.821	0.199	11.6	3.7
$C_{12}EO8$	2.650	0.069	7.6	8.0
	4.732	0.269	9.3	6.7
	6.309	0.255	11.0	2.6
	10.33	0.709	12.15	2.2
$C_{12}EO10$	3.348	0.074	8.4	1.9
	5.580	0.309	9.0	2.7
	10.33	0.990	10.6	2.0
$C_{12}EO6$[a]	0.202			2.4
	0.509			3.7
$C_{14}EO6$[a]	0.051			2.4
	0.509			7.7

[a] Data from reference121

(iv) Relationship of $|\varepsilon|$ to C

Figure13 shows plots of surface elasticity, $|\varepsilon|$, as a function of surfactant concentration C for the system $C_{12}EO4$, at two fixed frequencies: f = 0.1 and 0.05. The values of $|\varepsilon|$ were calculated by use of equation IV-5 from our dynamic surface tension data, obtained by the maximum bubble pressure method. The curves show shapes similar to those in the literature [116], as shown in the insert for Figure 13. The value of $|\varepsilon|$ increases through a maximum, and decreases with further increase in concentration.

It appears, therefore, that the parameters, $|\varepsilon|$, $|\varepsilon_{max}|$ and f^*, developed in this treatment show functions similar to those of other elasticity parameters in the literature.

(3) Relation of the Slope in the Curve γ_t versus log t to $|\varepsilon|$

Multiplying the both sides of equation IV-4 by t, we obtain

$$\frac{d\gamma}{d\ln t} = \Pi_m \frac{[\, -n\ t\ f^*(\ f^*\ /\ f\ )^{n-1}\ ]}{[\ 1\ +\ (f^*/\ f)^n\ ]^2} \qquad [IV-13]$$

Since $t = 1/f$, equation IV-13 becomes

$$\frac{d\gamma_t}{d\ln t} = \Pi_m \frac{[-n\ (\ f^*\ /\ f\ )^n\ ]}{[\ 1\ +\ (f^*/\ f)^n\ ]^2} \qquad [IV-14]$$

Comparing equation IV-14 with equation IV-5, we obtain

$$\left|\frac{d\gamma_t}{d\log t}\right| = \frac{2|\varepsilon|}{3 \times 2.303} = \frac{|\varepsilon|}{3.455} \qquad [IV-15]$$

Equation 15 shows that the absolute value of the slope of the curve γ_t versus log t is directly proportional to the surface elasticity. Miller[108] reported that the slope of surface tension, measured by the maximum bubble pressure method, with frequency can be related to a bubble surface elasticity property. Both results are qulititatively in agreement.

The maximum slope on the curve γ_t versus log t corresponds to the maximum value of $|\varepsilon|$, i.e. $|\varepsilon_{max}|$, which is a function of the parameters n and Π_m. Recall the discussion in Chapter III (p.50), which indicates that the slope in the linear portion of the curve of γ_t versus log t depends on the paramters n and Π_m ($= \gamma_t - \gamma_m$). The theoretical conclusion is in the agreement with the observation.

B. Prediction of Mechanism of Surface Tension Change with Time

(1) Theory

The adsorption of surfactant molecules from an aqueous solution below the critical micelle concentration can be controlled by the diffusion from bulk phase to sub-surface or by the transfer from sub-surface to surface, or the two processes may be of approximately equal importance. We have shown in equation IV-11' the relationship between t* and the relaxation time of the main dynamic process which controls surface tension change with time. Now, we define a

"subordinate relaxation time", t_2, as a measure of a dynamic process other than the main one.

As discussed above, the equation IV-5 has a maximum surface elasticity, $|\varepsilon_{max}|$, at the resonance frequency, f*. To obtain the ratio of (t_2 / t^*), we first use equation IV-5 and equation IV-7 to solve for the peak width, Δf, at half height, $|\varepsilon_{max}|/2$. Substituting $(|\varepsilon_{max}| / 2)$ into equation IV-5, we obtain

$$(1/2)\ (3\Pi_m n / 8) = (3\Pi_m n / 2)\frac{(f^* / f)^n}{[\ 1 + (f^* / f)^n\ ]^2} \qquad [IV-16]$$

Defining $X = (f^* / f)^n$, we obtain, from equation IV-16,

$$X^2 - 6X + 1 = 0 . \qquad [IV-16']$$

Solving equation IV-16', we obtain,

$$X = (f^* / f)^n = 3 \pm 2.828.$$

Hence, $\Delta f_{1/2} = f^* (0.172^{-1/n} - 5.828^{-1/n})$ [IV-17]

In nuclear magnetic resonance, the shape of a broadened line is usually described empirically by the Lorentz function, the width at the half height of a peak being related to the transverse relaxation time, T_2,[123] by equation IV-18

$$\Delta f_{1/2} = \frac{1}{\pi T_2} \qquad [IV-18]$$

By the method of similarities[124], we use the same relationship to estimate the relationship of $\Delta f_{1/2}$ to the subordinate relaxation time, t_2,

$$\Delta f_{1/2} = \frac{1}{\pi\, t_2} \qquad [IV-19]$$

Hence,

$$t_2 = \frac{1}{\pi\, \Delta f_{1/2}} = (1/f^*)\, \frac{1}{\pi\, (0.172^{-1/n} - 5.828^{-1/n})} \qquad [IV-20]$$

Since $1/f^* = t^*$,

$$\frac{t^*}{t_2} = \pi\, (0.172^{-1/n} - 5.828^{-1/n})\,. \qquad [IV-21]$$

Thus, the ratio of the relaxation times of the main and subodinate mechanisms can be determined from the value of n.

(2) Comparison with Other Criteria

Previous investigators have suggested some criteria to determine the mechanism which causes the surface tension change with time. Joos et al [80] suggested to use the slope of the $\Delta\gamma_t$ - log t curve as the criterion for dynamic surface tension data measured by the oscillating jet method, where $\Delta\gamma_t$ is the difference between the dynamic surface tension and the equilibrium surface tension, a slope between 0 and -0.5 indicates a diffusion-controlled mechanism, a slope about -1 indicates a relaxation mechanism other than diffusion, and a slope between -0.5 and -1 indicates a mixed mechanism. Ward and Tordai[64] suggested to use the apparent diffusion coefficient, D_{ap}, as the criterion: when D_{ap} calculated from dynamic surface tension data is the same order of magnitude

as the diffusion coefficient D, the diffusion process is slower than the other; when D_{ap} is smaller than D, the process by another mechanism is slower. Table XI shows a comparision of the present criterion with Joos' and Ward's for the system sodium di(2-ethyhexyl)- sulfosuccinate (DESS) in water (C = 6.77 x 10^{-4} mole / dm^3 and 8.85 x 10^{-4} mole / dm^3) at three temperatures. The present criterion shows that the relative relaxation time of the main process (assumed diffusion) to the subordinate process decreases with decrease in temperature for the two surfactant concentrations listed. Joos's criterion also shows the mechanism changes gradually from diffusion to the other with decrease in temperature. The comparision of D_{ap}, obtained from the dynamic surface tension, and D calculated from the Stokes-Einstein equation shows also that the effect of the mechanism other than diffusion increases with decrease in temperature.

Table XII shows a comparison of the present criterion with Joos' and Ward's for n-dodecyl ethers of polyoxyethylenated alcohols with homogeneous head group ($C_{12}EO7$ and $C_{12}EO8$) at a concentration range of 3 - 10 x 10^{-5} mole / dm^3 (below the cmc). The average t^*/ t_2 value is about 23 for $C_{12}EO7$ and $C_{12}EO8$, which indicates that the relaxation time of the main dynamic process, diffusion, is 23 times longer than the relaxation time of the other dynamic process, such as adsorption from sub-surface to surface. The average slopes of log $\Delta\gamma$ vs. log t for $C_{12}EO7$ and $C_{12}EO8$ fall in the region of 0 to -0.5. The average value of the apparent diffusion coefficient in either case is the same as the expected value of bulk phase diffusion (5-6 x 10^{-6} cm^2/s).

Table XI [a]

Criteria for Mechanism of Surface Tension Change with Time (1)

$C \times 10^4$ mole / dm^3	T K	n	t^* / t_2	slope	$D_{ap} \times 10^6$ cm^2 / s
6.77	283.1	1.84	7.0	-0.65	0.14 (2.3)[b]
	298.1	1.34	10.8	-0.54	0.48 (3.6)
	318.1	0.77	30.6	-0.30	8.4 (5.7)
8.85	283.1	1.68	7.9	-0.71	0.20 (2.3)
	298.1	1.32	11.1	-0.50	0.66 (3.6)
	318.1	0.70	38.6	-0.30	10.8 (5.7)

a The values of n, t^* / t_2, D_{ap}, and the slope of log $\Delta\gamma$ versus log t were obtained from our dynamic surface tension data, measured by the maximum bubble pressure method.

b The values in parentheses are diffusion coefficients calculated by use of the Stokes-Einstein equation with an estimated average radius of 6.9 A^o for the DESS molecule.

Table XII [a]

Criteria for Mechanism of Surface Tension Change with Time (2)

Compound	Log C (mole / dm^3)	n	t^* / t_2	slope	D_{ap} x10^6 cm^2 / s
$C_{12}EO7$	-4.536	1.00	17.7	-0.67	2.67
	-4.235	0.82	26.5	-0.40	6.51
	-3.986	0.86	23.9	-0.40	6.06
Average			22.7	-0.49	5.08
$C_{12}EO8$	-4.577	0.88	22.8	-0.29	4.45
	-4.325	0.92	20.8	-0.29	6.50
	-4.200	0.83	25.8	-0.40	5.86
	-3.986	0.94	20.0	-0.39	5.25
Average			22.4	-0.34	5.52

a The values of n, t^* / t_2, D_{ap}, and the slope of log $\Delta\gamma$ versus log t were obtained from our dynamic surface tension data, measured by the maximum bubble pressure method.

Another example is 1,9-nonanediol. The value of n at C = 8.3 x 10^{-5} mole/dm^3, calculated from the dynamic surface tension data of Joos et al.[80] is about 2.7, from which

$$\frac{t^*}{t_2} \geq 4$$

Here, the two relaxation times are closer than for polyoxyethylenated alcohols. The results are in agreement with the literature: n-dodecyl ethers of polyoxyethylenated alcohols have a diffusion-controlled mechanism[69,121] and 1,9-nonanediol has a mixed mechanism of sub-surface transfer and diffusion[81].

From above examples, we can see that the criterion suggested by this work gives a simple and semi-quantitative measure of the mechanisms involved in dynamic surface adsorption, in agreement with those in the literature.

C. Preliminary Experimental Results

(1) Surface Elasticity

Table XIII lists the maximum surface elasticity and resonance frequency in the concentration region of several tenths to several times the cmc for 13 systems. Figures 14-23 show the relatioships between the maximum surface elasticity and the bulk phase surfactant concentration. There appear to be two kinds of curves: in one case the maximum surface elasticity first increases with increase in the surfactant concentration to a maximum and then decreases with further

increase in the concentration (for example, systems $C_{12}EO4$, $C_{12}EO_2SNa$ in 0.5 N NaCl, $C_{14}BMG$, $C_{12}SNa$ in 0.1 N NaCl, DESS in 0.1 N NaCl and DESS in water); In the other case, the maximum surface elasticity increases slowly, if at all, with increase in the surfactant concentration at the relatively high concentration (for example, systems of $C_{12}EO7$, $C_{12}EO8$, $C_{12}EO10$, $C_{12}BMG$, $C_{12}EOSNa$ in 0.1 N NaCl and 0.5 N NaCl, and $C_{12}EO_2SNa$ in 0.1 N NaCl).

The question is what determines the concentration at the maximum point or the turning point on the curve of ε_{max} versus C. Acording to equation IV-7, the ε_{max} value depends on the values of Π_m and n. If n keeps approximately constant, then the concentration at this point will be approxomately the same as the CMC value, as shown for the systems of $C_{12}EOSNa$ in 0.1 N and 0.5 N NaCl, $C_{12}EO_2SNa$ in 0.1 and 0.5 N NaCl, DESS in 0.1 N NaCl, $C_{12}EO4$, and $C_{14}BMG$ (Figures 14, 16-20, and 22). In other hand, if the value of n changes with the surfactant concentration, the concentration at this point will be different with cmc, for example, DESS in water (Figure 21).

The relationship of log f* to log C (in mole/dm^3) is linear (Figure 24-36) over the concentration region listed in Table XIII for the systems investigated. The equations are:

log f* = 4.40 + 1.40 log C ---------- $C_{12}EO4$

log f* = 7.08 + 1.86 log C ---------- $C_{12}EO7$

log f* = 6.99 + 1.78 log C ---------- $C_{12}EO8$

log f* = 6.57 + 1.69 log C ---------- $C_{12}EO10$

log f* = 5.86 + 1.59 log C ---------- $C_{12}BMG$

$\log f^* = 4.78 + 1.47 \log C$ ----------	C_{14}BMG
$\log f^* = 6.17 + 1.64 \log C$ ----------	C_{12}SNa in 0.1 n NaCl
$\log f^* = 7.07 + 2.00 \log C$ ----------	C_{12}EOSNa in 0.1 N NaCl
$\log f^* = 5.90 + 1.72 \log C$ ----------	C_{12}EOSNa in 0.5 N NaCl
$\log f^* = 7.71 + 2.15 \log C$ ----------	$C_{12}EO_2$SNa in 0.1 N NaCl
$\log f^* = 6.50 + 1.87 \log C$ ----------	$C_{12}EO_2$SNa in 0.5 N NaCl
$\log f^* = 9.03 + 2.52 \log C$ ----------	DESS in water
$\log f^* = 5.72 + 1.50 \log C$ ----------	DESS in 0.1 N NaCl

Table XIII

Maximum Surface Elasticity and Resonance Frequency

Compound	C x10^4 [a] mole/dm^3	n	Π_m mN/m	$\lvert\varepsilon_{max}\rvert$ mN/m	Log f° (f° in s-1)
$C_{12}EO4$	0.324	1.07	31.7	12.7	-1.921
	0.518	0.88	37.4	12.3	-1.620
	0.647	0.87	40.7	13.3	-1.469
	1.036	1.11	43.2	18.0	-1.046
	1.294	1.28	43.2	20.7	-0.951
	3.236	0.98	44.3	16.3	-0.569
$C_{12}EO7$	0.291	1.00	26.9	10.1	-1.387
	0.582	0.82	32.7	10.1	-0.7645
	1.033	0.86	35.2	11.35	-0.279
	2.911	1.09	35.9	14.7	0.476
$C_{12}EO8$	0.265	0.88	20.5	6.77	-1.174
	0.473	0.92	25.3	8.73	-0.599
	0.631	0.83	30.7	9.56	-0.648
	1.032	0.94	33.0	11.63	-0.176
	1.893	- - -	- - -	- - -	0.398

Table XIII (continued)

Maximum Surface Elasticity and Resonance Frequency

Compound	C x10^4 [a] mole/dm^3	n	Π_m mN/m	$\lvert\varepsilon_{max}\rvert$ mN/m	Log f* (f* in s-1)
$C_{12}EO10$	0.335	0.83	23.9	7.44	-1.215
	0.558	0.69	26.5	6.86	-0.690
	1.033	0.71	30.6	8.14	-0.146
	1.86	0.86	31.2	10.06	0.222
	3.35	- - -	- - -	- - -	0.699
DESS	3.342	1.20	19.4	8.73	0.284
in water	5.844	1.28	24.9	12.0	0.769
	9.027	0.84	31.5	7.44	1.380
	12.52	0.63	35.4	8.36	1.921
	24.57	0.52	41.1	8.01	2.348
DESS					
in 0.1 N NaCl	1.228	1.69	40.2	25.5	-0.223
	1.474	1.90	41.3	29.4	-0.107
	1.965	1.88	42.6	30.0	0.180

Table XIII (continued)

Maximum Surface Elasticity and Resonance Frequency

Compound	C x10^4 [a] mole/dm^3	n	Π_m mN/m	$\lvert\varepsilon_{max}\rvert$ mN/m	Log f* (f* in s-1)
	2.457	1.57	44.3	26.1	0.367
	3.339	1.52	46.1	26.3	0.602
	5.848	1.64	45.6	26.0	0.903
	8.189	1.61	46.1	27.8	1.000
	10.65	1.44	46.1	24.9	1.222
C_{12}BMG	0.780	1.75	23.6	15.5	-0.592
(pH = 9)	1.493	1.39	27.2	14.2	-0.269
	1.991	1.32	30.1	14.9	-0.0757
	2.985	1.39	32.1	16.7	0.292
	3.890	1.13	34.7	14.7	0.468
	5.970	1.18	37.2	16.5	0.815
	10.19	1.17	37.4	16.4	1.086
C_{14}MBG	0.333	1.86	34.0	23.7	-1.745
(pH = 9)	0.508	1.79	35.6	23.9	-1.620

Table XIII (continued)

Maximum Surface Elasticity and Resonance Frequency

Compound	C x10^4 [a] mole/dm^3	n	Π_m mN/m	$\lvert\varepsilon_{max}\rvert$ mN/m	Log f* (f* in s-1)
	0.540	1.96	36.0	26.5	-1.495
	0.604	1.87	36.6	25.7	-1.377
	0.746	1.60	38.6	23.2	-1.284
	1.015	1.50	40.0	22.5	-1.057
$C_{12}SNa$	2.958	0.81	17.0	5.2	0.241
in 0.1 N NaCl	3.700	1.02	19.3	7.4	0.639
	5.284	0.91	22.0	7.5	0.796
	6.339	1.02	24.7	9.4	1.000
	12.05	0.72	29.0	7.8	1.310
$C_{12}EOSNa$	1.937	0.84	25.6	8.1	-0.269
in 0.1 N NaCl	2.970	0.84	28.9	9.1	-0.0179
	3.713	0.83	31.4	9.8	0.127
	4.950	0.94	36.8	13.0	0.443
	7.430	0.93	36.0	12.6	0.826

Table XIII (continued)

Maximum Surface Elasticity and Resonance Frequency

Compound	C x10^4 [a] mole/dm^3	n	Π_m mN/m	$\lvert\varepsilon_{max}\rvert$ mN/m	Log f* (f* in s-1)
	14.85	0.83	38.1	11.9	1.446
$C_{12}EOSNa$	0.598	1.06	27.5	10.9	-1.456
in 0.5 N NaCl	1.197	- - -	- - -	- - -	-0.709
	3.373	1.02	42.1	16.1	-0.071
	7.816	1.09	41.8	17.4	0.548
	18.58	1.11	42.4	17.3	1.196
$C_{12}EO_2SNa$	1.336	0.76	25.5	7.3	-0.643
in 0.1 N NaCl	2.229	0.83	27.0	8.4	-0.119
	2.570	0.84	30.4	9.6	0.0113
	3.342	0.93	35.55	12.4	0.280
	6.687	0.96	36.1	13.0	0.860
$C_{12}EO_2SNa$	0.411	1.00	28.5	10.7	-1.820
in 0.5 N NaCl	0.851	0.89	32.3	10.8	-1.092

Table XIII (continued)

Maximum Surface Elasticity and Resonance Frequency

Compound	C x10^4 [a] mole/dm^3	n	Π_m mN/m	$\lvert\varepsilon_{max}\rvert$ mN/m	Log f* (f* in s-1)
	1.560	1.00	38.45	14.4	-0.536
	3.122	1.10	38.1	15.7	-0.0232
	5.200	0.90	38.1	12.9	0.352
	9.354	0.86	38.4	12.4	0.726
	33.42	- - -	- - -	- - -	1.867

[a] underlined concentrations are above the CMC.

(2) Adsorption Mechanism

Table XIV lists the slopes of the plots of log f* versus log C. The value of the slope is near 2 for the systems of $C_{12}EO7$, $C_{12}EO8$, $C_{12}EO10$, $C_{12}EOSNa$ in 0.1 N and 0.5 N NaCl, $C_{12}EO_2SNa$ in 0.1 N and 0.5 N NaCl, and DESS in water. According to Section (A) (2) in Theory, a slope of 2 indicates a diffusion-controlled mechanism. The slope is near 1.5 for the systems of $C_{12}EO4$, $C_{12}BMG$, $C_{14}BMG$, $C_{12}SNa$ in 0.1 N NaCl, and DESS in 0.1 N NaCl. This indicates that the mechanism involved is not completely diffusion.

Table XIV also lists the value of n, which is related to t^*/t_2 by equation IV-21. The value of n in Table XIV varies from 0.5 to 2. In general, if the average value of n is equal to or less than 1, a diffusion-controlled mechanism is involved; if the average value of n is higher than 1, a mixed mechanism is involved.

The slope of the plot of log f* versus log C and the value of n give only qualitative information about the mechanism. The value of t^*/t_2 in Table XIV gives semi-quantitatively information about the adsorption mechanism. For example, in general, the systems of $C_{12}EO7$ and $C_{12}EO10$ have the same diffusion-controlled mechanism. However, a higher average value of t^*/t_2 for C_{12} EO10 than that for $C_{12}EO7$, shown in Table XIV, indicates that the time for transfer is less significant in the adsorption process of $C_{12}EO10$, compared to $C_{12}EO7$. The other example is shown by the systems of $C_{12}BMG$ and $C_{14}BMG$. The adsorption process for both systems is not completely diffusion-controlled,

however, a lower average value of t^*/t_2 for C_{14}BMG than for C_{12}BMG, shown in Table XIV, indicates that the time for transfer is more significant in the adsorption process of C_{14}BMG, compared to C_{12}BMG. However, since the error in measuring t^*/t_2 is as high as $\pm$20%, this method is only a semi-quantitative one.

Table XIV
Mechanism of Adsorption

System	Log C [a]	n	t^*/t_2	Slope[b]	Mechanism: Diffusion ?
$C_{12}EO4$	-4.489	1.07	15.7		
	-4.286	0.88	22.8		
	-4.189	0.87	23.3		
	-3.985	1.11	14.7		
	-3.888	1.28	11.6		
	-3.490	0.98	18.4		
Average		1.03	17.7±3.8	1.4	Not Completely
$C_{12}EO7$	-4.536	1.00	17.7		
	-4.235	0.82	26.5		
	-3.986	0.86	23.9		
	-3.936	1.09	15.2		
Average		0.94	20.8±4.4	1.9	Yes
$C_{12}EO8$	-4.577	0.88	22.8		
	-4.325	0.92	20.8		
	-4.200	0.83	25.8		

Table XIV (continued)

Mechanism of Adsorption

System	Log C [a]	n	t^*/t_2	Slope[b]	Mechanism: Diffusion ?
	-3.986	0.94	20.0		
Average		0.89	22.4 ±2.0	1.8	Yes
$C_{12}EO10$	-4.475	0.83	25.8		
	-4.254	0.69	40.0		
	-3.986	0.71	37.2		
	-3.731	0.86	23.9		
Average		0.77	31.7±6.9	1.7	Yes
$C_{12}BMG$	-4.108	1.75	7.4		
	-3.826	1.39	10.3		
	-3.701	1.32	11.1		
	-3.525	1.39	10.3		
	-3.410	1.13	14.3		
	-3.224	1.18	13.3		
	-2.992	1.17	13.4		
Average		1.33	11.5±1.9	1.6	No

Table XIV (continued)

Mechanism of Adsorption

System	Log C [a]	n	t^*/t_2	Slope[b]	Mechanism: Diffusion ?
C_{14}BMG	-4.478	1.86	6.9		
	-4.294	1.79	7.2		
	-4.268	1.96	6.4		
	-4.219	1.87	6.8		
	-4.127	1.60	8.4		
	-3.993	1.50	9.2		
Average		1.76	7.5 ±0.9	1.5	No
C_{12}EOSNa in	-3.713	0.84	25.2		
0.1 N NaCl	-3.527	0.84	25.2		
	-3.430	0.83	25.8		
	-3.305	0.94	20.0		
	-3.129	0.93	20.4		
	-2.828	0.83	25.2		
Average		0.87	23.6 ±2.3	2.0	Yes
C_{12}EOSNa	-4.225	1.06	15.9		
in 0.5 N NaCl	-3.472	1.02	17.1		

Table XIV (continued)

Mechanism of Adsorption

System	Log C [a]	n	t^*/t_2	Slope[b]	Mechanism: Diffusion ?
	-3.107	1.11	15.2		
	-2.731	1.09	14.7		
Average		1.07	15.7±0.78	1.7	Not completely
$C_{12}EO_2SNa$	-3.874	0.76	31.5		
in 0.1 N NaCl	-3.652	0.83	25.8		
	-3.590	0.84	25.2		
	-3.476	0.93	20.4		
	-3.175	0.96	19.2		
Average		0.86	24.4±3.7	2.0	Yes
$C_{12}EO_2SNa$	-4.386	1.00	17.7		
0.5 N NaCl	-4.070	0.89	22.3		
	-3.807	1.00	17.7		
	-3.506	1.10	14.9		
	-3.284	0.90	21.8		
	-3.029	0.86	23.9		
Average		0.96	19.7±3.0	1.7	Yes

Table XIV (continued)

Mechanism of Adsorption

System	Log C [a]	n	t^*/t_2	Slope[b]	Mechanism: Diffusion ?
$C_{12}SNa$	-3.529	0.81	27.2		
in 0.1 N NaCl	-3.432	1.02	17.1		
	-3.277	0.91	21.3		
	-3.198	1.02	17.1		
	-2.919	0.72	35.9		
Average		0.90	23.7±6.3	1.6	Yes
DESS	-3.911	1.69	7.8		
in 0.1 N NaCl	-3.832	1.90	6.7		
	-3.707	1.88	6.8		
	-3.610	1.57	8.6		
	-3.476	1.52	9.0		
	-3.233	1.64	8.1		
	-3.087	1.61	8.3		
	-2.973	1.44	9.7		
Average		1.66	8.1±0.8	1.5	No

Table XIV (continued)

Mechanism of Adsorption

System	Log C [a]	n	t^*/t_2	Slope[b]	Mechanism: Diffusion ?
DESS in water	-3.476	1.20	12.9		No
	-3.233	1.28	11.6		No
	-3.044	0.84	25.2		Yes
	-2.902	0.63	51.2		Yes
	-2.610	0.52	92.6		Yes
				2.5	

a underlined concentrations are above the CMC.

b The slope of log f^* vs. log C

In the range of concentration that we have investigated, which is restricted to that in which the plot of γ_{eq} versus log C is linear (equilibrium surface saturation), there appears to be a relationship between the maximum surface excess concentration, Γ_{max}, and the average t^*/t_2 value. A compound with a higher maximum surface excess concentration (Γ_{max}) has a lower value of t^*/t_2. Table XV shows the relationship of t^*/t_2 to Γ_{max}. For example, the value of t^*/t_2 increases with increase in EO number in the nonionic, whereas the value of Γ_{max} decreases with increase in EO number. The system of $C_{12}EOSNa$ or $C_{12}EO_2SNa$ in 0.5 N NaCl with a higher value of Γ_{max} has a lower value of t^*/t_2 than that in 0.1 N NaCl; and $C_{14}BMG$ with a higher Γ_{max} value has a lower t^*/t_2 value than that for $C_{12}BMG$. The results indicate that the time for transfer from the sub-surface to the surface is more significant in the adsorption process for the surfactant with higher maximum surface excess concentration.

Table XV

Relationship of t^*/t_2 to Equilibrium Maximum Surface Excess Concentration

(25 ^{0}C)

System	Γ_{max} x 10^{10} (mole/cm^2)	Averg. t^*/t_2
$C_{12}EO4$	3.61	17.7
$C_{12}EO7$	2.90	20.8
$C_{12}EO8$	2.52	22.4
$C_{12}EO10$	2.11	31.7
$C_{12}EOSNa$ (in 0.1 N NaCl)	3.81	23.6
$C_{12}EOSNa$ (in 0.5 N NaCl)	4.41	15.7
$C_{12}EO_2SNa$ (in 0.1 N NaCl)	3.46	23.9
$C_{12}EO_2SNa$ (in 0.5 N NaCl)	3.78	18.2
DESS (in water)	1.45	11.6 - 92.6
DESS (in 0.1 N NaCl)	2.34	8.1
in water		
$C_{12}BMG$ (pH 9)	3.07	11.5
$C_{14}BMG$ (pH 9)	4.22	7.5

D. Thermodynamics of Dynamic Surface Process

Most of the usual physicochemical processes like diffusion, conduction of heat or electicity, chemical reaction, etc., are irreversible processes. Since the diffusion process strongly affects surface tension change with time, we have done some preliminary reseach by use of irreversible thermodynamics.

(1) Gibbs Equation for Dynamic Surface Tension

Since basic thermodynamic relationships are valid for both equilibrium and non-equilibrium thermodynamics[125], we have

$$-d\gamma_t = \Gamma_t \, d\,\mu_2^{st} \qquad [I\,V\text{-}22]$$

for nonionic surfactant solutions, where μ_2^{st} is the chemical potential of a surfactant at its surface phase at time t, Γ_t is the surface excess concentration at time t, and γ_t is the surface tension of a surfactant solution at time t.

In a non-equilibrium process, the chemical potential in the surface phase of a surfactant, μ_2^{st}, is not equal to the chemical potential in the bulk phase, μ_2^{b}. Thus,

$$\mu_2^{st} - \mu_2^{b} = \Delta\mu^t, \qquad [I\,V\text{-}23]$$

where $\Delta\mu^t$ is the difference between the chemical potential of the surface phase and that of the bulk phase at time t, which is a negative value in the process of dynamic adsorption. From equation IV-23, we obtain

$$d\,\mu_2^{st} = d\,\mu_2^{b} + d\Delta\mu^t . \qquad [I\,V\text{-}24]$$

Also,

$$\mu_2^b = \mu_2^{b0} + RT \ln a,$$

and $$d\mu_2^b = RT\, d \ln a, \qquad [IV-25]$$

where μ_2^{b0} is the standard chemical potential in bulk phase, and a is the activity of the surfactant in the bulk phase at the equilibrium condition. Substituting equations IV-24 and IV-25 into equation IV-22, we obtain

$$-d\gamma_t = \Gamma_t (RT\, d \ln a + d\, \Delta\mu^t)$$

$$= \Gamma_t RT [d \ln a + d \ln (\exp (\Delta\mu^t / RT))]$$

$$= \Gamma_t RT\, d \ln [a (\exp (\Delta\mu^t / RT))] \qquad [IV-26]$$

Defining $a^t = a (\exp (\Delta\mu^t / RT))$, we obtain [IV-27]

$$-d\gamma_t = \Gamma_t RT\, d \ln a^t . \qquad [IV-28]$$

This form is similar to the Gibbs equation for equilibrium surface adsorption. We designate equation IV-28 as the Gibbs equation for dynamic surface adsorption. In the limiting case, as $\Delta\mu^t \rightarrow 0$, $a^t \rightarrow a$, $\Gamma_t \rightarrow \Gamma$, and equation IV-28 reduces to the conventional Gibbs equation.

(2) Pseudo-Phase Separation in a Non-equilibrium State

The plots of dynamic surface tension vs. log of concentration for pure nonionic surfactant $C_{12}EO8$ at different fixed surface ages are shown in Figure 11. Each curve shows a rapid decrease in surface tension with increase in log C over a certain concentration range and then no change or a gradual change with the further increase in concentration above a concentration which we symblize, C^*.

To explain this discontinuty, we derivatize equation IV-28 with respect to

In C, at concentration equal to or above C*. Assuming Γ_t reaches to its maximum value at a sufficiently high concentration, we obtain in the range above C*

$$\left(\frac{-\partial\gamma_t}{\partial \ln C}\right)_T = RT\Gamma_t\left(\frac{\partial \ln a^t}{\partial \ln C}\right)_T \qquad [IV-29]$$

Since Γ_t is a finite number, if the term ($\partial\gamma_t$ / ∂lnC) equals approximately zero, the term (∂ ln a^t / ∂ ln C) must be equal approximately to zero. This means that the activity keeps approximately constant with increase in surfactant concentration.

In the case of sparingly soluble substances such as C_6H_6 or $C_{10}H_{21}OH$ in water, the activity increase is almost in proportion to the concentration of solute up to the saturation concentration of single dispersed species, but it does not increase after the excess solute phase appears. These two phenomena are thermodynamicly similar[126]. From the dynamic surface tension versus concentration data, we are forced to conclude that micelle formation, which resembles the phase separation phenomenon, occurs at the turning region, which is generally higher than the equilibrium CMC at short surface ages. Since this is only a theoretical prediction, and a further experimental proof is necessary (not within the scope of thesis), we designate temporarily the turning concentration in the curve of dynamic surface tension versus log C as C*. From Figure 11 we can see that the shorter the surface age is, the higher C* is. This implies that surface age effects micelle formation in dynamic process.

In real phase separation such as precipitation, the curves of physical

properties versus the concentration of a solution change sharply at the point of phase separation. For most of aqueous surfactant solutions, curves of equilibrium surface tension versus log C also show sharp break at their CMC's. However, the curves of dynamic surface tension versus log C at short surface ages usually have no sharp change at their C* (see Figure 11). This implies that micelle size is smaller at short surface ages than at equilibrium (experimental proof is not within the scope of this thesis).

Chapter V: Results of Phenomenological Studies

In many important rapid interfacial processes involving surfactants, such as high speed wetting of textiles, coating of solid surfaces, some hard surface cleaning processes, and high speed foaming and emulsification, equilibrium conditions are not attained. As a result, surface or interfacial properties under dynamic (non-equilibrium) conditions would appear to be more important than equilibrium properties in determining the effect of the surfactant on the process. For example, in a process where the surface area is being increased by a value, ΔA, at a short time, t, the minimum work required to achieve that surface area expansion is the product of the surface tension, γ_t, at time t, and the interfacial area increase. For rapid interfacial processes, therefore, the questions to be answered are:

(i) what bulk phase concentration of surfactant is necessary to attain a significant reduction of the surface tension of the system in a short time (for example,1 second)?

(ii) how much of a reduction of the surface tension can be attained in such a time?

(iii) what time is needed to achieve a significant reduction of the surface tension at a particular bulk phase concentration of surfactant?

The surface tension at meso-equilibrium (γ_m) is the lowest surface tension value that can be reached by the system in a short time at a particular surfactant concentration. The time at the begining of the meso-equilbrium region, t_m, by

definition (p.49), is the time for the surface tension to be depressed about 91% of the value at meso-equilibrium. The parameters at meso-equilbrium are useful in intermediate-time dynamic processes or fast processes, depending on the meso-equilibrium time, t_m, for a particular surfactant.

We investigated the parameters of dynamic surface tension at 1 second because the surface tension at 1 second has been shown (Section F, below) to correlate well with wetting time for 23 commonly used surfactants. Hence we consider the dynamic behavior at 1 second as representive of fast processes.

A. Definitions for Parameters of Surface Tension at 1 Second and at Meso-equilibrium

Figure 37 shows a generalized plot of surface tension at 1 sec surface age (γ_{1s}), a plot of surface tension at meso-equilbrium (γ_m), and a plot of equilibrium surface tension (γ_{eq}), all vs. log of surfactant molar concentration (log C). The curves for γ_{1s} and γ_m are similar in shape to that for equilibrium surface tension: the surface tension at first decreases rapidly with increase in the surfactant concentration, followed by a point in the curve where the surface tension begins to decrease gradually. Because of this similarity between dynamic and equilibrium curves, we have created a data treatment pattern similar to that used with equilibrium data, and compare the dynamic parameters to the equilibrium ones (CMC, and surface tension at CMC).

From the intersection of the two linear portions of the curve above and below it, or by taking the midpoint (the intersection of the two broken lines) of

the transition region, we obtain from the γ_{1s} versus log C plot the point symbolized C^*_{1s}, the concentration at which the surface tension at 1 second shows slow change with increase in surfactant concentration; from the γ_m versus log C curve, the point symbolized C^*_m, the minimum concentration at which the surface tension shows little further change with increase either in time or in surfactant concentration. C^*_m therefore represents the minimum surfactant concentration required to approach maximum reduction (i.e. maximum effectiveness) of surface tension reduction. Higher surfactant concentrations give only small increase in effectiveness.

The experimental results for systems of $C_{12}EO4$, $C_{12}EO7$, $C_{12}EO8$, $C_{12}EO10$, C_8PY, $C_{10}PY$, $C_{12}SO_4Na$ in water, $C_{10}SNa$ in water, and in 0.1 N NaCl, $C_{12}SNa$ in 0.1 N NaCl, $C_{12}EOSNa$ in water and in 0.1 N NaCl and in 0.5 N NaCl, $C_{12}EO_2SNa$ in water and in 0.1 N NaCl and in 0.5 N NaCl, DESS in water and in 0.1 N NaCl, $C_{10}BMG$ (pH = 9), $C_{12}BMG$ (pH = 9) and $C_{14}BMG$ (pH = 9) are shown in Tables A I- A XXI in Appendix, and in Figures A1- A21 in Appendix, which include the same set of plots as in Figure 37.

B. Definition of Effectiveness Percentage in Surface Tension Reduction

We define the effectiveness percentage in dynamic surface tension reduction, P_t, as the percentage of the equilibrium surface tension reduction that is attained in a time t with a given molar bulk phase concentration of surfactant.

$$P_t = \frac{(\gamma_o - \gamma_t)}{(\gamma_o - \gamma_{eq})} \times 100\% = \frac{\Pi_t}{\Pi_{eq}} \times 100\% \qquad [V-1]$$

where γ_0 is the surface tension of pure solvent, γ_t the surface tension at time t, γ_{eq} the equilibrium surface tension, Π_t the surface pressure at time t, and Π_{eq} the equilibrium surface pressure. A high value of P_t means that the dynamic state at time t is close to equilibrium. We use P_{1s} to represent the effectiveness percentage at 1 second, and P_m, the effectiveness percentage at meso-equilibrium. The physical meaning of P_{1s} is the degree of equilibrium attainment at 1 secod, which is equal to the average rate of equilibrium attainment at 1 second.

C. Parameters and Features of the Surface Tension at 1 Second

(1) 1-Sec. Critical Reduction Concentration, C^*_{1s}

Table XVI shows the comparison of values of C^*_{1s}, obtained from the plots of γ_{1s} versus log C in the figures in the Appendix, with equilibrium critical micelle concentration (CMC). The data indicate that the value of C^*_{1s} is never lower than the CMC and is generally higher than it. For the investigated materials with CMCs lower than about 5 x 10^{-4} mole/ dm^3, the C^*_{1s} value appears to fall in the range 5 -10 x 10^{-4} mole/ dm^3, for those whose CMCs are 5 x10^{-4} mole/ dm^3 or more, the C^*_{1s} value is just slightly higher than the value of the CMC. The value in parenthesis for $C_{12}EO4$ and $C_{14}BMG$ is the concentration at their solubility limit, which is below their C^*_{1s} value. The C^*_{1S}/CMC ratio is also listed in Table XVI. For materials whose CMC value is less than 5 X10^{-4} mole/ dm^3, the ratio increases with decrease in the value of CMC. Since the CMC value

can be considered a measure of the "surface activity" of the surfactant[127], here the deviation from the equilibrium value increases with increase in surface activity of the surfactant.

Table XVI
Comparison of Values of C^*_{1s} and CMC

Surfactant	$C^*_{1s} \times 10^4$ mole/dm^3	CMC $\times 10^4$ mole/dm^3	C^*_{1s}/ CMC
$C_{12}EO4$	(3.2)[a]	0.645	
$C_{12}EO7$	7.9	0.82	9.6
$C_{12}EO8$	7.9	1.09	7.2
$C_{12}EO10$	7.9	1.20	6.6
$C_{12}EOSNa$ in 0.1 N NaCl	10	4.3	2.3
$C_{12}EOSNa$ in 0.5 N NaCl	7.9	1.3	6.1
$C_{12}EO_2SNa$ in 0.1 N NaCl	6.9	2.9	2.4
$C_{12}EO_2SNa$ in 0.5 N NaCl	8.9	1.00	8.9
$C_{14}BMG$	(1)[a]	0.61	
DESS in 0.1 N NaCl	5.0	3.47	1.4
**********	**********	**********	**********
$C_{10}BMG$ (pH 9)	56.2	45.7	1.2

Table XVI (continued)

Comparison of Values of C^{*}_{1s} and CMC

Surfactant	$C^{*}_{1s} \times 10^{4}$ mole/dm^3	CMC x 10^4 mole/dm^3	C^{*}_{1s}/CMC
C_{12}BMG (pH 9)	5.5	5.10	1.1
DESS in water	20.0	20.0	1.0
$C_{12}SO_4Na$ in water	95.5	79.4	1.2
C_{12}EOSNa in water	43.7	39.1	1.1
$C_{12}EO_2SNa$ in water	31.6	28.8	1.1
C_{10}SNa in water	452	427	1.1
C_{10}SNa in 0.1 N NaCl	224	211	1.1

(2) Surface Tension at 1 Second Surface Age (γ_{1s})

This addresses the question of how low the surface tension of the solvent can be reduced in a short time. Values of γ_{1s} are listed in Table XVII, together with equilibrium surface tension values, γ_{eq}. Since the value of γ_{1s} depends upon the bulk phase concentration of the surfactant, in order to permit comparison with equilibrium values, γ_{1s} and γ_{eq} values were both taken at the equilibrium critical micelle concentration of the surfactant. A plot of $\Delta\gamma_{1s}$ (= γ_{1s} - γ_{eq}) vs. log CMC is shown in Figure 38. From the figure, it is apparent that, when the CMC of the substance is less than 5-10 $x10^{-4}$ molar (log CMC = -3.0 to -3.3), a large deviation of γ_{1s} from γ_{eq} can be expected. Since the CMC value can be considered a measure of the "surface activity" of the surfactant[127], hence the deviation from the equilibrium value increases with increase in surface activity of the surfactant. Figure 39 shows a plot of $\Delta\gamma_{1s}$ versus C^*_{1s}. In general, the value of $\Delta\gamma_{1s}$ decreases with increase in C^*_{1s}. It appears that the value of $\Delta\gamma_{1s}$ rapidly increases when $C^*_{1s} < 10^{-3}$ mole/dm^3, however, it is about 1 to 3 mN/m when $C^*_{1s} > 10^{-3}$ mole/dm^3. The value of $\Delta\gamma_{1s}$ for compounds $C_{12}EO4$ and $C_{14}BMG$ are unusually high, because their solubility limit is below their C^*_{1s} values.

Table XVII

γ_{1s} and γ_{eq} Values at CMC

Surfactant	γ_{1s}	γ_{eq} mN/m	$\Delta\gamma_{1s}$ mN/m	log CMC mN/m
$C_{12}EO4$	70.5	28.6	41.9	-4.190
$C_{12}EO7$	62.9	33.6	29.3	-4.086
$C_{12}EO8$	58.4	34.6	23.8	-3.963
$C_{12}EO10$	56.4	37.0	19.4	-3.921
C_{10}BMG (pH 9)	38.7	33.8	4.9	-2.340
C_{12}BMG (pH 9)	38.8	32.8	6.0	-3.292
C_{14}BMG (pH 9)	71.4	31.7	39.7	-4.215
C_{12}EOSNa in 0.1 N NaCl	50.0	33.7	16.3	-3.367
C_{12}EOSNa in 0.5 N NaCl	68.0	30.6	37.4	-3.886
$C_{12}EO_2$SNa in 0.1 N NaCl	53.3	35.6	17.7	-3.538
$C_{12}EO_2$SNa in 0.5 N NaCl	68.5	32.9	35.6	-4.000
DESS in water	31.2	29.8	1.4	-2.699
DESS in 0.1 N NaCl	32.1	25.5	6.6	-3.460
C_{10}SNa in water	43.4	41.0	2.4	-1.370
C_{10}SNa in 0.1 N NaCl	42.8	39.7	3.1	-1.676
C_{12}SNa in 0.1 N NaCl	40.2	35.9	4.3	-2.607
$C_{12}SO_4$Na in water	43.0	39.5	3.5	-2.100
C_{12}EOSNa in water	44.0	39.2	4.8	-2.408
$C_{12}EO_2$SNa in water	45.0	41.4	3.6	-2.541

(3) Features of Plot of γ_{1s} Versus Log C

We have noted that the surface tension at a short time such as 1 second in some cases is less sensitive to the effects of structure, electrolyte, organic additives, and temperature than at longer surface age, or at equilibrium. Some examples follow:

Figure 40 shows plots of γ_{1s} versus log C in different solvents: water, 0.1 N NaCl, and 0.5 N NaCl, for the system of $C_{12}EOSNa$. The plots of γ_{1s} versus log C for the surfactant in 0.1 N and 0.5 N NaCl fall on one line at the concentrations below 4 x10 $^{-4}$ mole/dm^3. The difference in the nature of the solvent (0.1 N and 0.5 N) seems to vanish at short surface ages such as 1 second and at low surfactant concentrations. Figure 41 shows the same set of plots for the system of $C_{12}EO_2SNa$. Again the plots of γ_{1s} versus log C for the surfactant in 0.1 N NaCl and 0.5 N NaCl fall on one line at concentrations below 2 x 10^{-4} mole/dm^3. However, there is a great decrease in the surface tension at 1 second from aqueous solution to 0.1 N NaCl.

Figure 42 (a) shows plots of surface tension at 1 second versus log C for the mixture of the $C_{12}SO_4Na$ and dodecyl alcohol ($C_{12}OH$) in water with the molar ratio of alcohol / surfactant = 1:10, cmpared to the same plot for pure surfactant in water. Figure 42(b) shows plots for the surface tension at 10 seconds versus log C for same systems as in Figure 42 (a). We found that the "impurity" ($C_{12}OH$) has no effect on the surface tension at 1 second at a concentration of about 4 x 10^{-3} mole/dm^3, whereas it causes a significant

decrease of the surface tension of $C_{12}SO_4Na$ at 10 seconds over the concentration region investigated. The additive, dodecyl alcohol, therefore shows less effect on the surface tension of sodium dodecyl sulfate at 1 second than at 10 seconds. Mysels[90] reported the effect of purification of an aqueous solution of sodium dodecyl sulfate on dynamic surface tension, measured by the maximum bubble pressure method. He found also that the effect of purification was small when the surface is fresh at short age and increased markedly as the surface age increased Hence, he suggested that for less precise determination on less pure systems, measurements made at short times are closer to the true values for the pure system than those made at long times. Our result is in agreement with Mysels' result.

Figure 43 shows the plot of γ_{1s} versus log C for $C_{12}EO7$, $C_{12}EO8$, and $C_{12}EO10$. At concentrations lower than $\sim 10^{-4}$ mole/dm^3, the surface tensions at 1 second for $C_{12}EO7$, $C_{12}EO8$, and $C_{12}EO10$ fall on one line, indicating no structural effect on γ_{1s} in this region. However, the curve of $C_{12}EO10$ begins to separate from the stem at $\sim 10^{-4}$ mole/dm^3; the curve of $C_{12}EO8$ at $\sim 3 \times 10^{-4}$ mole/dm^3.

Figure 44 shows the plots of γ_{1s} versus log C for $C_{12}EO_xSNa$ in 0.1 N NaCl, where x =1, 2. At the concentrations below $\sim 4 \times 10^{-4}$ mole/dm^3, the plots fall on one line. Again this indicates no structural effect on γ_{1s} in this region. However, the curves separate from each other after 7×10^{-4} mole/dm^3, and graduately reach constant values: 38.5 mN/m for the surfactant with higher equilibrium surface tension (x=2, γ_{eq} = 35.6 mN/m), and 35.2 mN/m for the other (γ_{eq} =

33.7 mN/m).

(4) Effectiveness Percentage at 1 Second, P_{1s}

Table XVIII portrays the effect of surfactant concentration on the effectiveness percentage at 1 second for the systems, $C_{12}EO7$, $C_{12}BMG$, and $C_{12}EO_2SNa$ in water and in 0.1 N NaCl. The data indicate that the effectiveness percentage at 1 second increases monotonously with increase in surfactant concentration at the range investigated, and at high concentration the value of P_{1s} approaches 100%, which is an indication of equilibrium state.

Table XVIII

Effectiveness Percentage at 1 Second

- Concentration Effect

System	Log C	γ_{1s} mN/m	Π_{1s} mN/m	γ_{eq} mN/m	P_{1s} (%)
$C_{12}EO7$					
	-4.536	71.6	1.0	41.1	3.2
	-4.235	65.6	6.4	35.9	17.7
	-3.986	59.5	12.5	33.6	32.6
	-3.536	45.1	26.9	33.6	70.0
	-3.277	42.0	30.0	33.6	78.1
	-2.944	38.3	33.7	33.6	87.8
	-2.608	35.6	36.4	33.6	94.8
	-2.424	35.6	36.4	33.6	94.8
$C_{12}BMG$					
	-4.108	70.8	1.2	46.6	4.7
	-3.826	64.4	7.6	41.9	25.2
	-3.701	59.0	13.0	39.7	40.2
	-3.525	48.6	23.4	36.7	66.3
	-3.410	43.7	28.3	34.8	76.1
	-3.224	37.7	34.3	32.8	87.5

Table XVIII (continued)

Effectiveness Percentage at 1 Second

- Concentration Effect

System	Log C	γ_{1s} mN/m	Π_{1s} mN/m	γ_{eq} mN/m	P_{1s} (%)
	-2.992	36.5	35.5	32.8	90.6
	-2.792	35.0	37.0	32.8	94.4
	-2.491	34.0	38.0	32.8	96.9
$C_{12}EO_2SNa$ in water					
	-2.777	52.9	19.1	47.9	79.3
	-2.652	48.5	23.5	44.5	85.5
	-2.476	43.6	28.4	41.4	91.9
	-2.294	44.0	28.0	41.4	91.5
	-2.044	43.5	28.5	41.4	93.1
	-1.692	42.4	29.6	41.4	96.7

Table XVIII (continued)

Effectiveness Percentage at 1 Second

- Concentration Effect

System	Log C	γ_{1s} mN/m	Π_{1s} mN/m	γ_{eq} mN/m	P_{1s} (%)
$C_{12}EO_2SNa$					
in 0.1 N NaCl					
	-3.874	66.4	5.6	62.2	55.4
	-3.652	60.7	11.3	56.2	70.2
	-3.590	56.4	15.6	50.9	72.9
	-3.476	48.9	23.1	45.0	84.6
	-3.175	40.7	31.3	35.6	85.3
	-2.476	39.1	32.9	35.6	89.6
	-2.018	38.5	33.5	35.6	91.3

Since P_{1s} changes with concentration, a comparison between compounds or different conditions is only possible at same molar concentration.

Table XIX lists the effectiveness percentage at 1 second, P_{1S}, for different compounds at same bulk molar concentrations and for the same compound under different molecular environment conditions, together with the γ_{eq} and Π_{1s} ($= \gamma_0 - \gamma_{1s}$) values on which they are based.

The P_{1S} value reflects the position of the surfactant concentration relative to C^*_{1s} and increases as the ratio, concentration / C^*_{1s}, increases. The value of P_{1S} also reflects the difference between the value of γ_0, the surface tension of the system in the absence of surfactant, and the equilibrium value, γ_{eq}. The larger the difference between these two values, the smaller will be P_{1S}. General speaking, a dynamic property is a modulated equilibrium property. When the modulating function is large, the dynamic property will be far from the equilibrium one; when the modulating function is small, the dynamic property approaches the equilibrium property. The ratio of concentration / C^*_{1s} is a measure of the modulating function at 1 second surface age.

Since for surfactants with CMC values below 5×10^{-4} mole/dm^3, the C^*_{1S} value falls in a fairly narrow range ($5 - 10 \times 10^{-4}$ mole/dm^3), it is to be expected that their P_{1S} values will reflect the γ_{eq} value, with higher γ_{eq} values yielding higher P_{1S} values. Thus, for the polyoxyethylenated compounds, $C_{12}EO_4$ - $C_{12}EO10$, since γ_{eq} increases with increase in the number of oxyethylene units in the molecule, the P_{1S} values decrease as the γ_{eq} values decrease. Since the

concentration at which the compounds are compared is much lower than their C^*_{1S} values, the values of P_{1S} are all small.

For compounds $C_{12}EOSNa$ and $C_{12}EO_2SNa$ in water, 0.1 N NaCl, and 0.5N NaCl, the C^*_{1S} values in water are several times higher than those in 0.1 N NaCl and 0.5 N NaCl, which are fairly close together, and close to the concentration at which all the systems are compared. Thus, although γ_{eq} in water is higher than those in 0.1 M NaCl and 0.5M NaCl, where again the values are close together, the P_{1S} values in water are considerably lower than the values in 0.1M NaCl and 0.5M NaCl.

In similar fashion, the P_{1S} value for DESS in 0.1 M NaCl is larger than in water because the C^*_{iS} value is 5 times smaller in 0.1 M NaCl than in water, and the increased γ_{eq} in water is not sufficient to compensate for this.

For compounds $C_{12}SO_4Na$, $C_{12}EOSNa$, $C_{12}EO_2SNa$, in water the C^*_{1S} value for $C_{12}SO_4Na$ is 2 - 3 times higher than those for the oxyethylenated compounds, which are fairly close together. This would make P_{1S} lower for the first compound. However, its γ_{eq} value is higher than those of the other two compounds which, again, are fairly close together. The combined result is that the P_{1S} values for all these compounds are fairly close together. Since they are all compared at a surfactant concentration considerably above their C^*_{1S} values, their P_{1S} values are high.

Regarding temperature effect, we expect that when values of C^*_{1S} for the same compound at different temperatures are close, then the P_{1S} will depend mainly on γ_{eq}. The values of γ_{eq} for DESS in water at the three temperatures

listed are close, consequently the P_{1s} values are very close; the value of γ_{eq} for $C_{12}EO8$ decreases with increase in temperature, consequently the P_{1s} value decreases with increase in temperature.

Table XIX

Effectiveness Percentage at 1 Second

System	Log C	γ_{1s} mN/m	γ_{eq} mN/m	Π_{1s} mN/m	P_{1s} (%)
in water					
$C_{12}EO4$	-4.20	69.5	28.6	2.2	5.8
$C_{12}EO7$	-4.20	65.2	35.4	6.4	18.6
$C_{12}EO8$	-4.20	64.4	37.9	7.9	22.3
$C_{12}EO10$	-4.20	64.2	40.3	7.0	24.6
in water					
$C_{12}SO_4Na$	-2.40	52.2	49.4	19.8	87.6
$C_{12}EOSNa$	-2.40	43.0	39.2	29.0	88.4
$C_{12}EO_2SNa$	-2.40	43.8	41.4	28.2	92.2
$C_{12}EOSNa$					
in water	-3.1	67.0	59.8	5.0	41.0
in 0.1 N NaCl	-3.1	41.1	33.6	31.2	79.8
in 0.5 N NaCl	-3.1	40.3	30.6	32.2	77.1

Table XIX (continued)

Effectiveness Percentage at 1 Second

System	Log C	γ_{1s} mN/m	γ_{eq} mN/m	Π_{1s} mN/m	P_{1s} (%)
in water $C_{12}EO_2SNa$					
in water	-3.1	64.8	56.1	7.2	45.3
in 0.1 N NaCl	-3.1	40.4	35.6	31.9	86.9
in 0.5 N NaCl	-3.1	42.3	32.9	30.2	76.7
**********					
DESS					
in water	-3.23	49.5	40.7	22.5	71.9
in 0.1 N NaCl	-3.23	28.2	26.7	44.1	97.4
**********					
DESS in water	-3.05				
10 ^{0}C		46.0	40.0	28.3	82.5
25 ^{0}C		43.6	38.0	28.4	83.5
45 ^{0}C		42.3	37.2	26.5	83.9
**********					
$C_{12}EO8$	-3.99				
10 ^{0}C		54.5	39.7	19.8	57.2
25 ^{0}C		55.0	35.2	27.0	46.2
45 ^{0}C		52.5	32.7	16.3	45.2

(5) Efficiency of 1-Second Surface Tension Reduction, $pC_{20\ (1s)}$

By analogy with equilibrium surface tension, we define the efficiency of 1-second surface tension reduction by a surfactant as the negative logarithm of the bulk phase molar concentration of surfactant required to depress the surface tension of the system by 20 mN/m in one second, and symbolize it $pC_{20(1s)}$. This is one approach to the question: what bulk phase concentration of surfactant is necessary to attain a significant reduction of the surface tension of the system in a short time?

Data are shown in Table XX and Figure 45 (a), where $pC_{20(1s)}$ values for 20 different systems, containing 6 different individual anionic surfactants, 5 different nonionic surfactants, and 2 zwitterionic surfactants are plotted against their respective equilibrium pC_{20} values. The function in Figure 45 (a) is polynomial. However, for convenience of application we use an approximate linear relationship to replace it, as shown in Figure 45 (b). The the best fitting equation by the computer is

$$pC_{20\ (1s)} = 1.12 + 0.52\ pC_{20\ (eq)} \qquad [V-2]$$

where $pC_{20\ (eq)}$ is the efficiency in equilibrium surface tension reduction.

Surfactants that are more efficient at reducing surface tension under equilibrium conditions are more efficient at reducing it in a short time. Thus, in pure water, nonionic surfactants are more efficient than zwitterionic which, in turn, are more efficient than ionic, surfactants with the same number of carbon atoms in their hydrophobic groups. Ionic surfactants are more efficient in

electrolyte solution than in pure water. Surfactants with the same hydrophilic head groups become more efficient when the alkyl chain of their hydrophobic group is lengthened, while polyoxyethylenated nonionics with the same hydrophobic group become less efficient with the number of oxyethylene units in the molecule is increased.

The difference, $\Delta pC_{20\ (eq)}$, between the equilibrium value, $pC_{20\ (eq)}$, and the 1-second efficiency value, $pC_{20\ (1s)}$ is listed in Table XX. In all cases, the 1-second efficiency is less than the equilibrium value. In addition, the difference between them increases with increase in the value of $pC_{20\ (eq)}$. Since the pC_{20} value is a measure of the tendency of the surfactant to adsorb at aqueous solution/air interface[127], i.e. its "surface activity", this means that the greater the surface activity of the surfactant, the more will its 1 second efficiency vary from its equilibrium efficiency.

Table XX

Relationship of Dynamic and Equilibrium Efficiency in Surface Tension Rreduction, $pC_{20(1s)}$ and $pC_{20(eq)}$

#	System	$pC_{20\ (1s)}$	$pC_{20(eq)}$	$\Delta pC_{20(eq)}$
1.	$C_{10}SO_3Na$ in water	1.64	1.685	0.045
2.	$C_{12}SO_3Na$ in water	2.30	2.36	0.06
3.	$C_{12}SO_4Na$ in water	2.39	2.48	0.09
4.	$C_{12}EOSNa$ in water	2.65	2.83	0.18
5.	$C_{12}EO_2SNa$ in water	2.76	2.92	0.16
6.	DESS in water	3.32	4.02	0.70
7.	$C_{10}SO_3Na$ in 0.1 N NaCl	2.21	2.28	0.67
8.	$C_{12}SO_3Na$ in 0.1 N NaCl	3.26	3.38	0.12
9.	$C_{12}EOSNa$ in 0.1 N NaCl	3.47	4.23	0.76
10.	$C_{12}EO_2SNa$ in 0.1 N NaCl	3.47	4.36	0.89
11.	DESS in 0.1 N NaCl	3.85	5.30	1.45
12.	$C_{12}EOSNa$ in 0.5 N NaCl	3.47	4.80	1.33
13.	$C_{12}EO_2SNa$ in 0.5 N NaCl	3.43	4.98	1.55
14.	C_8PY in water	2.88	3.13	0.25
15	$C_{10}PY$ in water	3.365	4.27	0.905
16.	$C_{12}EO7$ in water	3.78	5.26	1.48

Table XX (continued)

Relationship of Dynamic and Equilibrium Efficiency in Surface Tension Reduction, $pC_{20(1s)}$ and $pC_{20(eq)}$

#	System	$pC_{20\ (1s)}$	$pC_{20(eq)}$	$\Delta pC_{20(eq)}$
17.	$C_{12}EO8$ in water	3.81	5.20	1.39
18.	$C_{12}EO10$ in water	3.72	5.15	1.43
19.	$C_{10}BMG$ in water (pH =9)	2.97	3.46	0.49
20.	$C_{12}BMG$ in water(pH = 9)	3.54	4.45	0.91

$\Delta pC_{20(eq)} = pC_{20(eq)} - pC_{20(1s)}$

D. Parameters and Features of meso-equilbrium surface tension

(1) Meso-equilibrium Critical Reduction Concentration, C^*_m

As mentioned above, this is the minimum bulk phase molar surfactant concentration at which the surface tension shows little further change with increase either in time or in surfactant concentration. Table XXI lists values of C^*_m, the equilibrium CMC, and the ratio of C^*_m to the equilibrium CMC. The C^*_m values appear to parallel the equilibrium CMC value. Thus, C^*_m decreases with decrease in EO number for nonionics, with increase in electrolyte content for anionic surfactants, and with increase in hydrocarbon chain length, the same trends as shown for the equilibrium CMC. The value of the C^*_m/CMC ratio is 1-2.5 in all cases investigated, and it appears to decrease with increase in EO number in nonionics, with decrease in chain length in zwitterionics, and decrease in salt concentration for ionics, implying that the ratio is decreased by increase in the hydrophilic character of the surfactant. The ratio of C_{10}BMG is slightly higher than C_{12}BMG, which may be due to experimental error.

Table XXI

Parameters at Meso-equilibrium (1): C^*_m and C^*_m/CMC Ratio

Surfactant	$C^*_m \times 10^4$ mole/dm^3	CMC $\times 10^4$ mole/dm^3	C^*_m/ CMC
$C_{12}EO4$	0.87	0.645	1.35
$C_{12}EO7$	1.15	0.82	1.40
$C_{12}EO8$	1.29	1.09	1.18
$C_{12}EO10$	1.20	1.20	1.00
$C_{10}BMG$	56.2	45.7	1.23
$C_{12}BMG$	5.50	5.10	1.08
$C_{14}BMG$	> 1.00	0.61	> 1.64
$C_{12}SO_4Na$ in water	95.5	79.4	1.20
$C_{12}EOSNa$ in water	43.7	39.1	1.12
$C_{12}EOSNa$ in 0.1 N NaCl	7.20	4.30	1.67
$C_{12}EOSNa$ in 0.5 N NaCl	3.20	1.30	2.46
$C_{12}EO_2SNa$ in water	31.6	28.8	1.10
$C_{12}EO_2SNa$ in 0.1 N NaCl	3.50	2.90	1.20
$C_{12}EO_2SNa$ in 0.5 N NaCl	1.45	1.00	1.45
$C_{10}SNa$ in water	436.5	427	1.02
$C_{10}SNa$ in 0.1 N NaCl	219	211	1.04

Table XXI (continued)

Parameters at Meso-equilibrium (1): C^{*}_{m} and C^{*}_{m}/CMC Ratio

Surfactant	$C^{*}_{m} \times 10^{4}$ mole/dm^3	CMC x 10^4 mole/dm^3	C^{*}_{m}/ CMC
DESS in water	20.0	20.0	1.00
DESS in 0.1 N NaCl	3.47	3.47	1.00

(2) Meso-equilibrium time

This addresses the question of what time is needed to achieve a significant reduction of the surface tension at a particular bulk phase concentration of surfactant. The time needed is greatly dependent upon the bulk phase concentration of surfactant. Consquently, the reference bulk phase surfactant chosen here is C^*_m, rather than a fixed surfactant concentration. This yields t^*_m as the minimum time required (for a particular surfactant under given molecular environmental conditions) to obtain a surface tension value (γ^*_m) that does not change much with increase in the surfactant concentration. The t^*_m values were obtained from a plot of γ_t versus log t at fixed surfactant concentration, C^*_m, or by interpolation of the linear plot of log t^* versus log C.

Table XXII lists the values of meso-equilibrium time, t^*_m, in three groups. For the systems studied, it is apparent from the data that, in general, the larger the value of C^*_m, the smaller the value of t_m. Quantitatively, Fgure 46 shows the approximate linear relationships between log t^*_m and log C^*_m: the top line in Figure 46 is for the compounds in the group 1 in Table XXII, the lower line is for the compounds in the group 2 in Table XXII. The linear equations are as follows:

$$\log t^*_m = -6.09 - 2.04 \log C^*_m \quad \text{(group 1)} \qquad [V-3]$$

$$\log t^*_m = -6.21 - 1.88 \log C^*_m \quad \text{(group 2)} \qquad [V-4]$$

Since the values of C^*_m in group 3 are much higher than that for the compounds in the groups 1 and 2, the values of t^*_m fall in the range of less than

0.1 second. Because of experimental limitation, more exact data could not be obtained.

Table XXII also lists the equilibrium maximum surface excess concentration, $\Gamma_{max.}$ The data indicate that compounds with values of Γ_{max} less than 3.1 X 10^{-10} mole/dm^3 fall on the lower line in Figure 46, while compounds with values of Γ_{max} greater than 3.5 X 10^{-10} mole/dm^3 fall on the upper line in Figure 46. That is, compounds with lower values of Γ_{max} show shorter meso-equilibrium times than that do compounds with higher values of Γ_{max} at the same C^*_m. The two lines also distinguish compounds of higher surface activity (upper line) from those of lower surface activity (lower line) in each surfactant class of surfactants studied. This may provide an explanation for the repeated above observation that more surface-active materials deviate more from equilibrium behavior in their dynamic behavior than do less surface-active ones. Compounds having higher equilibrium surface excess concentrations may need more time to reach these concentrations (and to exhibit equilibrium properties) than those with lower equilibrium concentrations. Since meso-equilibrium parallels equilibrium, the same may be true for meso-equilibrium behavior. The third group of compounds in Table XXII are the least surface-active and have such high C^*_m values that t^*_m is less than 1 second.

Table XXII

Parameters at Meso-equilibrium (2): Meso-equilibrium Time, t_m

Surfactant	Log C^*_m (in mole/dm^3)	t^*_m (Second)	Log t^*_m	Γ_{max} X 10^{10} (mole/cm^2)
$C_{12}EO4$	-4.060	182	2.26	3.61
$C_{12}EOSNa$				
in 0.1 N NaCl	-3.143	2.3	0.36	3.81
in 0.5 N naCl	-3.495	12.1	1.08	4.41
$C_{12}EO_2SNa$				
in 0.1 N NaCl	-3.456	6.9	0.84	3.46
in 0.5 N NaCl	-3.839	54.3	1.73	3.78
$C_{14}BMG$ (pH 9)	>-4	< 100	< 2	4.22
**********				
$C_{12}EO7$	-3.940	20.0	1.30	2.90
$C_{12}EO8$	-3.759	8.71	0.94	2.52
$C_{12}EO10$	-3.640	19.3	1.285	2.11
$C_{12}BMG$ (pH 9)	-3.260	1.2	0.079	3.07
DESS in 0.1 N NaCl	-3.460	1.2	0.079	2.34

Table XXII

Parameters at Meso-equilibrium (2): Meso-equilibrium Time, t_m

Surfactant	Log C^*_m (in mole/dm^3)	t_m (Second)	Log t_m	Γ_{max} X 10^{10} (mole/cm^2)
$C_{12}SO_4Na$ in water	-2.020	< 0.1	< -1	
$C_{12}EOSNa$ in water	-2.360	< 0.1	< -1	
$C_{12}EO_2SNa$ in water	-2.500	< 0.1	< -1	
DESS in water	-2.700	< 0.1	< -1	

(3) Effectiveness of Surface Tension Reduction, Π^*_m

Since the meso-equilibrium surface tension at the discontinuity in the γ_m versus log C plot (C^*_m) changes only gradually both with time and with surfactant concentration, we can use the reduction of the surface tension of the solvent, or surface pressure, Π^*_m ($= \gamma_0 - \gamma^*_m$), achieved at this point as a measure of the effectiveness of dynamic surface tension reduction, by analogy with the effectiveness of equilibrium surface tension reduction, Π_{cmc}, the surface pressure at the discontinuity in the plot of equilibrium surface tension versus the log C (i.e., at the CMC). Table XXIII shows a comparison of dynamic and equilibrium effectivenesses.

In general, effectiveness of dynamic surface tension reduction appears to parallel effectiveness of equilibrium surface tension reduction. Figure 47 shows an approximately linear relationship between them. The linear equation is as follows:

$$\Pi^*_m = -1.78 + 1.015\ \Pi^*_{cmc}. \qquad [V-5]$$

In Table XXIII, the value of $\Delta\Pi^*$ ($= \Pi^*_m - \Pi_{cmc}$) falls in the range of 0 to -3.8 mN/m, i.e. Π^*_m is equal or somewhat smaller than Π_{cmc}. It appears that the absolute value of $\Delta\Pi^*_m$ increases with increase in molecular weight in the same chemical family under same molecular environmental condition, and increase with increase in NaCl concentration for most of the ionics in Table XXIII.

These results may account for the fact that the performance of surfactants in some dynamic phenomena often can be predicted successfully from the equilibrium surface values, especially if the surfactant concentration is not too

low. Thus, in Ross-Miles foaming, the initial foam height obtained in many cases correlates well[121] with the equilibrium surface tension of the surfactant solution. The lower the equilibrium surface tension, the higher the initial foam height. The test is conducted at a surfactant concentration of 1-2.5 g/l, equivalent to 2-12.5 X 10^{-3} mole/dm^3 for surfactants of 200 - 500 molecular weight. This concentration range is above the CMC value of many surfactants and, consequently, the C^*_{1s} value (Table XVI) is exceeded. This means that a surface tension value close to the equilibrium value will be obtained in less than 1 second. For small molecules with high CMC values, on the other hand, the C^*_{1s} value may possibly not be exceeded. However, when the molar concentration is above10^{-2}, the t^*_m value is probably less than one second (Table XXII) and γ_{1s} is close to γ_{eq} (Table XVIII). Thus, under the conditions of the test, in most cases the surface tension of the surfactant solution during the foaming process is probably close to its equilibrium value.

Table XXIII

Effectiveness of Dynamic Surface Tension at C^*_m

Surfactant	Π^*_m mN/m	Π_{cmc} mN/m	$\Delta\Pi^*$ mN/m
$C_{12}EO4$	43.4	43.4	0
$C_{12}EO7$	36.0	38.4	-2.4
$C_{12}EO8$	34.4	37.4	-3.0
$C_{12}EO10$	31.2	35.0	-3.8
$C_{12}SO_4Na$ in water	32.3	32.4	0
$C_{12}EOSNa$ in water	32.8	32.8	0
$C_{12}EO_2SNa$ in water	29.2	30.6	-1.4
$C_{12}EOSNa$ in 0.1 N NaCl	38.5	38.5	0
$C_{12}EO_2SNa$ in 0.1 N NaCl	35.7	36.7	-1.0
$C_{12}EOSNa$ in 0.5 N NaCl	41.7	42.3	-0.6
$C_{12}EO_2SNa$ in 0.5 N NaCl	37.9	40.0	-2.1
$C_{10}SNa$ in water	30.5	31.0	-0.5
$C_{10}SNa$ in 0.1 N NaCl	31.1	32.6	-1.5
DESS in water	40.9	42.3	-1.4
DESS in 0.1 N NaCl	46.1	46.8	-0.7
C_{10}BMG (pH 9)	37.2	38.2	-1.0
C_{12}BMG (pH 9)	37.0	39.2	-2.2

$\Delta\Pi^*_m = \Pi^*_m - \Pi^*_{cmc}$

(4) Effectiveness Percentage at Meso-equilibrium, P_m

Table XXIV portrays the concentration effect on the effectiveness percentage at meso-equilibrium, P_m for systems $C_{12}EO7$, $C_{12}BMG$, $C_{12}EO_2SNa$ in water and in 0.1 N NaCl. The data indicate that (i) the meso-equilibrium states at the concentrations investigated are close to the equilibrium, as shown by the high values of P_m; (ii) the value of P_m increases with increase in the surfactant concentration in the range investigated and at high concentration reaches 100%, which is an indication of the equilibrium state (Small variations in the P_m value are due to experimental error.) .

Table XXIV

Effectiveness Percentage at Meso-equilibrium: Concentration Effect

System	Log C	γ_m mN/m	Π_m mN/m	γ_{eq} mN/m	P_m (%)
$C_{12}EO7$					
	-4.536	45.1	26.9	41.0	86.8
	-4.235	39.3	32.7	36.0	90.8
	-3.986	36.9	35.1	33.6	91.4
	-3.536	36.1	35.9	33.6	93.5
	-3.277	35.7	36.3	33.6	94.5
	-2.944	35.0	37.0	33.6	96.4
	-2.608	34.4	37.6	33.6	97.9
	-2.424	34.4	37.6	33.6	97.9
$C_{12}BMG$ in water (pH 9)					
	-4.108	48.4	23.6	46.6	92.9
	-3.826	44.8	27.2	41.9	90.4
	-3.701	41.9	30.1	39.8	93.5
	-3.525	39.9	32.1	36.8	91.2
	-3.410	37.3	34.7	34.9	93.5

Table XXIV (continued)

Effectiveness Percentage at Meso-equilibrium: Concentration Effect

System	Log C	γ_m mN/m	Π_m mN/m	γ_{eq} mN/m	P_m (%)
	-3.244	34.8	37.2	32.8	94.9
	-2.992	34.6	37.4	32.8	95.4
	-2.792	33.9	38.1	32.8	97.2
	-2.419	32.9	39.1	32.8	99.7
$C_{12}EOSNa$					
in water					
	-2.731	54.0	18.0	49.4	79.6
	-2.607	48.6	23.4	45.3	87.6
	-2.430	41.5	30.5	39.8	94.7
	-2.270	41.5	30.5	39.2	93.0
	-2.174	39.8	32.2	39.2	98.2
	-2.094	39.1	32.9	39.2	~100
	-1.794	39.1	32.9	39.2	~100

Table XXIV (continued)

Effectiveness Percentage at Meso-equilibrium: Concentration Effect

System	Log C	γ_m mN/m	Π_m mN/m	γ_{eq} mN/m	P_m (%)
$C_{12}EOSNa$ in 0.1 N NaCl					
	-3.713	46.7	25.6	41.8	83.9
	-3.527	43.4	28.9	37.6	83.3
	-3.430	40.9	31.4	35.3	84.9
	-3.305	35.5	36.8	33.7	95.3
	-3.129	36.3	36.0	33.7	93.3
	-2.828	34.2	38.1	33.7	98.7
	-2.420	34.2	38.1	33.7	98.7
	-1.793	33.0	39.3	33.7	~100

E. Induction Time

Chapter III has shown that there always exists an induction time before the surface tension of a solution of surfactant shows a significant decrease with time. We have defined the induction time, t_i, as the time for the reduction of the surface tension to be 1/11 of its value at meso-equilibrium, i.e., $(\gamma_o - \gamma_t) / (\gamma_t - \gamma_m) = 1/10$, where γ_o is the surface tension of the pure solvent, γ_t, the surface tension at time t, and γ_m, the surface tension at meso-equilibrium.

Figures 48 and 49 show that the induction time changes both with the structure of the surfactant and with the molar concentration of the surfactant in the solution. This raises the questions: (i) Why does the induction time change with the structure of a surfactant? (ii) What is the relationship between induction time and surfactant concentration?

(1) A Simplified Picture of Dynamic Surface Adsorption

Surfactant molecules begin to move from the bulk phase to the freshly formed surface at time 0, the time needed to arrive at the surface being dependent on (i) the speed of diffusion from the bulk phase to the sub-surface, which is a layer just below the surface; (ii) the distance from the bulk phase to the sub-surface; (iii) the energy barrier for surface adsorption from the sub-surface to the surfacce.

(2) Semi-quantitative Criterion for Determing the Mechanism of Dynamic Surface Adsorption

In Chapter IV we suggested a parameter, t^*/ t_2, to measure the mechanisms involved in dynamic surface adsorption. The parameter, t^*, is a measure of the relaxation time for diffusion in the bulk phase and t_2 is a measure of the relaxation time for transfer from the sub-surface to the surface. A larger ratio indicates that the diffusion process is slower than the other, the smaller ratio indicates that the transfer mechanism plays a significant part. In the chemical literature[69,115], the dynamic adsorption of $C_{12}EO7$ or $C_{12}EO8$ is considered to be a diffusion-controlled process, the t^*/ t_2 value for which is about 22 according to our work. Hence, if t^*/ t_2 is 22 or more, the mechanism is considered to be completely diffusion-controlled; on the other hand, the dynamic adsorption of 1,9-nonanediol is considered[80,81] to occur by a mixed mechanism of diffusion in the bulk phase and transfer to the surface, the t^*/ t_2 value of which we have found to be about 4.

(3) Mean Distance from Bulk Phase to Surface

Addison[3] suggested a treatment to elucidate the surface tension change with time, in which he supposed that the surfactant molecules at a surface of unit cross-sectional area were drawn from a disc of unit cross-sectional area placed with one face in the surface. He then calculated the thickness of this disc, which we designate as mean distance, d, from the bulk phase to the surface, as follows

$$d = \frac{\Gamma_{eq}}{C} \qquad [V-6]$$

where Γ_{eq} is the equilibrium surface excess concentration (approximately equal to the surface concentration) in mole/cm^2, C is the surfactant concentration in the bulk phase in mole/cm^3. Obviously, parameter, d, changes with C and Γ_{eq}. At a fixed surfactant concentration, the value of d is proportional to Γ_{eq}. Addison's concept of d as the mean distance from the bulk phase to the surface provides a visual picture of the dynamic adsorption process.

(4) Induction Time

Table XXV lists factors affecting the induction time. To permit comparison, we have arranged the data in four groups and set the surfactant concentration at 7.9×10^{-8} mole/ cm^3, where Γ_{eq} is a maximum in all cases from the plot of γ_{eq} -log C. Values of the maximum surface excess, Γ_{max}, are listed in Table XXV, together with values of d calculated from Γ_{max} by use of equation V-6.

For the group of n-dodecyl ethers of polyoxyethylenated alcohols, the diffusion coefficient, D, may decrease slightly from $C_{12}EO4$ to $C_{12}EO10$. However, no great difference is expected between them because the diffusion coefficient depends mainly upon the average radius of the surfactant molecule and the polyoxyethylene chain is believed to be coiled in aqueous solution, hence the length of the hydrocarbon controls the radius of the molecule and all of the compounds in the first group have the same carbon chain length. $C_{12}EO4$ has the

longest induction time for two reasons: (i) it has the largest mean distance, d, from the bulk phase to the surface (Table XXV); (ii) the average value t^*/t_2 is lower than for the other members (Tablel XXV), indicating that some mechanism other than diffusion, possibly an energy barrier to adsorption, is significant in this case and increases the value of t_i. The induction time decreases from $C_{12}EO7$ to $C_{12}EO10$ in Table XXV because the mean distance, d, decreases and t^*/t_2 increases in that direction.

The second and third groups in Table XXV compare the sodium salts of sulfated n-dodecyl ethers of polyoxyethylenated alcohol in 0.1 N and in 0.5 N NaCl. The diffusion coefficients, D, are all fairly close. The induction time in 0.5 N NaCl is longer than in 0.1 N NaCl for two reasons: (i) a larger mean distance, d, from the bulk phase to the surface and (ii) a smaller average value t^*/t_2 in 0.5 N NaCl (overcoming an energy barrier is more significant in 0.5 N NaCl than in 0.1 N NaCl).

The last group in Table XXV is a comparison of C_{12}- and C_{14}-N-alkyl-N-benzyl-N-methylglycines. The C_{14}- compound has a longer induction time than the C_{12}- because of three reasons: (i) a smaller diffusion coefficient; (ii) a larger mean distance, d; (iii) a smaller t^*/t_2 value.

Table XXV

Factors Affecting Induction Time (C = 7.9×10^{-8} mole/cm3)

System	Γ_{max} x 10^{10} mole / cm^2	d x 10^3 cm	Average t^* / t_2	Relative Order of D	t_i sec.
$C_{12}EO4$	3.61	4.57	17.7	largest	2.2
$C_{12}EO7$	2.90	3.67	20.8		0.29
$C_{12}EO8$	2.52	3.19	22.4		0.19
$C_{12}EO10$	2.11	2.67	31.7	smallest	0.13
$C_{12}EOSNa$ in 0.1 N NaCl	3.81	4.82	23.6	close to each	0.88
$C_{12}EOSNa$ in 0.5 N NaCl	4.41	5.58	15.7	other	1.8
$C_{12}EO_2SNa$ in 0.1 N NaCl	3.46	4.38	23.9	close to each	0.51
$C_{12}EO_2SNa$ in 0.5 N NaCl	3.78	4.78	18.2	other	1.6
$C_{12}BMG$	3.07	3.89	11.5	larger	1.3
$C_{14}BMG$	4.22	5.34	7.5	smaller	4.7

(6) Relationship of Induction Time (t_i) to Bulk Phase Surfactant Molar Concentration (C)

For diffusion-controlled surface adsorption, at very short surface age, the simplified Ward and Tordai equation can be used.

$$\log t_i = \log \frac{(\Gamma_t)^2 \pi \times 10^6}{4D} - 2 \log C \qquad [V\text{-}7]$$

where Γ_t is the surface adsorption excess (approximately equal to surface concentration) at time t_i, D is the bulk phase diffusion coefficient, C is the bulk phase surfactant concentration in mole/dm^3. Plots of log t_i to log C should be linear with a slope of 2 for a diffusion-controlled adsorption. Figures 50 - 57 show the plots of log t_i to log C for ten systems, they are all linear. The slopes are -1.96 and -1.75 for $C_{12}EOSNa$ in 0.1 N NaCl and 0.5 N NaCl, respectively; -2.11 and -1.75 for $C_{12}EO_2SNa$ in 0.1 N NaCl and 0.5 N NaCl, respectively; -1.64 for DESS in 0.1 N NaCl; -1.44, -1.73, -1.44, and -2.06 for the nonionics ($C_{12}EO4$, $C_{12}EO7$, $C_{12}EO8$, and $C_{12}EO10$) in water, respectively; and -1.88 for $C_{12}BMG$ in water (pH 9). The values of the slopes for the systems fall between -1.4 to -2.1, this is because some of systems are not completely diffusion-controlled ($C_{12}EO4$, DESS in 0.1 N NaCl, $C_{12}EOSNa$ and $C_{12}EO_2SNa$ in 0.5 N NaCl, and $C_{12}BMG$), and also because of experimental error (The adsorption process for $C_{12}EO8$ is diffusion-controlled, but the slope of the plot is -1.44). Nevertheless a linear plot of log t_i versus log C with a slope near 2 gives a convenient estimation for applications.

F. An example of Application: Relationship of Dynamic Surface Tension to Wetting Time

Wetting on cotton skeins is considered as a fast process. We have tried to relate the wetting out times (WOT) to the dynamic surface tension of both highly purified and industrial surfactants. The Draves-Clarkson Sinking Test, as described in Chapter II, was used in this work. The systems investigated were 14 nonionics and 1 zwitterionic in distilled water and 7 anionics in 0.1 N NaCl. The nonionics were t-octylphenol, nonylphenol, and C_{12-14} alcohols oxyethylenated with 7 to 12.5 moles of ethylene oxide and included both pure, homogeneous compounds and commercial materials; n-octyl-2-pyrrolidone; dodecyl oxyethylenated mercaptan; and methoxy terminated etheroxylated silicones. The anionics included such commmercial materials as the sodium salts of linear dodecylbezenesulfonate, di-(2-ethylhexyl) sulfosuccinate, sulfated oxyethylenated C_{12} - C_{14} alcohol, secondary C_{12} and C_{14} alkanesulfonates, and two isomeric sodium salts of sulfated oxyethylenated branched C_{16} alcohols with 5 oxyethylene units.

Log WOT versus dynamic surface tension at 0.4 second, 1 second, and 10 seconds for 23 surfactants at 71 concentrations, along with the plots of log WOT versus γ_{eq} are shown in Figure 58 -61 with data listed in Table XXVI. There appears to be no correlation between wetting out time and equilibrium surface tension, but a fairly good correlation between the log of WOT and dynamic surface tension at 1 second. The linearities of log WOT versus $\gamma_{0.4\ sec}$ and $\gamma_{10\ sec}$ are not

as good as versus γ_{1s}.

Thus, in some dynamic interfacial phenomena, such as high speed wetting, data at short surface age (for example, 1 second) rather than equilibrium data are better able to predict perfomance.

From the Figure 59, it appears that for a wetting time of 25 seconds or less, the value of γ_{1s} should be 40 mN/m or less; for 10 seconds or less, 35 mN/m or less.

The Draves wetting test is commonly conducted at a concentration of 1.0 g/l. For surfactants with molecular weight of 200-500, this corresponds to a concentration of 2-5 $x10^{-3}$ mole/dm^3. For materials with CMC values below 5 x 10^{-4} mole/dm^3, this test concentration is considerably above their C^*_{1s} value and consequently γ_{1s} is close to the minimum γ_{eq} value (at or above the CMC of the surfactant). The minimum γ_{eq} value of the surfactant will therefore determine the wetting time.

For surfactants with CMC values above the (2-5 x 10^{-3} mole/dm^3) concentration at which the test is conducted, the γ_{1s} value will be not only above their minimum γ_{eq} value (at or above the CMC of the surfactant) but also significantly above the γ_{eq} value for the surfactant at the test concentration. Consequently, these surfactants will show high wetting time in the test, even if they reduce the surface tension to low values above their CMC.

Table XXVI

Wetting and Surface Tension

Surfactant	C (g/1)	Log WOT	γ_{1sec} mN/m	γ_{eq} mN/m
$C_{12}EO7$	1.00	0.77	36.2	33.6
	0.50	1.23	38.2	33.6
	0.25	1.68	42.4	33.6
$C_{12}EO8$	1.00	0.92	40.1	34.6
	0.50	1.30	41.6	34.6
	0.25	1.72	43.0	34.6
CO720	1.00	1.36	38.4	33.2
	0.50	1.81	42.2	33.2
	0.25	2.33	47.5	33.0
CO630	1.00	0.98	35.4	31.3
	0.50	1.50	38.7	31.3
	0.25	2.07	44.6	31.3
CA620	1.00	1.07	35.0	29.4
	0.50	1.47	36.0	29.3
	0.25	1.89	40.9	29.2
CA630	1.00	0.97	35.5	---
	0.50	1.41	38.8	30.4

Table XXVI (continued)

Wetting and Surface Tension

Surfactant	C (g/1)	Log WOT	γ_{1sec} mN/m	γ_{eq} mN/m
	0.38	1.62	40.1	30.2
	0.25	2.13	44.3	29.3
CA720	1.00	1.26	39.2	33.4
	0.50	1.76	48.0	32.7
	0.25	2.75	48.0	31.2
$C_{14}EO9$	1.00	1.78	43.4	37.0
	0.75	1.84	45.0	37.0
	0.50	2.02	46.7	37.0
	0.25	2.81	52.9	37.0
LAS(0.1 N NaCl)	1.00	0.90	35.1	30.2
	0.50	1.23	37.8	30.2
	0.25	1.77	40.3	30.6
N25(0.1 N NaCl)	1.00	1.32	38.2	32.4
	0.50	1.69	41.5	32.4
	0.25	2.10	45.3	32.7
$C_{12}SAS$(0.1 N NaCl)	1.00	1.96	41.2	31.0
	1.50	0.97	37.8	30.6

Table XXVI (continued)

Wetting and Surface Tension

Surfactant	C (g/l)	Log WOT	γ_{1sec} mN/m	γ_{eq} mN/m
	2.00	0.59	35.1	31.5
C_{14}SAS(0.1 N NaCl)	0.49	0.86	34.7	31.2
	0.25	1.81	38.2	31.6
DESS (0.1 N NaCl)	1.00	0.48	28.0	25.7
	0.50	0.72	29.3	25.8
	0.25	1.06	31.7	25.8
	0.09	2.46	45.5	28.6
$C_{16}LGSO_4Na$	1.00	1.09	38.2	30.2
(0.1 N NaCl)	0.50	1.41	43.9	30.2
	0.25	1.79	52.3	30.2
$C_{16}BGSO_4Na$	1.00	0.84	32.2	28.6
(0.1 N NaCl)	0.50	1.16	35.9	28.6
	0.25	1.60	43.1	28.6
CDMB	1.50	1.59	38.0	32.7
	1.00	1.73	39.4	32.6
	0.50	1.96	42.2	32.0
S-260	1.00	1.11	36.7	28.6
	0.50	1.43	38.5	28.6

Table XXVI (continued)

Wetting and Surface Tension

Surfactant	C (g/1)	Log WOT	γ_{1sec} mN/m	γ_{eq} mN/m
	0.25	1.91	43.3	28.6
S-SK	1.00	0.87	32.7	29.4
	0.50	1.38	37.3	29.1
	0.25	2.01	42.2	29.4
S-218	1.00	0.91	34.2	30.4
	0.50	1.53	37.1	30.3
	0.25	2.39	44.0	30.3
L7600	1.00	2.38	47.9	25.1
	0.50	2.80	55.3	26.0
	0.25	3.32	60.4	26.4
L7607	1.00	1.52	37.8	23.4
	0.50	2.08	44.9	23.8
	0.25	3.11	52.9	24.2
TMN-6	1.00	0.68	31.1	26.8
	0.50	1.29	34.6	27.8
	0.25	2.56	42.7	28.6

Table XXVI (continued)

Wetting and Surface Tension

Surfactant	C (g/1)	Log WOT	γ_{1sec} mN/m	γ_{eq} mN/m
C_8PY	1.00	0.54	33.1	30.8
	0.75	1.24	38.4	34.1
	0.50	2.67	44.0	38.7

Legend of Figures

Figure 1 (a) Block diagram of maximum bubble pressure apparatus.

1. N_2 gas cylinder regulator; 2. Capillary for stabilizing gas flow; 3. Flow control meter; 4. Sample beaker and capillary; 5. Gas pressure transducer; 6. Computer; 7. Printer.

Figure 1 (b) Computer printout of signal from transducer.

Figure 2. Calibration curve of transducer: voltage to pressure.

Figure 3. Calibration curve: voltage to surface tension.

Radius of the capillaries : (1) ⊡ 0.088 mm, (2) ◆ 0.135 mm, (3) ■ 0.238 mm, (4) ◇ 0.318 mm.

Figure 4. Reproducibility of dynamic surface tension data.

(a) γ_t vs. log t curve for aqueous 5.844 x 10^{-4} mole/dm^3 solution of DESS in water at 25 ^{0}C. The symbols, ◆ + ⊡, represent the data measured on three consecutive days.

(b) γ_t vs. log t curve for aqueous solution of C_{12}SNa at 25 ^{0}C at concentration: 3.012 x 10^{-3} mole/dm^3, measured on two consecutive days (⊡ ◆); 6.024 x10^{-3} mole/dm^3, measured on two consecutive days (◇ ■).

(c) γ_t vs. log t curve for aqueous 6.58 x 10^{-3} mole/dm^3 solution (pH 9) of C_{14}BMG , measured by use of two capillaries. Radius of capillaries: ⊡ 0.24 mm; ◆ 0.32 mm.

Figure 5. Convergence of dynamic surface tension values to that of the solvent. ⊡ C_{12}EO4 in water (1.94 x 10^{-5} mole/dm^3), ◆ C_{12}EO4 in water (3.24 x 10^{-5} mole/dm^3), ◇ C_{12}PY in water

(9.59×10^{-5} mole/dm^3), ⊡ $C_{12}EOSNa$ in 0.5 N NaCl (5.99×10^{-5} mole/dm^3), X $C_{12}EO_2SNa$ in 0.5 N NaCl (4.11×10^{-5} mole/dm^3).

Figure 6. Comparison between dynamic surface tension measured by the maximum bubble pressure approach and the equilibrium data measured by the Wilhelmy plate method.

(a) ⊡ C_8PY in water (6.53×10^{-3} mole/dm^3), ◆ $C_{10}SNa$ in 0.1 N NaCl (6.35×10^{-3} mole/dm^3), ■ $C_{10}SNa$ in 0.1 N NaCl (1.60×10^{-2} mole/dm^3). Numbers in parentheses are the equilibrium surface tension values.

(b) ⊡ DESS in 0.1 N NaCl (1.15×10^{-2} mole/dm^3), ◆ $C_{12}BMG$ in water, pH 9 (3.23×10^{-3} mole/dm^3), ■ $C_{12}SO_4Na$ in water (5.06×10^{-2} mole/dm^3), ◇ $C_{12}EO_2SNa$ in 0.5 N NaCl (9.00×10^{-3} mole/dm^3).

Numbers in parentheses are the equilibrium surface tension values.

Figure 7. Generalized dynamic surface tension, γ_t, vs. log time, t, curve - Region I: induction; Region II: rapid fall; Region III: meso-equilibrium; Region IV: equilibrium.

Figure 8. Diagram illustrating relationship of $(\gamma_0 - \gamma_t)$ to $(\gamma_0 - \gamma_m)$.

Figure 9. Model curve of equation III-1.

(a) For n =2, $t^* = 0.67$ s, $(\gamma_0 - \gamma_m)$ equals (I) 10.0 mN/m, (II) 19.4 mN/m, (III) 38.8 mN/m.

(b) For n =2, $(\gamma_0 - \gamma_m) = 19.4$ mN/m, t^* equals (I) 0.67 s, (II)

0.33 s, (III) 0.23 s.

(c) For $(\gamma_0 - \gamma_m)$ = 19.4 mN/m, (I) t^* = 0.67 s, n =2, (II) t^* = 0.33 s, n =1, (III) t^* =0.23 s, n = 0.5.

Figure10. An example of the validity of equation III-1 and III-6.

(a) γ_t vs. log t curve for aqueous solution (pH 9) of C_{12}BMG in log C ⊡ -2.992, ⊙ -3.224, ◈ -3.410, △ -3.525, ● -3.701, ⌀ -3.826, ◆ -4.108. Solid lines calculated by equation III-1 using constants from Table IX .

(b) log $(\gamma_0 - \gamma_t)/(\gamma_t - \gamma_m)$ vs. log t, log C in water equals ⊡ -2.992, ⊙ -3.224, ◈ -3.410, ● -3.525, △ -3.701, ⌀ -3.826, ◆ -4.108. Solid lines are drawn using least squares constants from Table IX.

Figure 11. Typical plot of γ_t vs. log C at constant times, together with γ_{eq} vs. log C for C_{12}EO8 in water, 25 ^{0}C. Fixed time: (1) 0.32 s, (2) 1.00 s, (3) 3.16 s, (4) 10.0 s, (5) 20.0 s, (6) 31.6 s, (7) 100 s.

Figure 12. Relationship of log f^* and log ω_0 to log C. ▲ Systems C_{12}EO7, C_{12}EO8, and C_{12}EO10 in present work, ⊡ Systems C_{12}EO6, C_{14}EO6 in reference 121.

Figure 13. Relationship of surface elasticity to surfactant concentration, C for C_{12}EO4. The insert figure is for C_{12}EO3 in reference 122.

Figure14. Maximum surface elasticity vs. surfactant concentration, C, in mole/dm^3, for nonionics C_{12}EOX.

Figure 15. Maximum surface elasticity vs. surfactant concentration, C, in

versus log C for $C_{12}EOSNa$ in water (⊡), in 0.1 N NaCl (◆), and in 0.5 N NaCl (+).

Figure 41. Effect of electrolyte on dynamic surface tension at 1 second, γ_{1s}, versus log C for $C_{12}EO_2SNa$ in water (⊡), in 0.1 N NaCl (◆), and in 0.5 N NaCl (+).

Figure 42. Effect of dodecyl alcohol on the dynamic surface tension of $C_{12}SO4Na$ in water. Molar ratio of alcohol / surfactant = 1: 10.
(a) ◆ γ_{1s} versus log C for the mixture of $C_{12}SO_4Na$ and $C_{12}OH$, together with ⊡ γ_{eq} versus log C;
(b) ◆ γ_{10s} versus log C for the mixture of $C_{12}SO_4Na$ and $C_{12}OH$, together with ⊡ γ_{eq} versus log C.

Figure 43. Effect of EO number on dynamic surface tension at 1 second for $C_{12}EOX$: ◇ $C_{12}EO4$, ■ $C_{12}EO7$, ⊡ $C_{12}EO8$, ◆ $C_{12}EO10$.

Figure 44. Effect of EO number on dynamic surface tension at 1 second for $C_{12}EOxSNa$ in 0.1 N NaCl: ⊡ x=1, ◆ x=2.

Figure 45 (a) Relationship of pC_{20} (1s) to pC_{20} (eq), curve-fitting.

Figure 45 (b) Relationship of pC_{20} (1s) to $pC_{20(eq)}$, linear line-fitting.

Figure 46. Relationship of log of meso-equilibrium time at C^*_m, t^*_m, to log of surfactant concentration, C in mole/dm^3.

Figure 47. Maximum surface pressure at meso-equilibrium versus maximum equilibrium surface pressure.

Figure 48. Structural effect on induction time: surface tension at time, t, versus log t (in second) for $C_{12}EO4$ and $C_{12}EO8$ at log C, -4.2.

Figure 49. Concentration effect on induction time: surface tension at time, t,

Figure 1 (a)

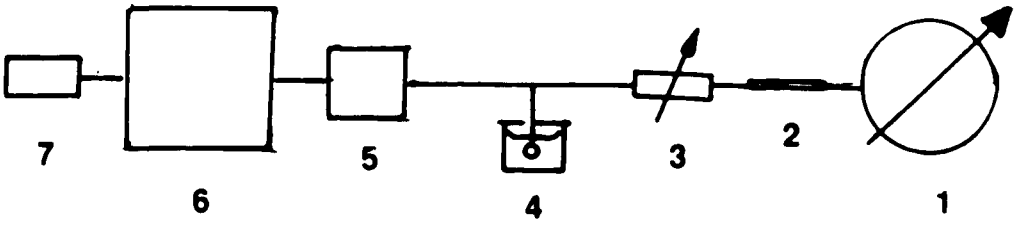

Figure 1 (b)

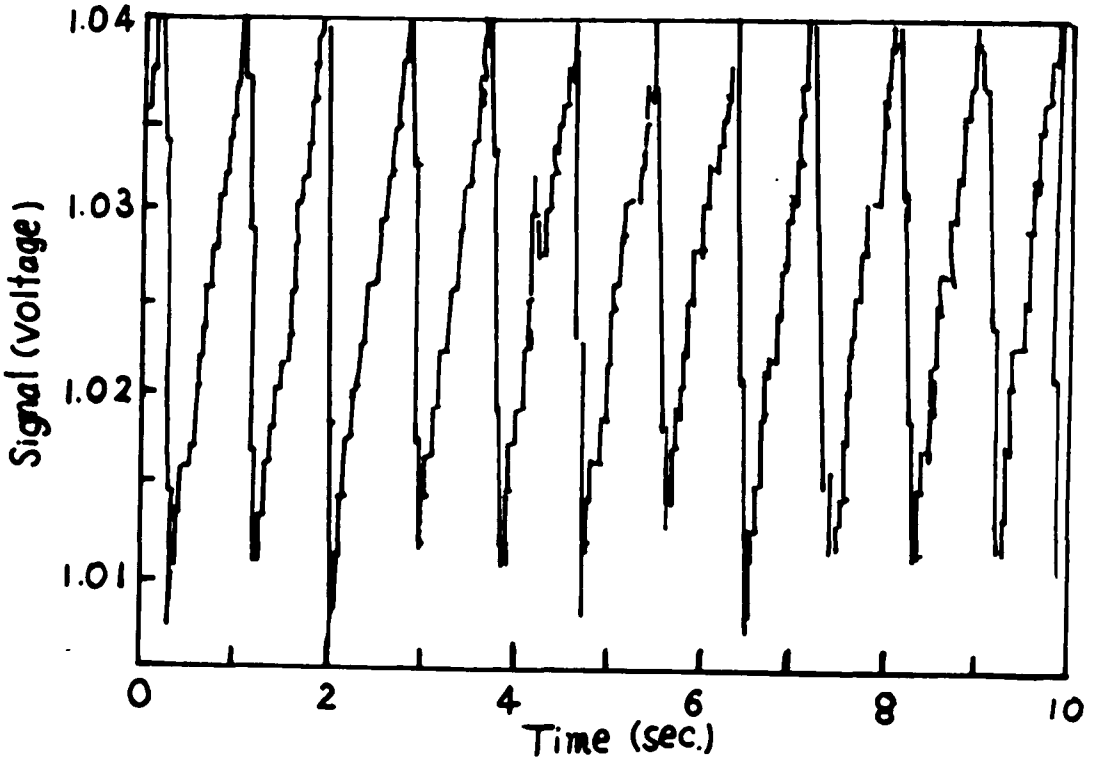

Figure 2

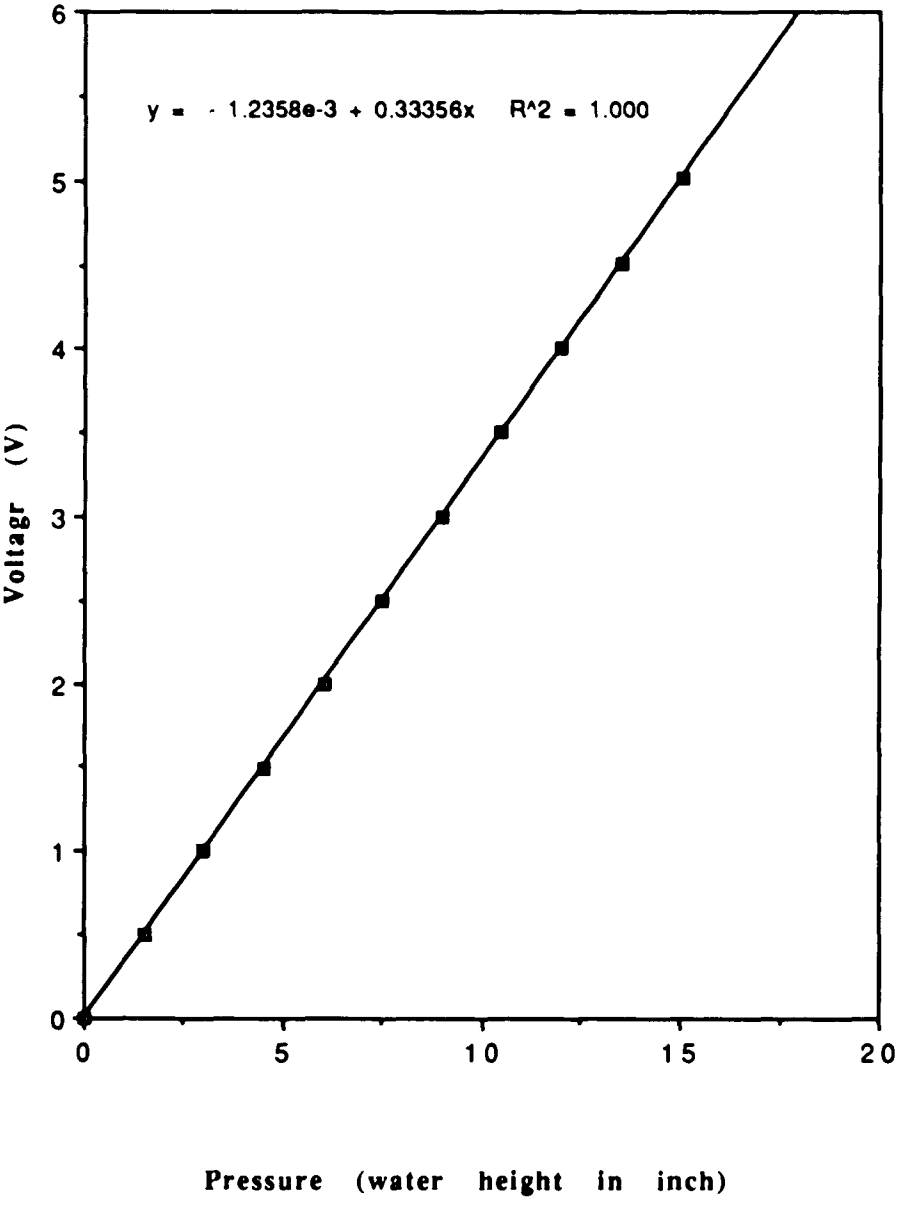
y = - 1.2358e-3 + 0.33356x R^2 = 1.000
Voltagr (V)
0
1
2
3
4
5
6
0
5
10
15
20
Pressure (water height in inch)

Figure 3

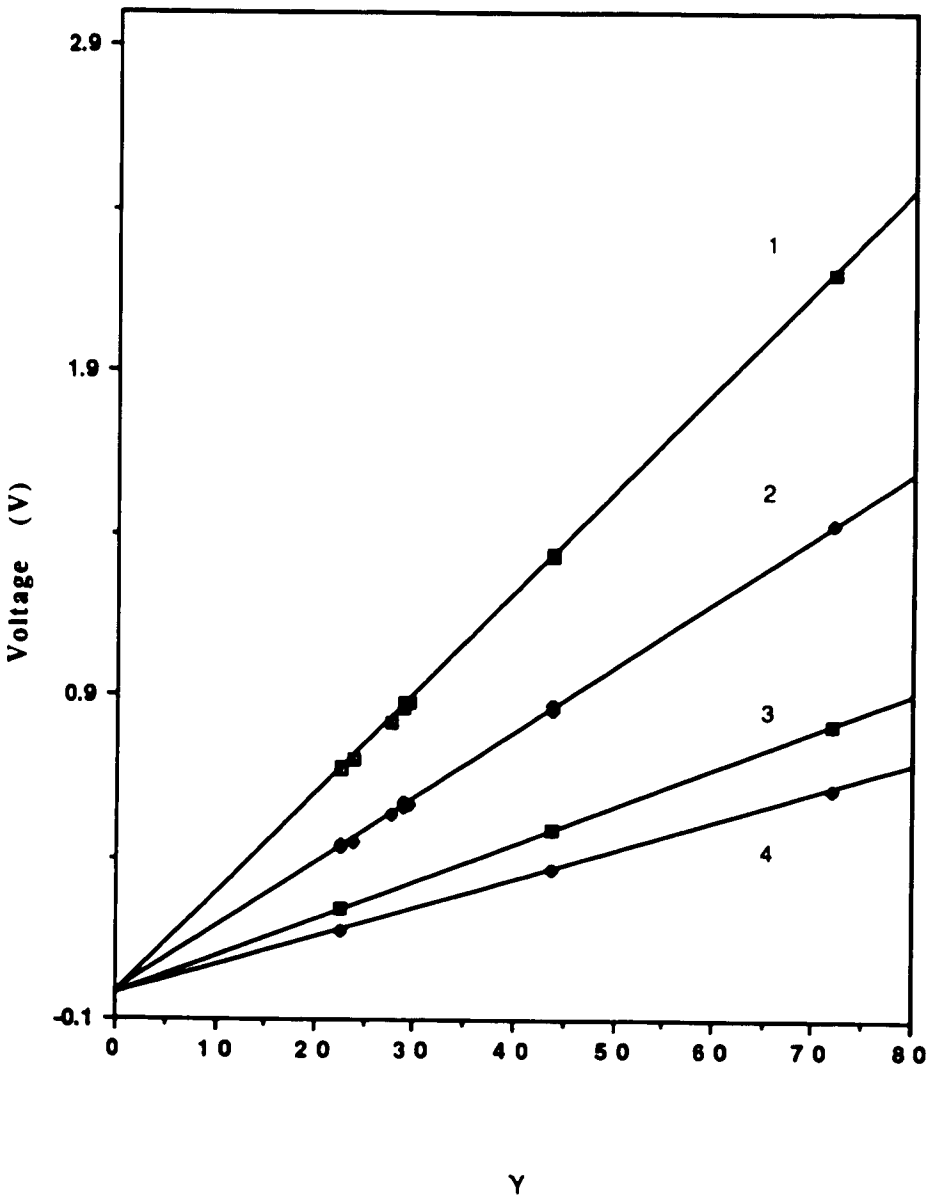

Figure 4 (a)

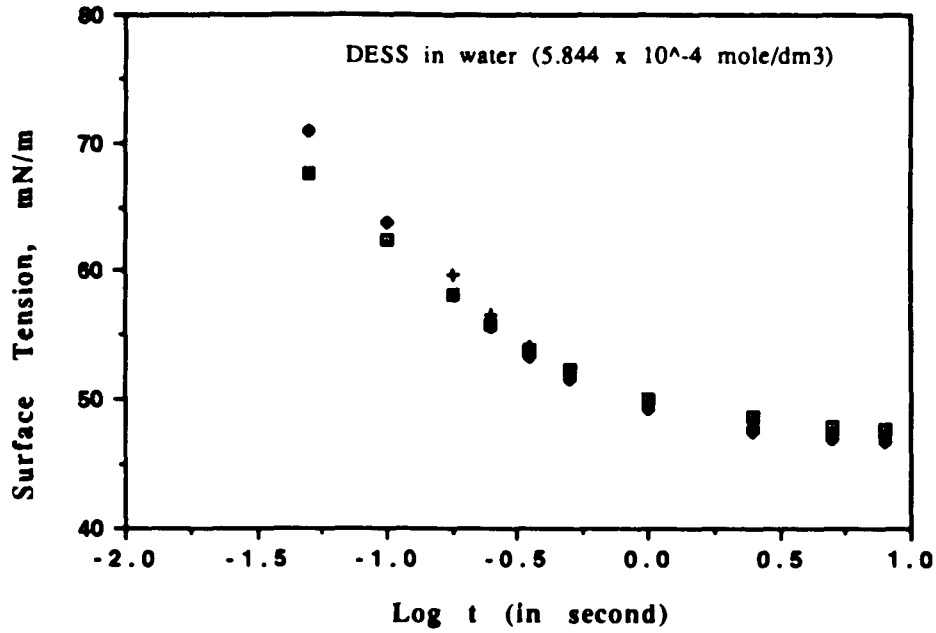

Figure 4 (b)

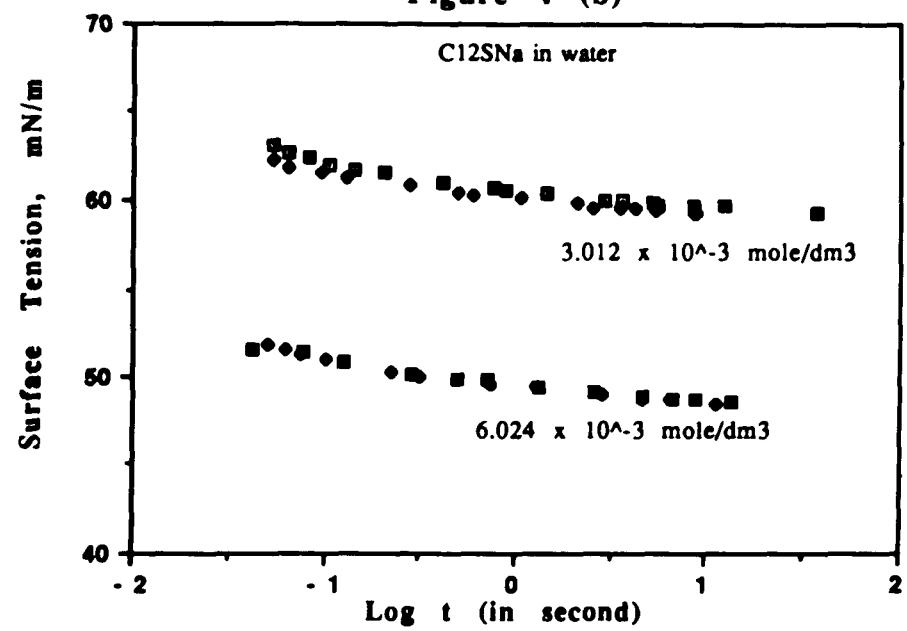

Figure 4 (c)

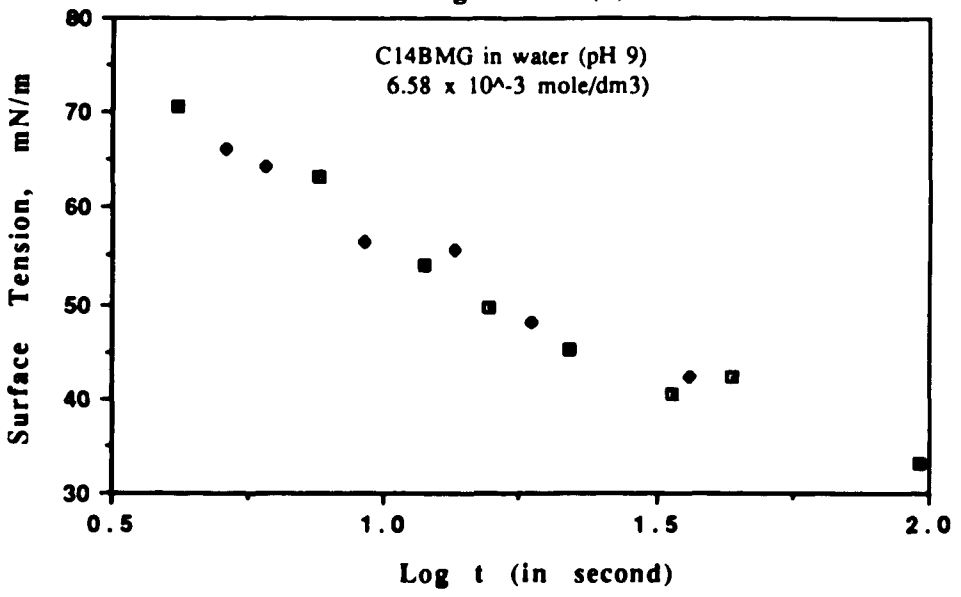

Figure 5

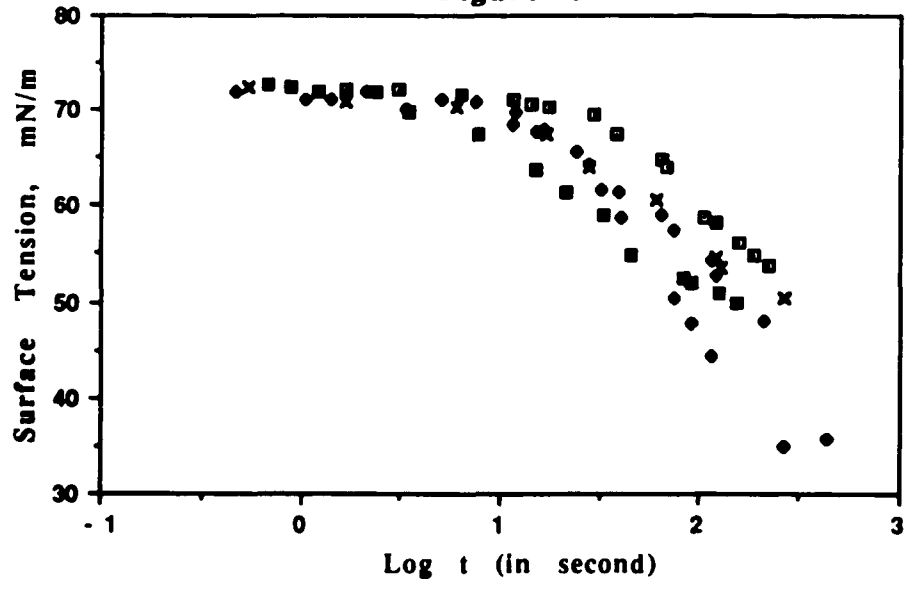

Figure 6 (a)

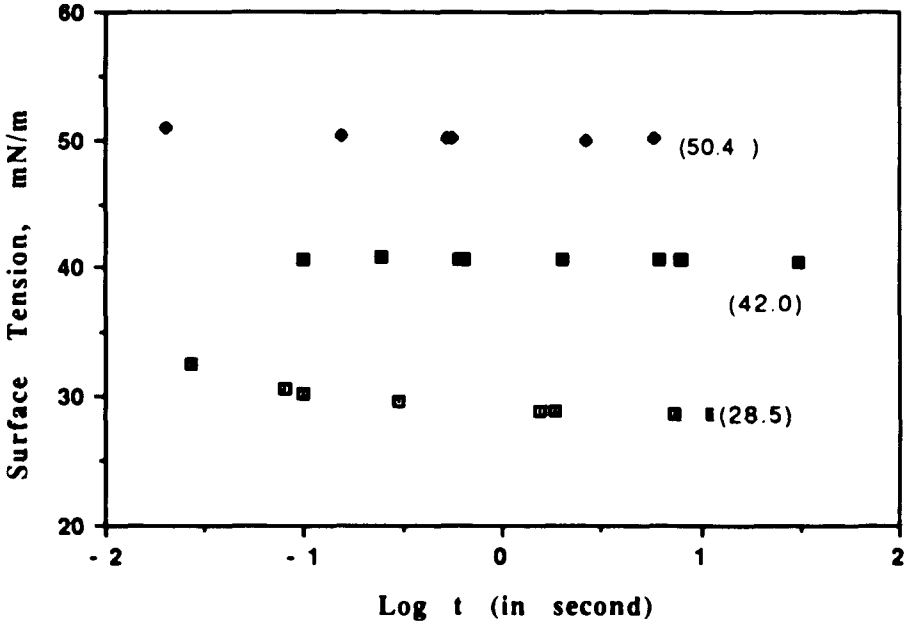

Figure 6 (b)

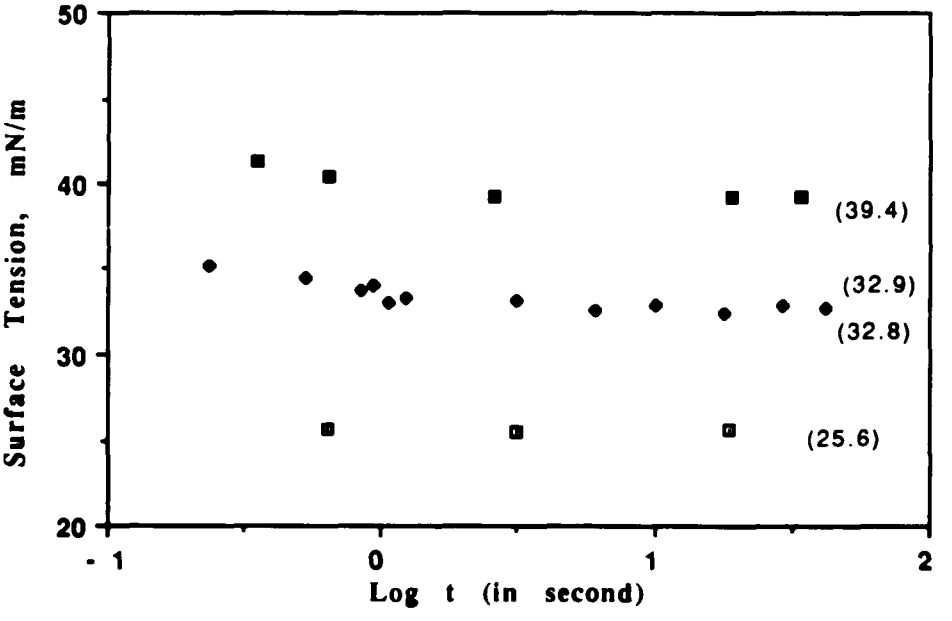

Figure 7

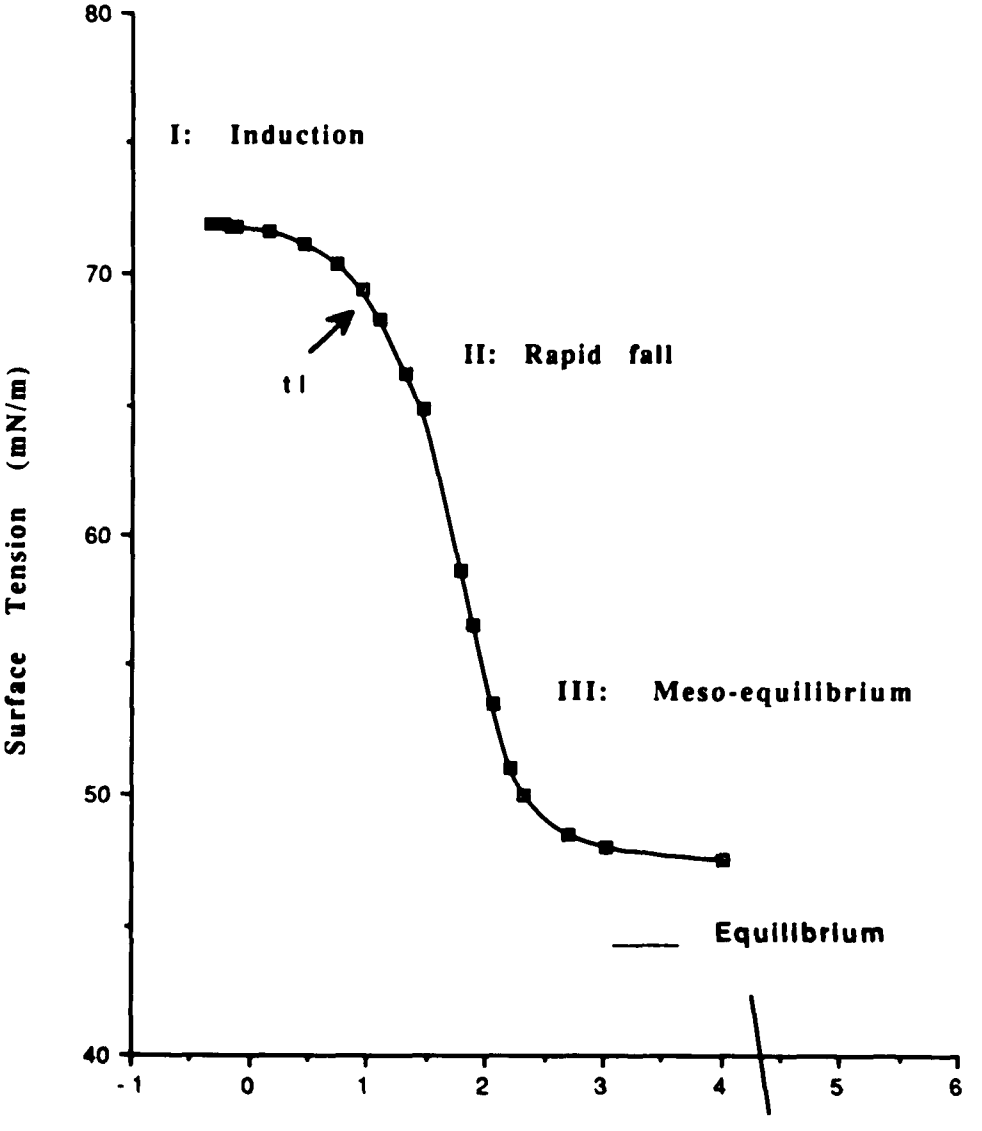
80
70
60
50
40
-1
0
1
2
3
4
5
6
I: Induction
II: Rapid fall
III: Meso-equilibrium
t l
Equilibrium
Surface Tension (mN/m)
Log t (in second)

Figure 8

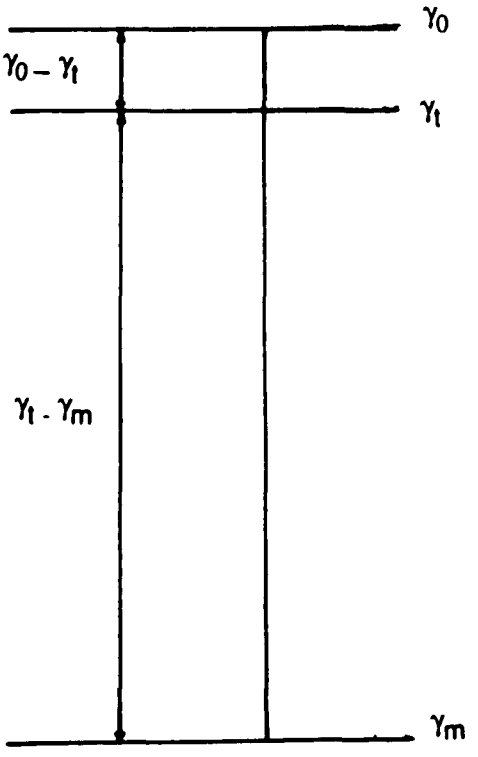

Figure 9

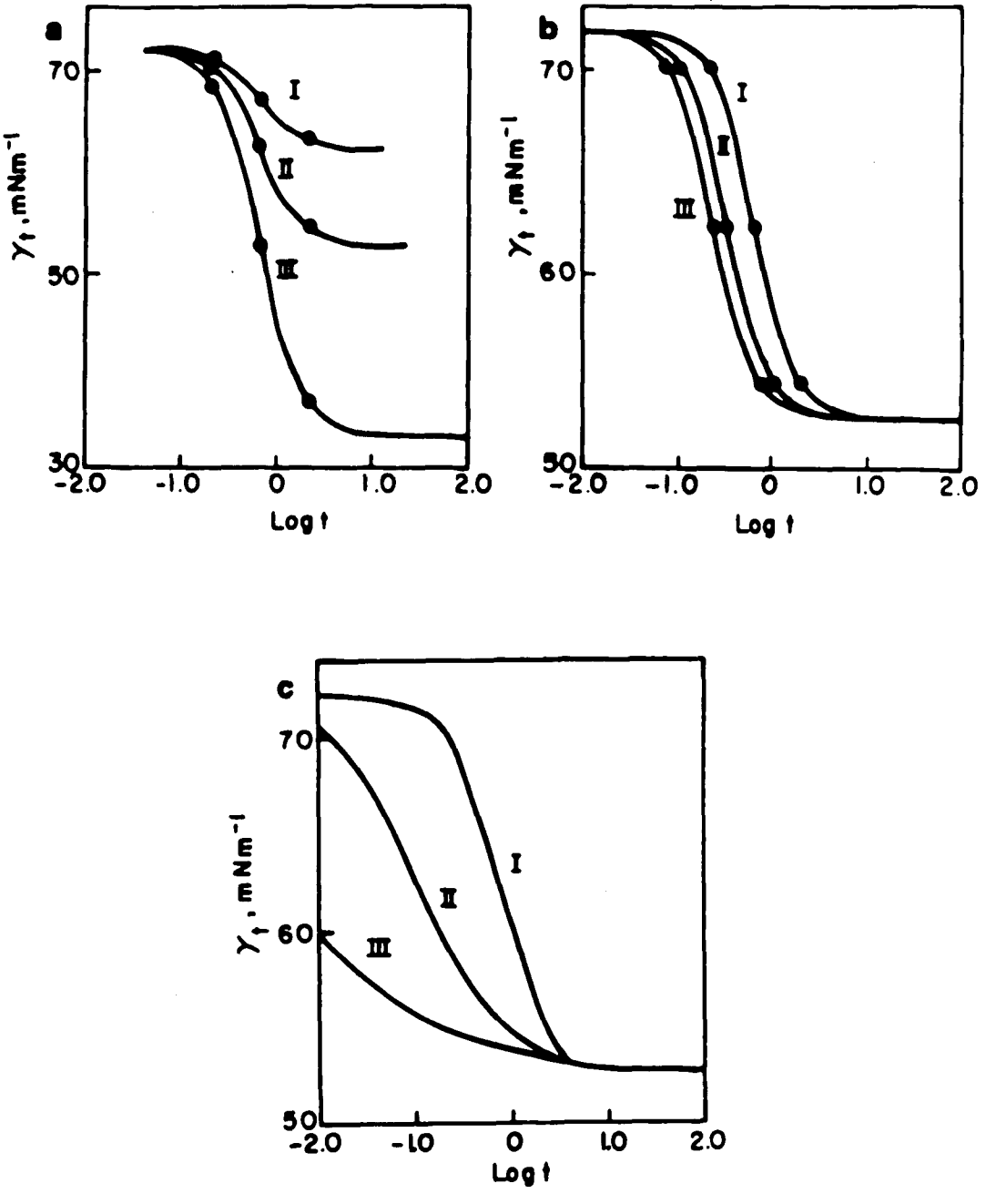
a
70
50
30
-2.0
-1.0
0
1.0
2.0
Log t
γ_t, mNm^{-1}
I
II
III
b
70
60
50
-2.0
-1.0
0
1.0
2.0
Log t
γ_t, mNm^{-1}
I
II
III
c
70
60
50
-2.0
-1.0
0
1.0
2.0
Log t
γ_t, mNm^{-1}
I
II
III

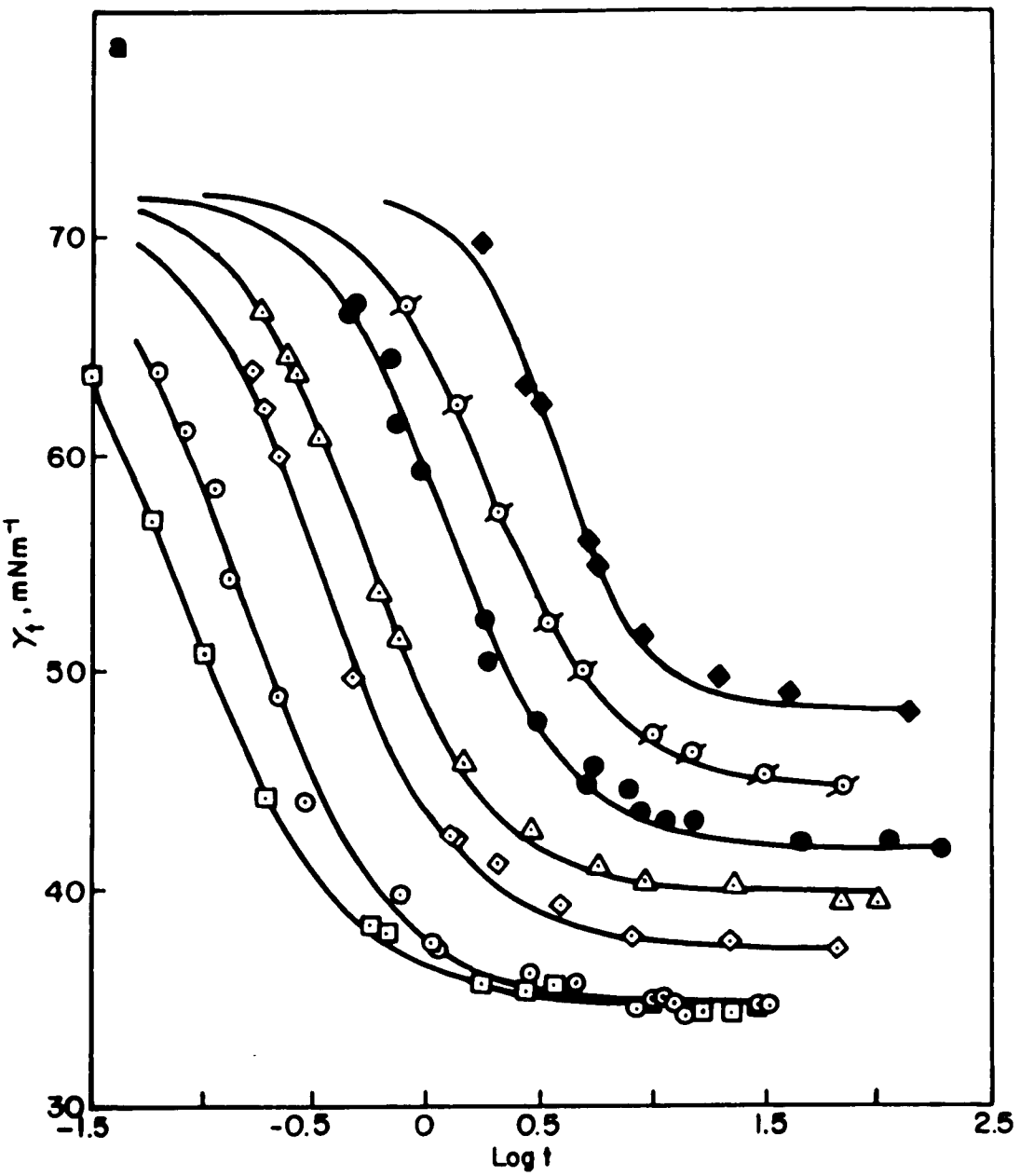

Figure 10 (a)

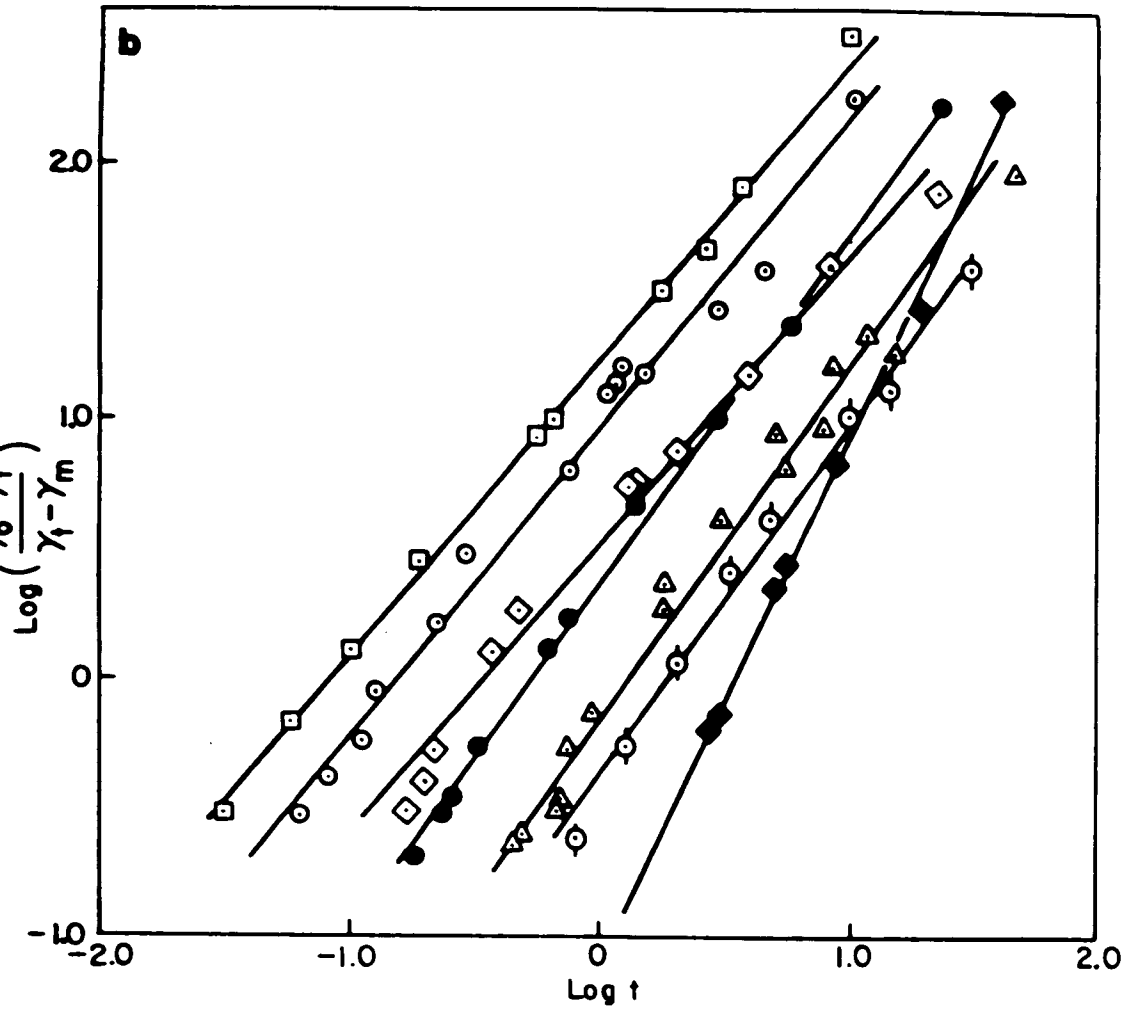

Figure 10 (b)

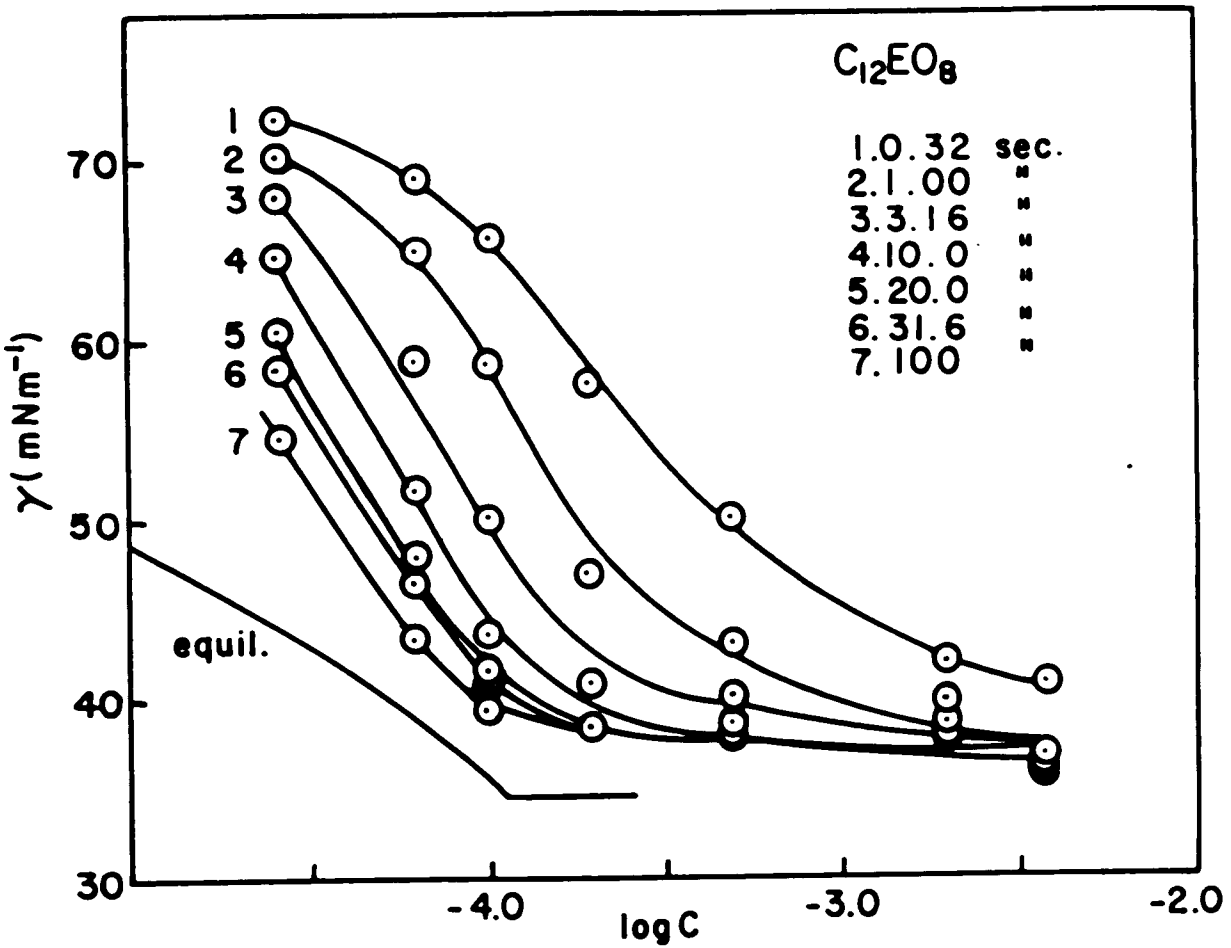
$C_{12}EO_8$
1.0.32 sec.
2.1.00 "
3.3.16 "
4.10.0 "
5.20.0 "
6.31.6 "
7.100 "
1
2
3
4
5
6
7
equil.
70
60
50
40
30
γ(mNm⁻¹)
-4.0
-3.0
-2.0
log C

Figure 11

Figure 12

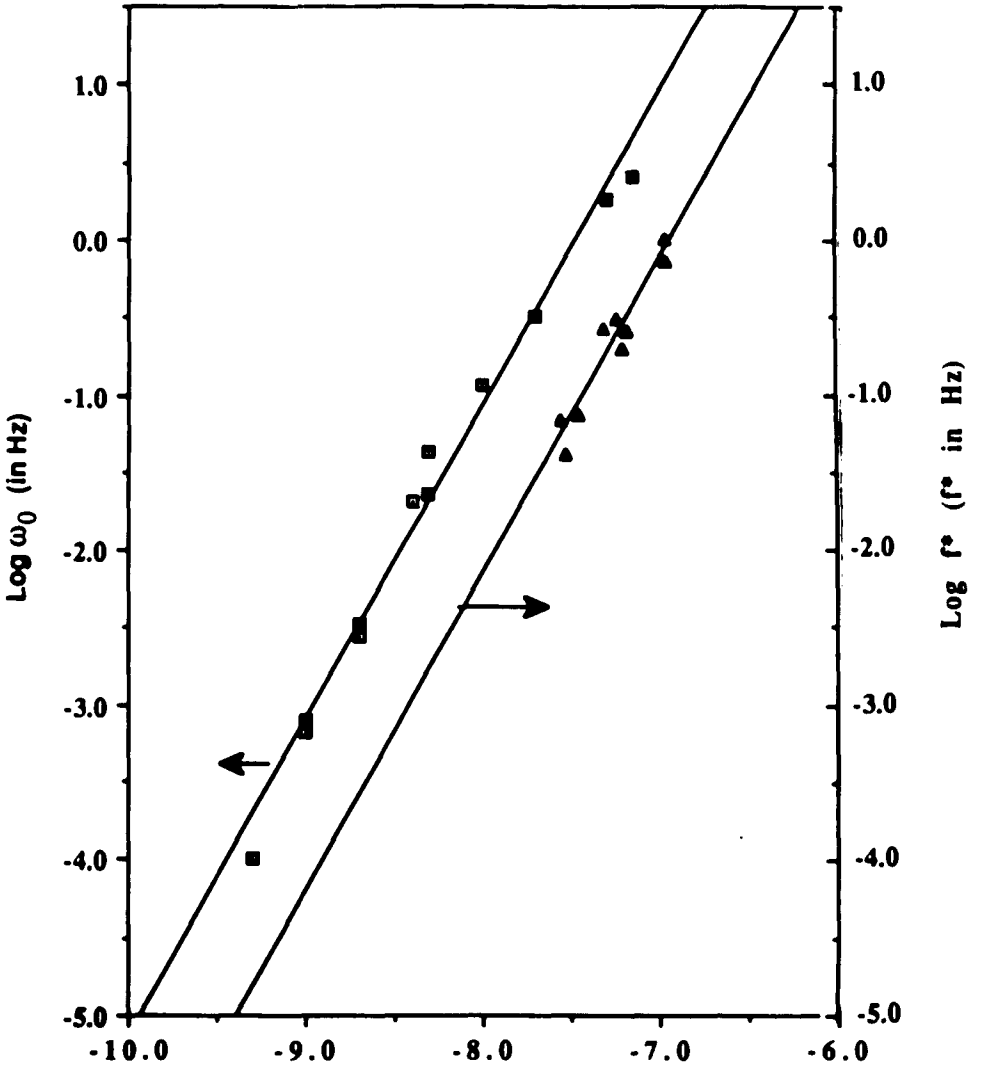
1.0
0.0
-1.0
-2.0
-3.0
-4.0
-5.0
-10.0
-9.0
-8.0
-7.0
-6.0
Log ω_0 (in Hz)
Log f^* (f^* in Hz)
Log C (in mole/cm3)

Figure 13

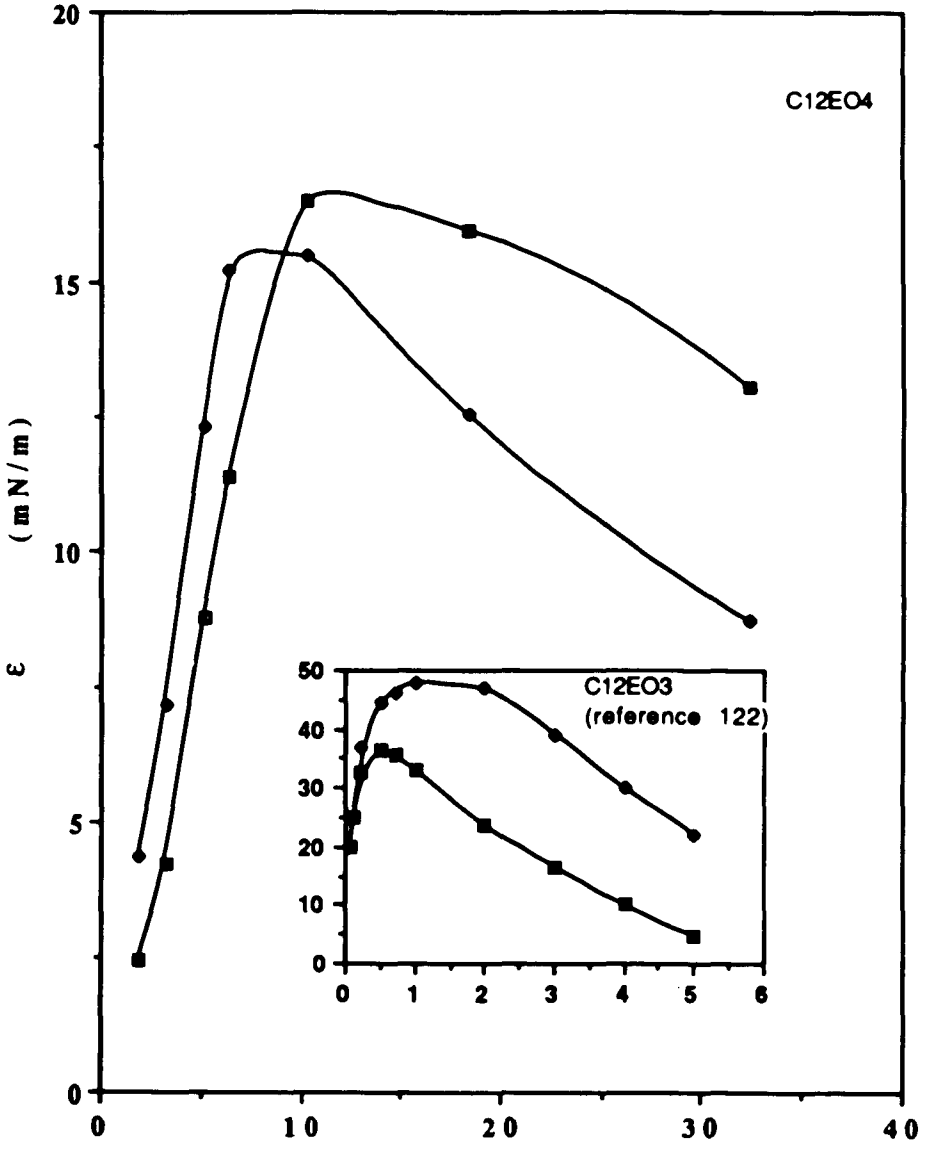
C12EO4
C12EO3
(reference 122)
ε (mN/m)
C x 10^8 (mole/cm3)
0
5
10
15
20
0
10
20
30
40
0
10
20
30
40
50
0
1
2
3
4
5
6

Figure 14

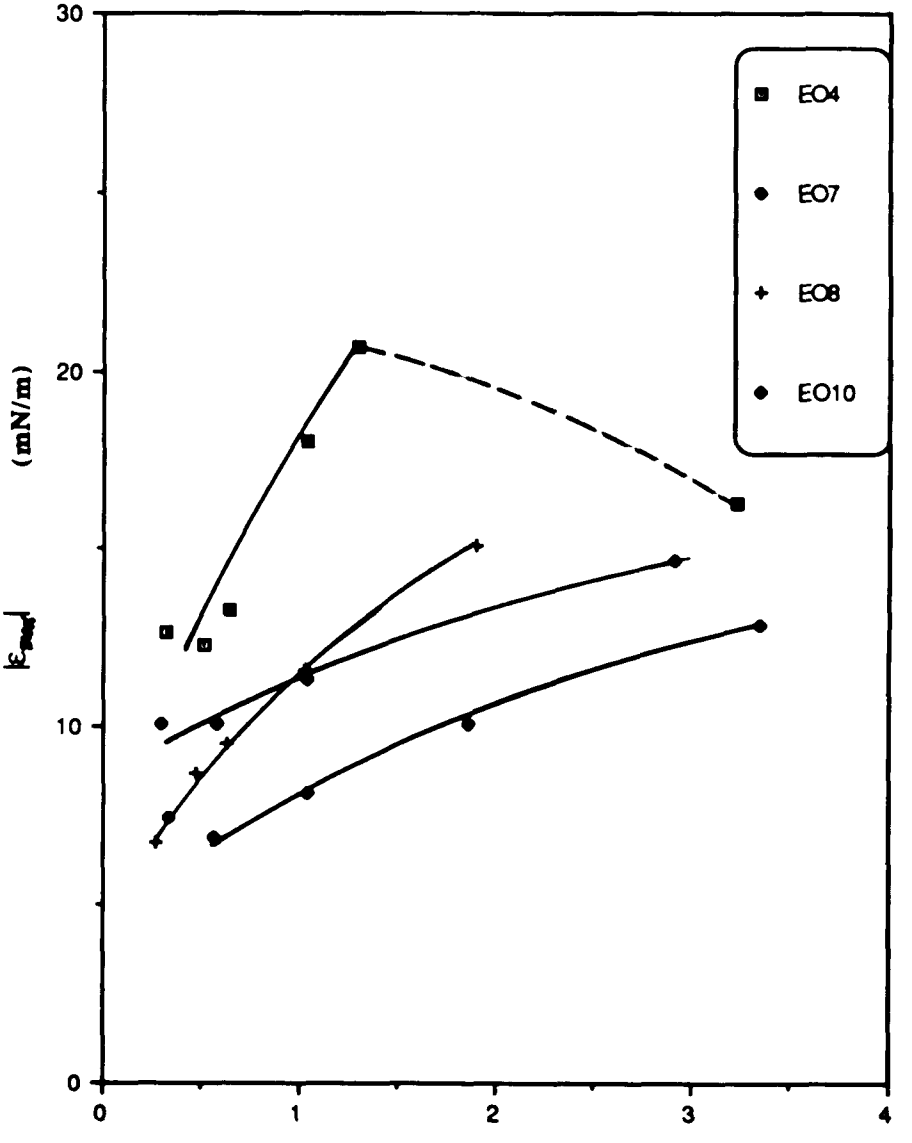

Figure 15

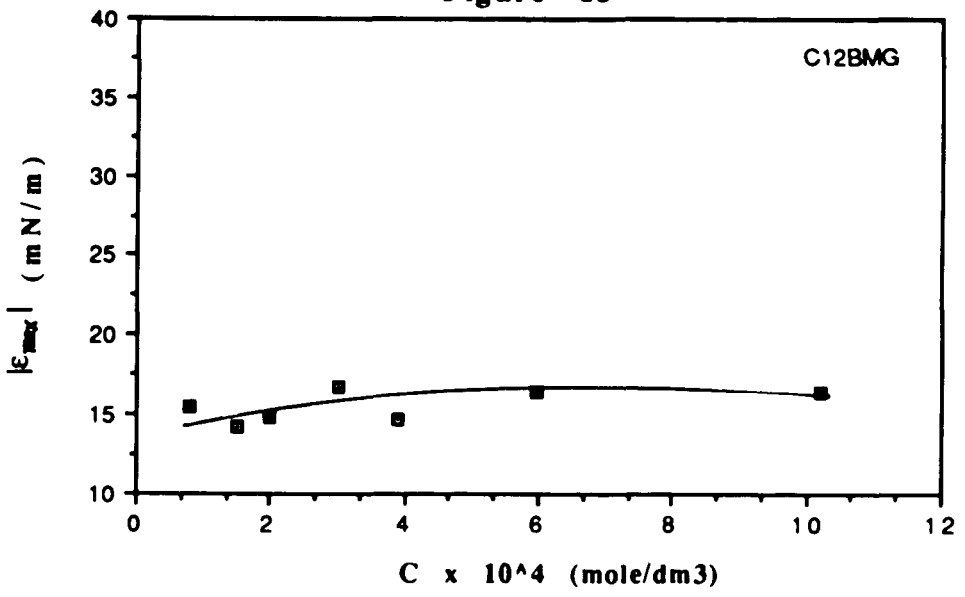

Figure 16

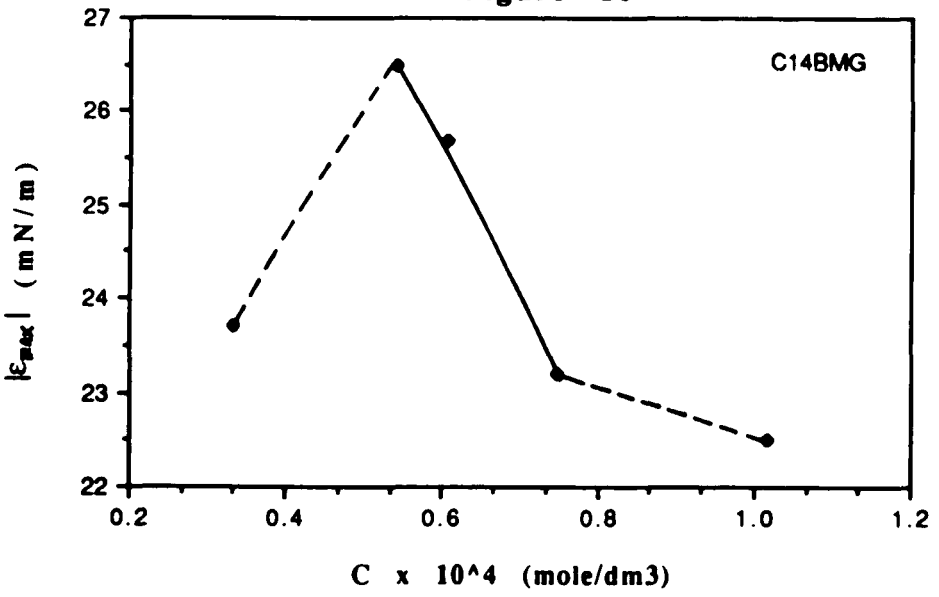

Figure 17

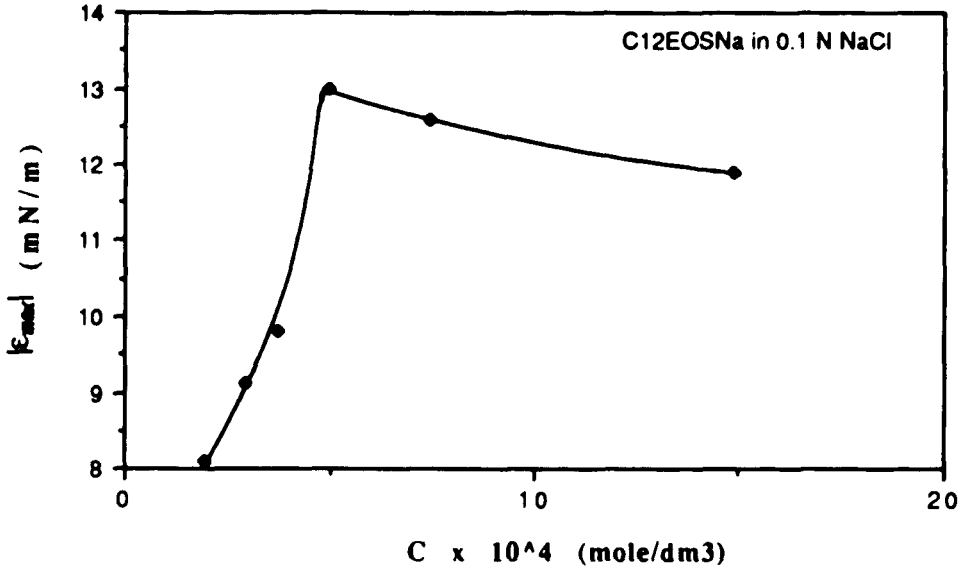

Figure 18

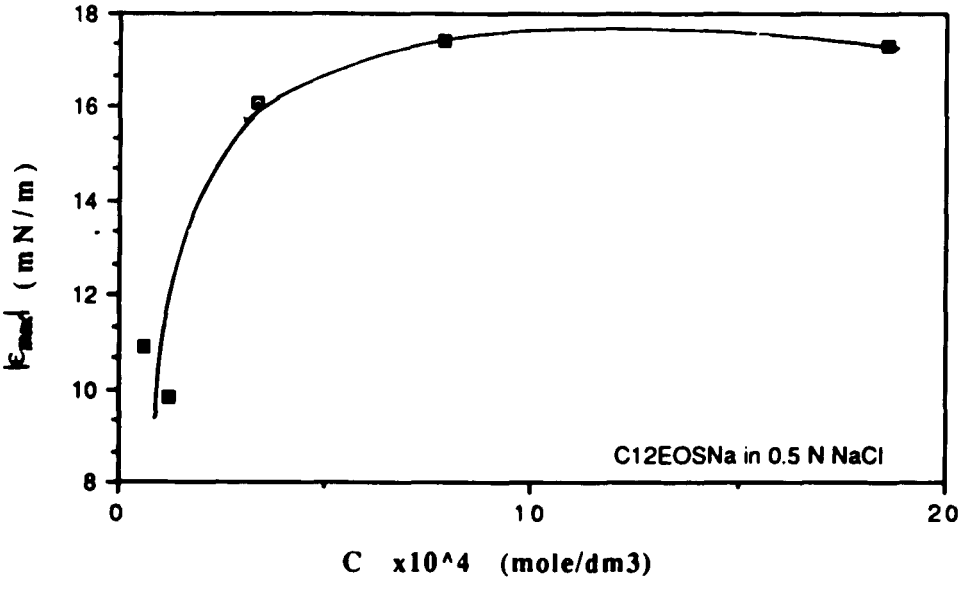

Figure 19

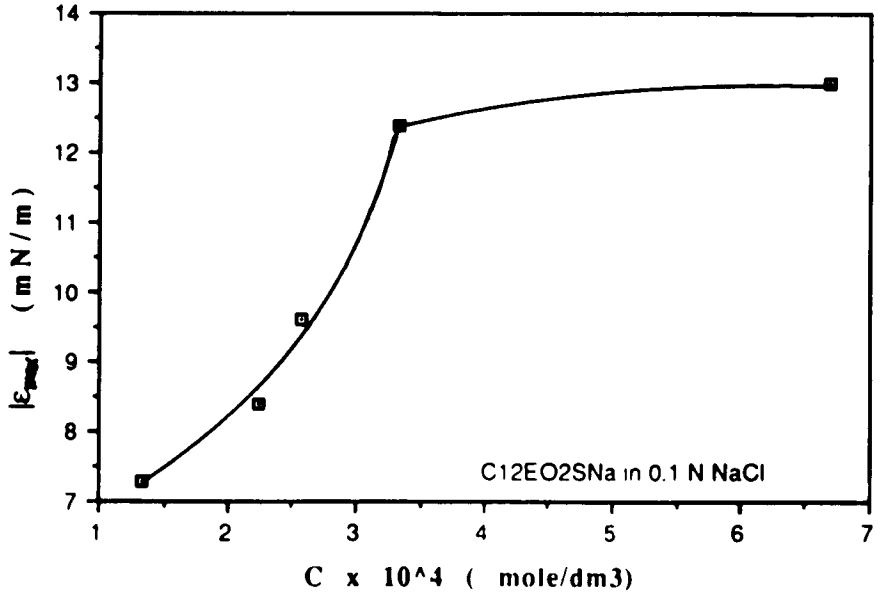

Figure 20

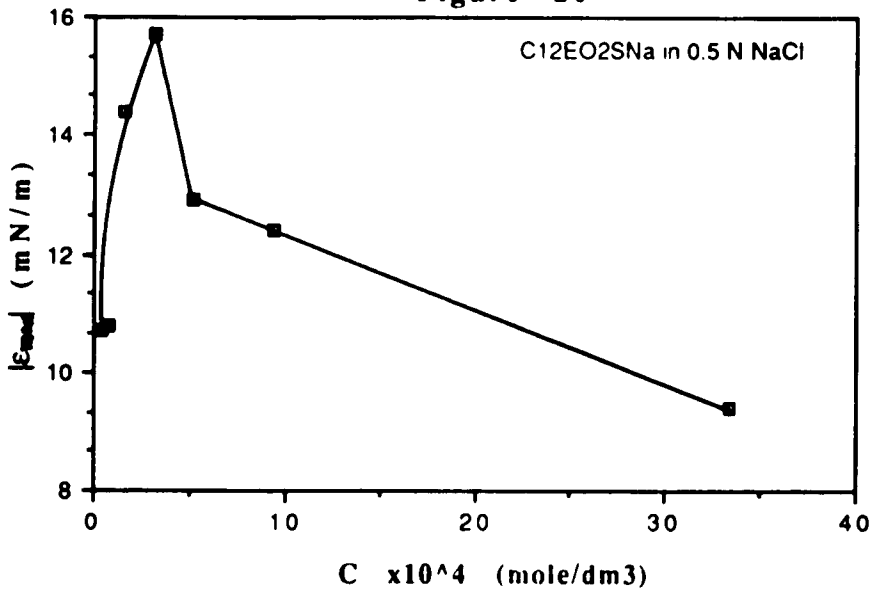

Figure 21

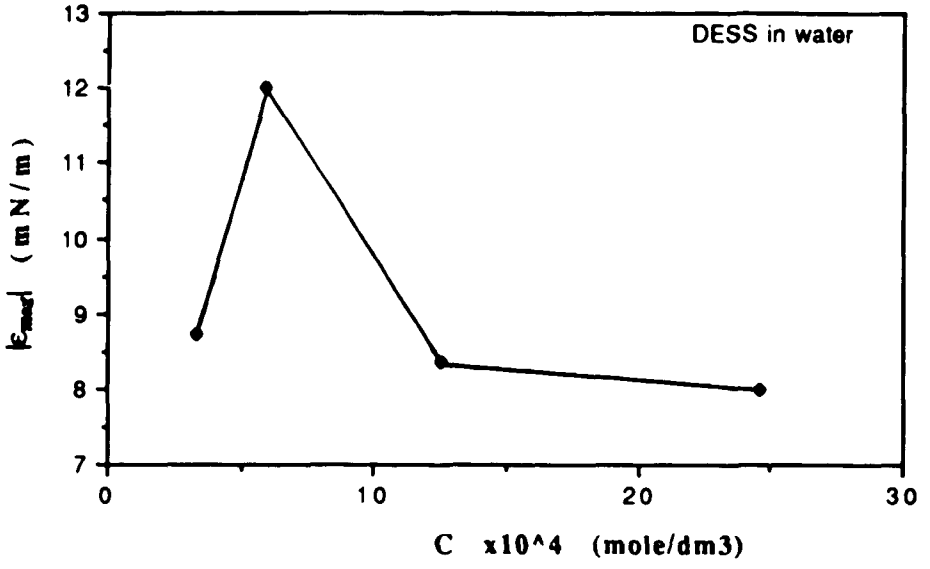

Figure 22

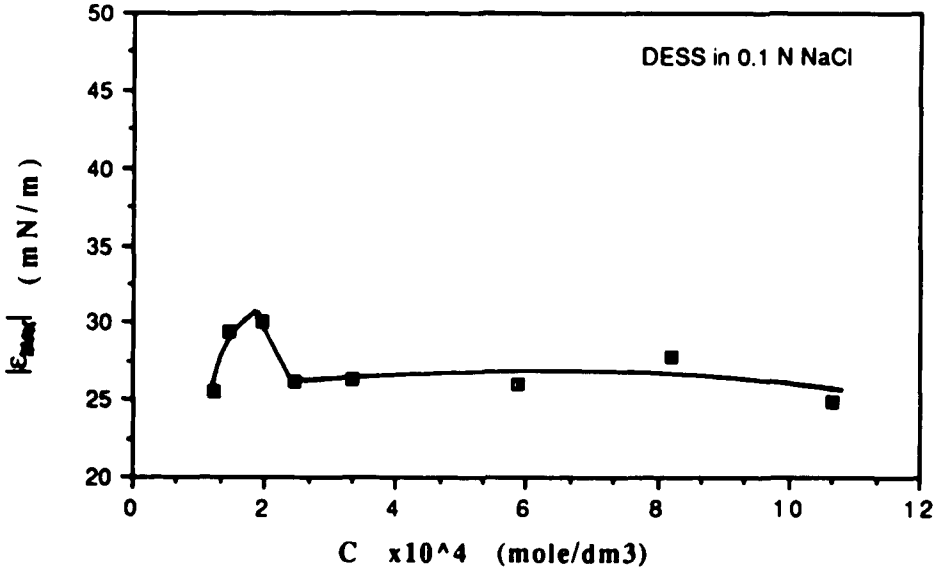

Figure 23

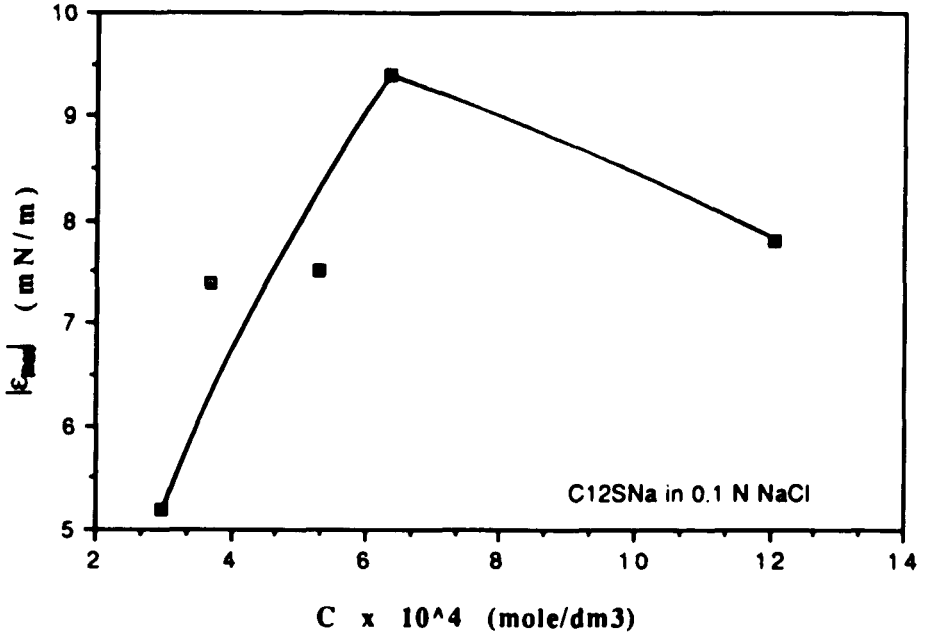

Figure 24

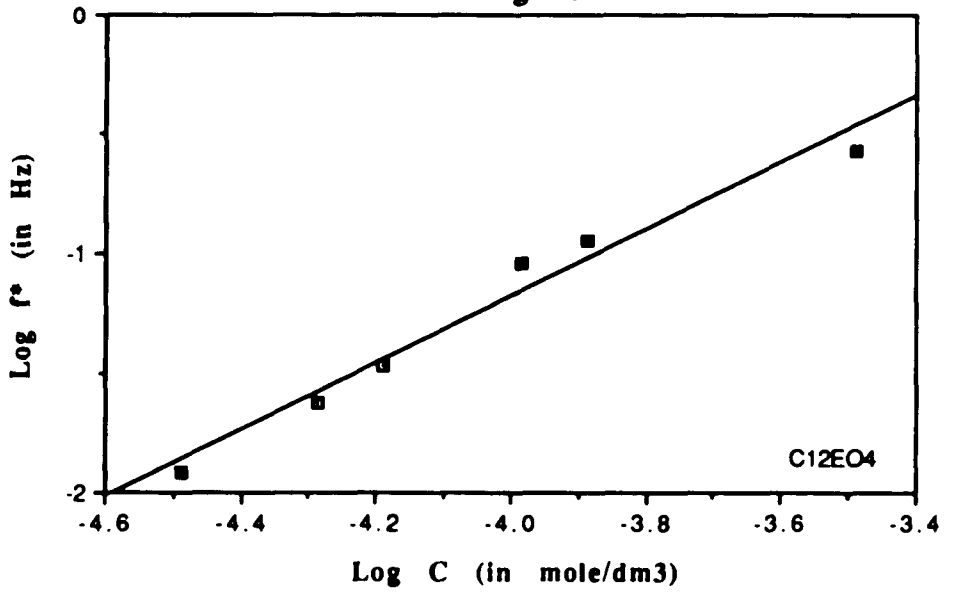

Figure 25

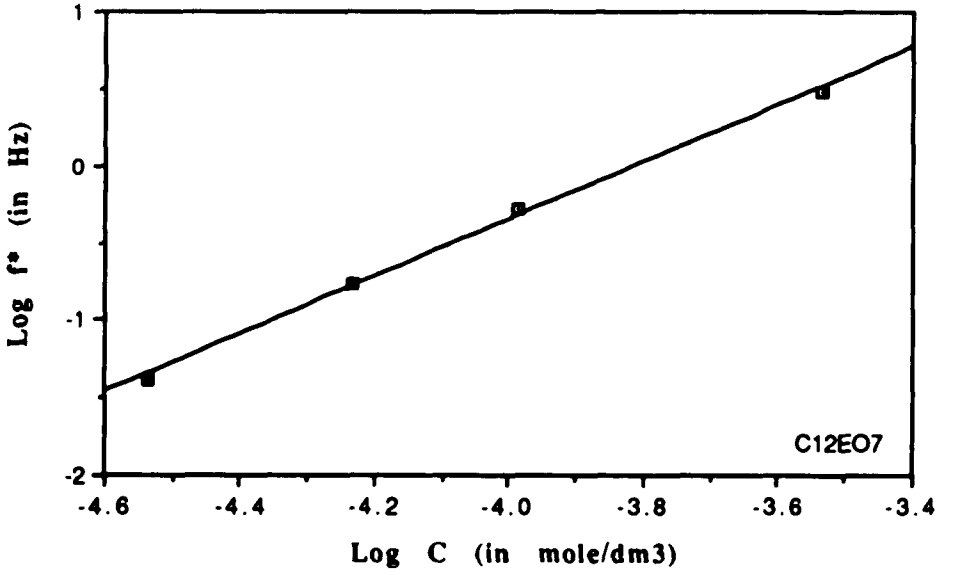

Figure 26

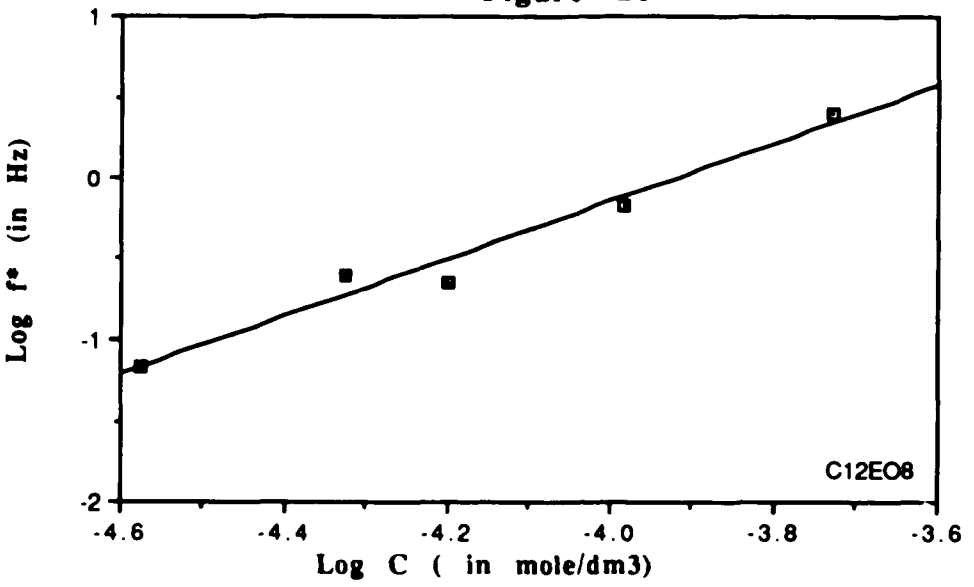

Figure 27

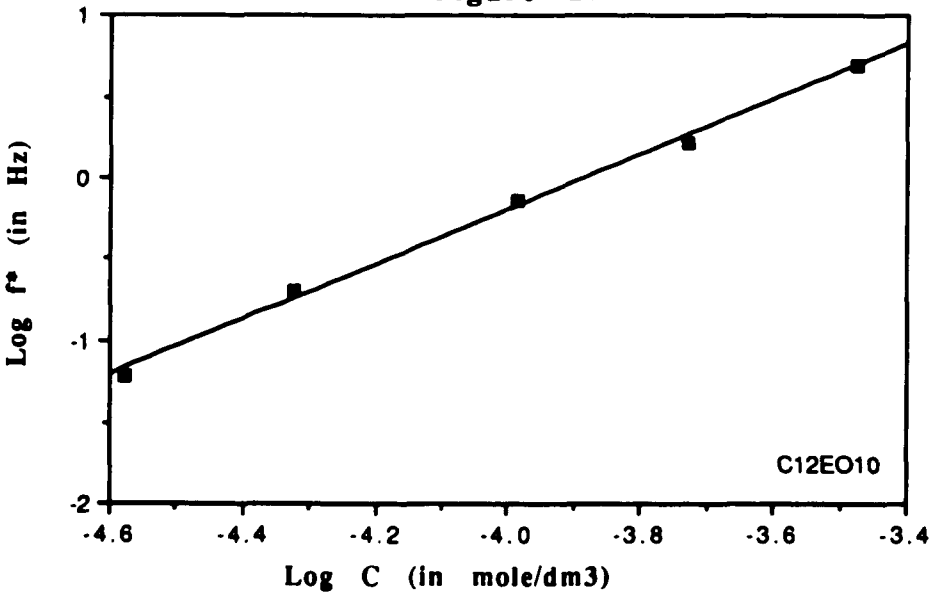

Figure 28

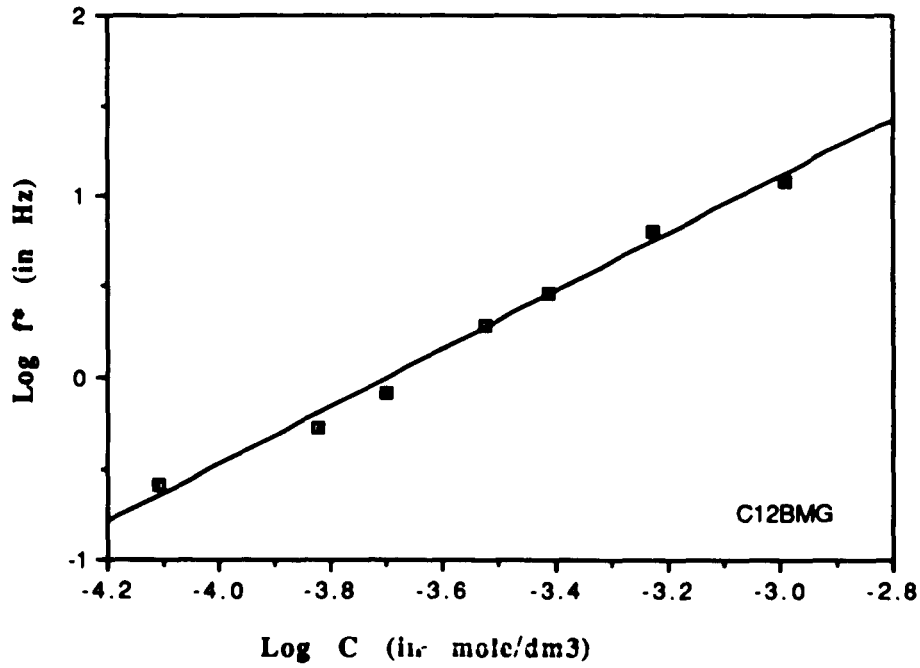

Figure 29

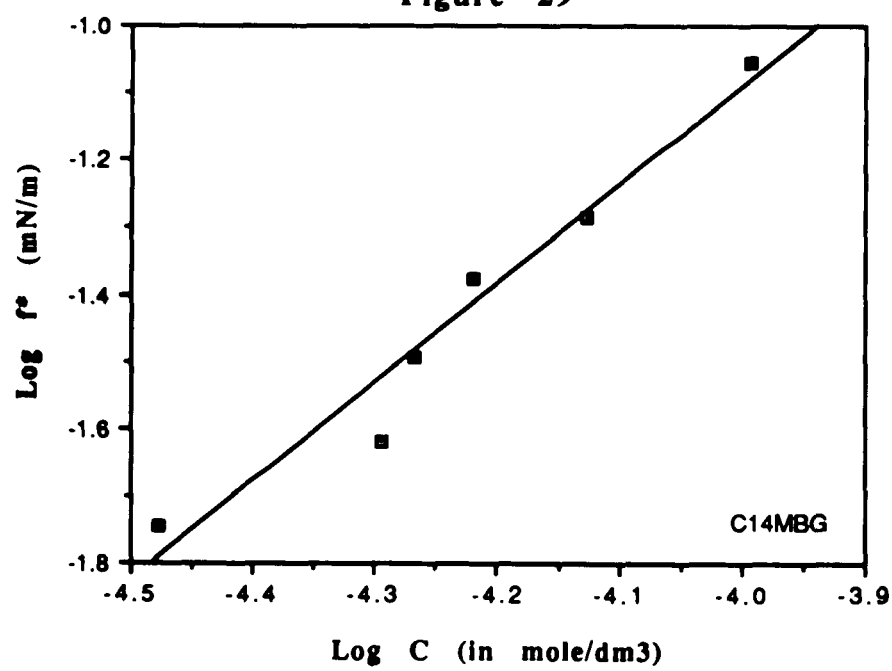

Figure 30

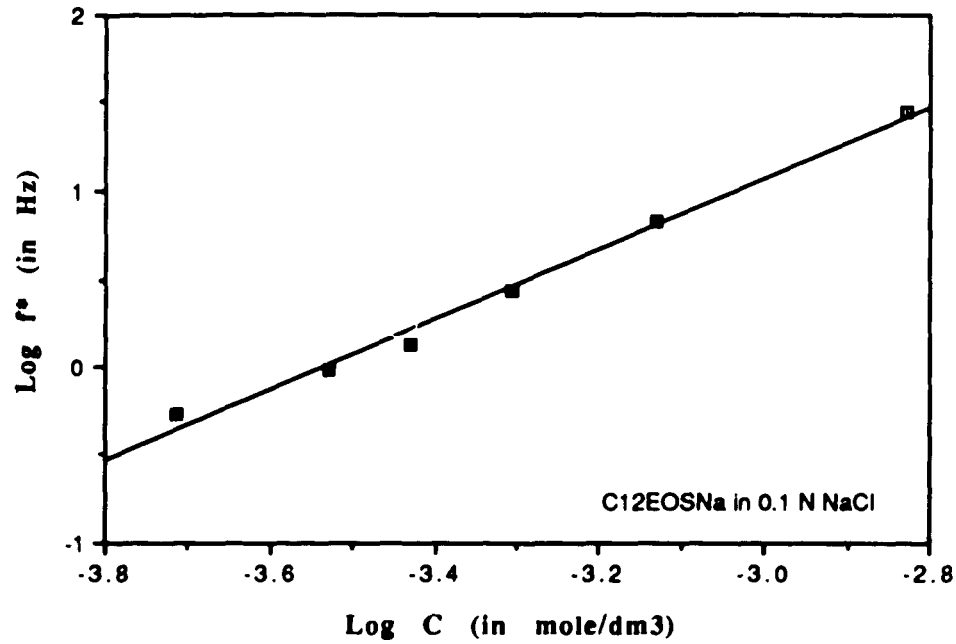

Figure 31

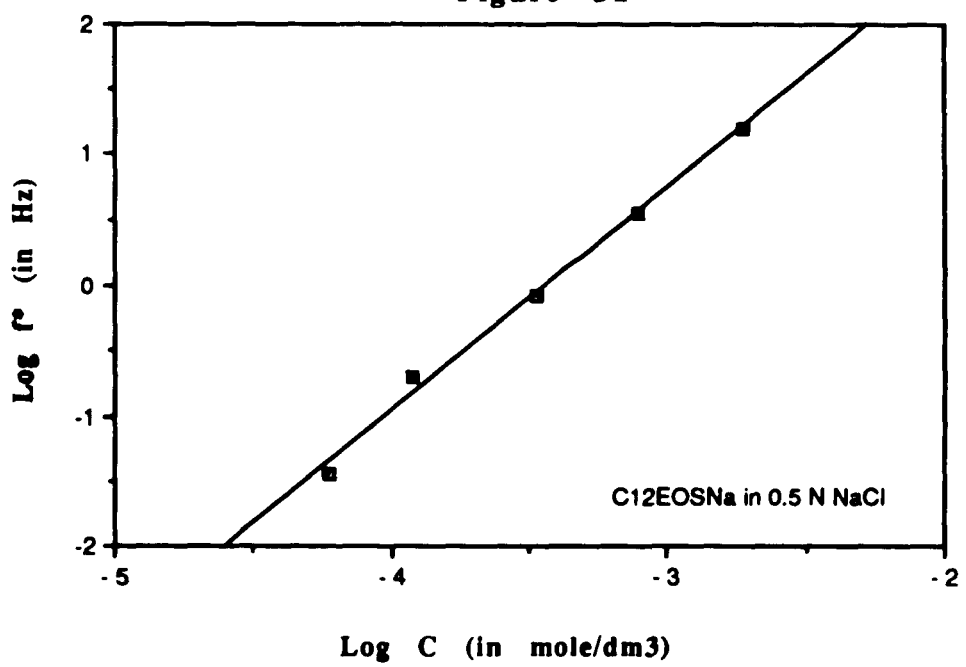

Figure 32

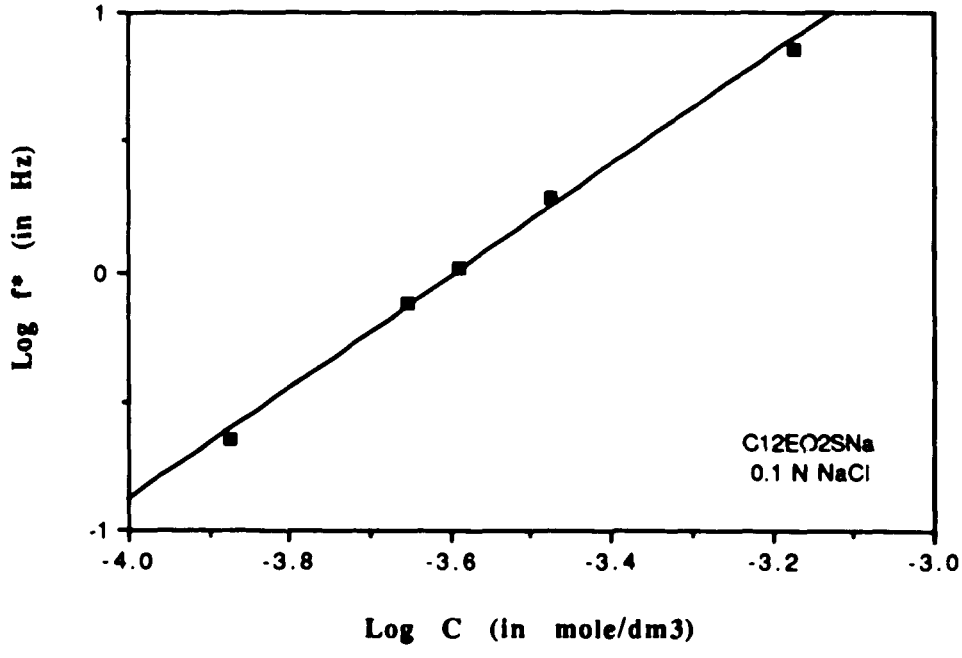

Figure 33

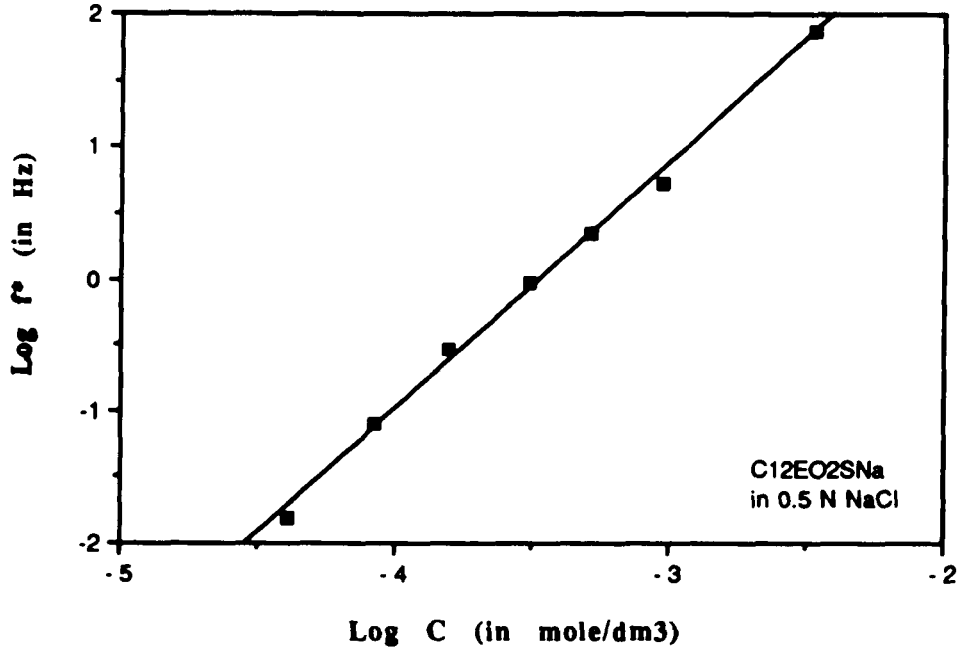

Figure 34

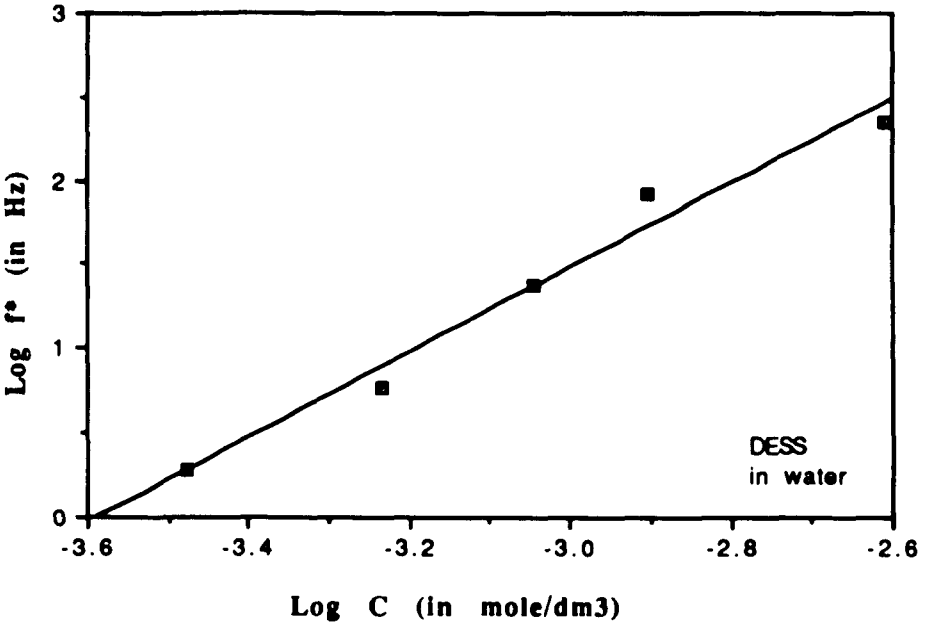

Figure 35

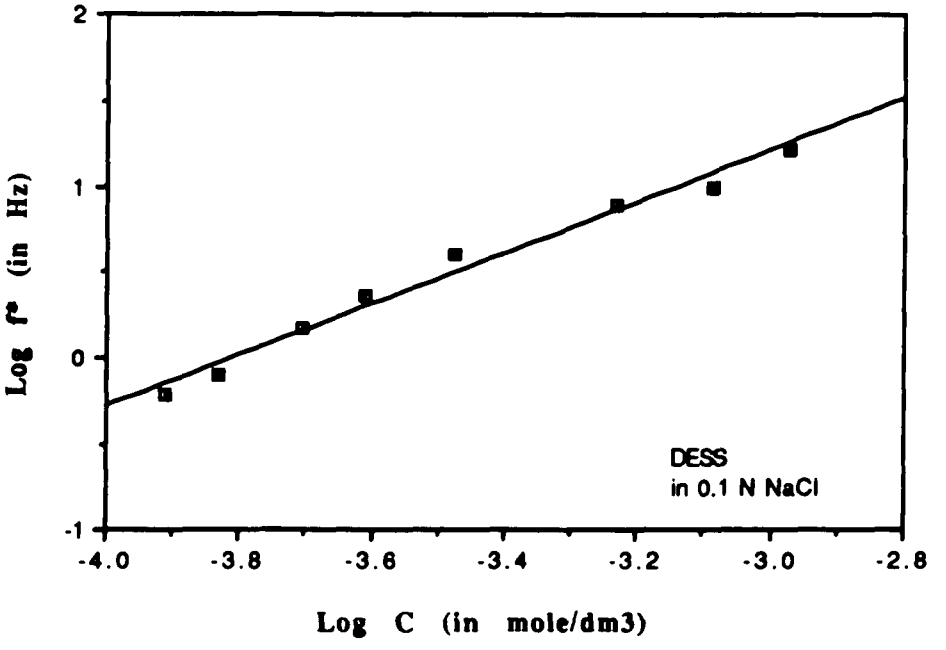

Figure 36

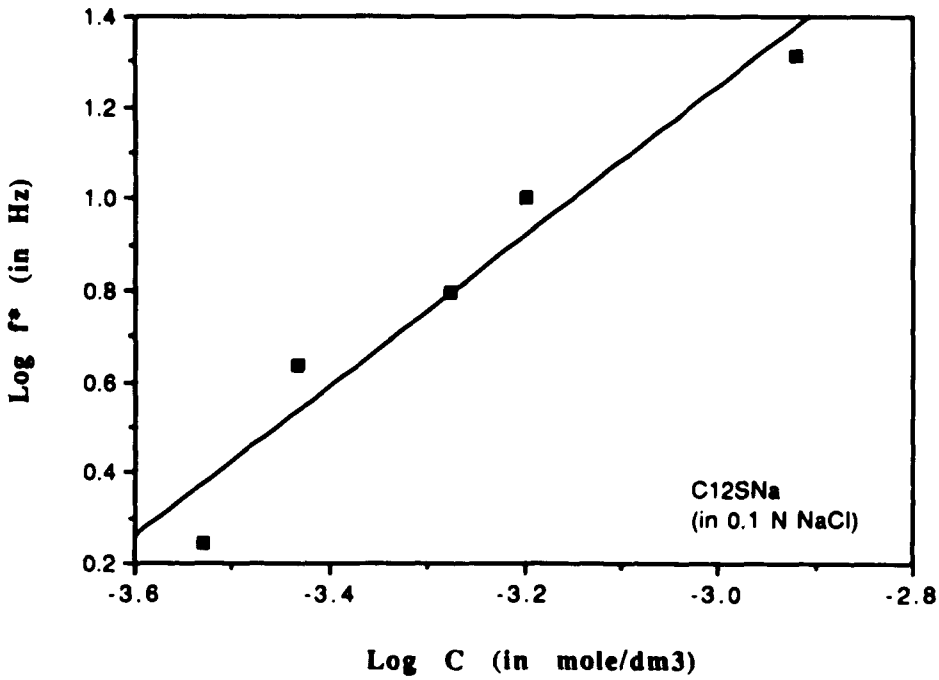
1.4
1.2
1.0
0.8
0.6
0.4
0.2
Log f* (in Hz)
-3.6
-3.4
-3.2
-3.0
-2.8
Log C (in mole/dm3)
C12SNa
(in 0.1 N NaCl)

Figure 37

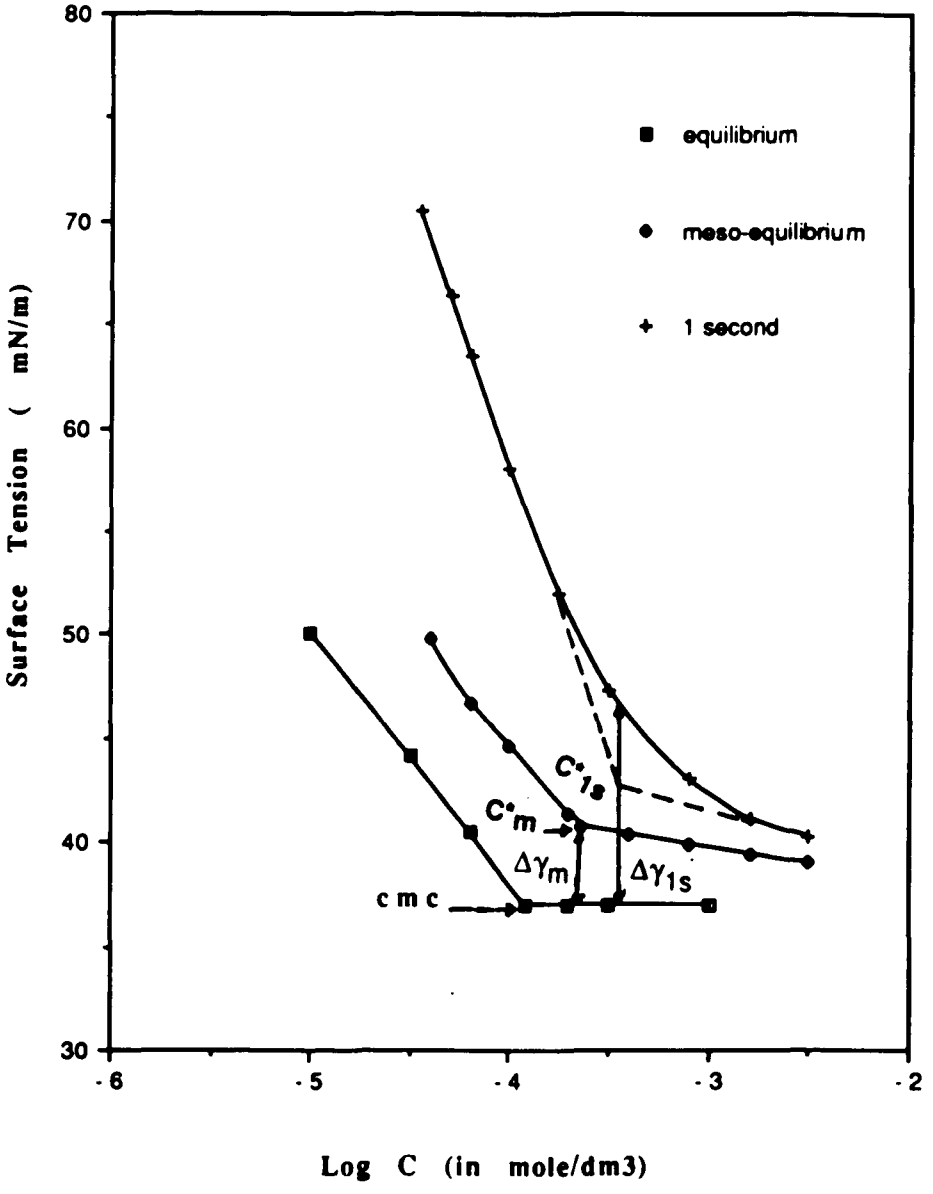
80
70
60
50
40
30
-6
-5
-4
-3
-2
Surface Tension (mN/m)
Log C (in mole/dm3)
equilibrium
meso-equilibrium
1 second
C*1s
C*m
Δγm
Δγ1s
c m c

Figure 38

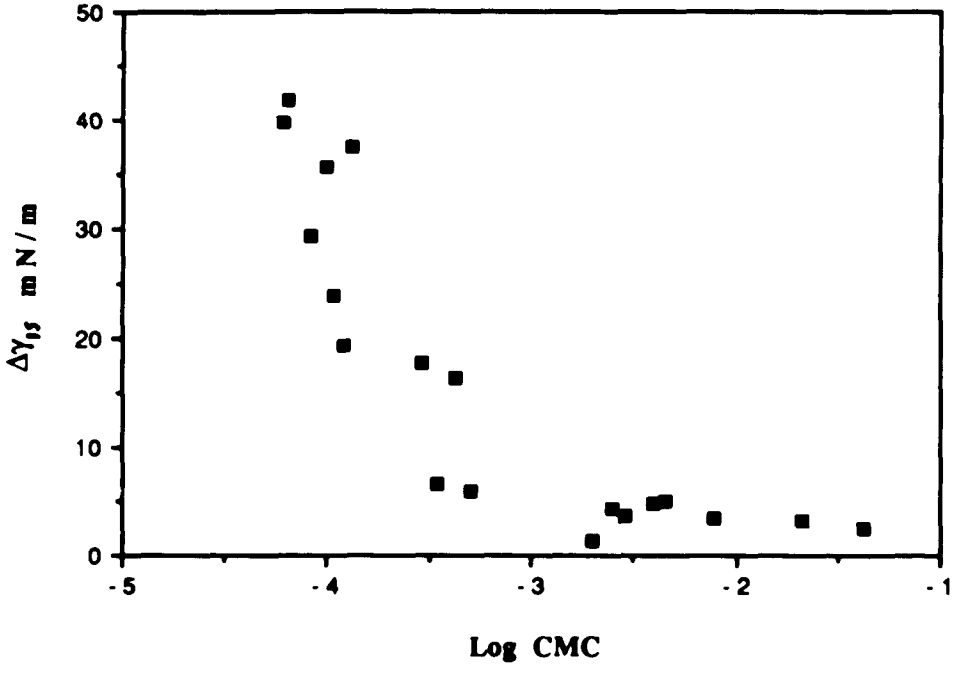

Figure 39

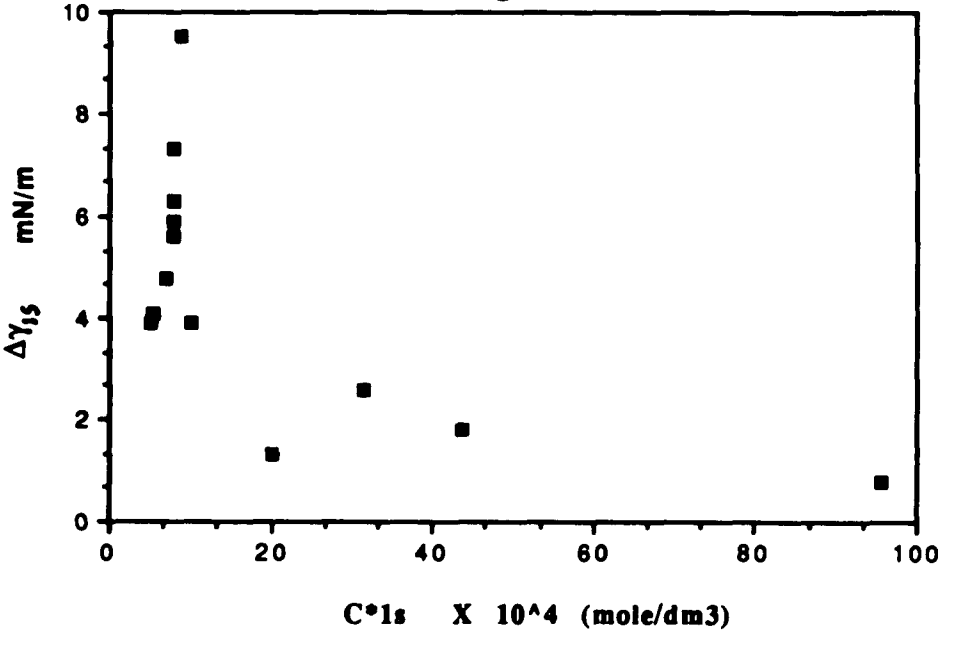

Figure 40

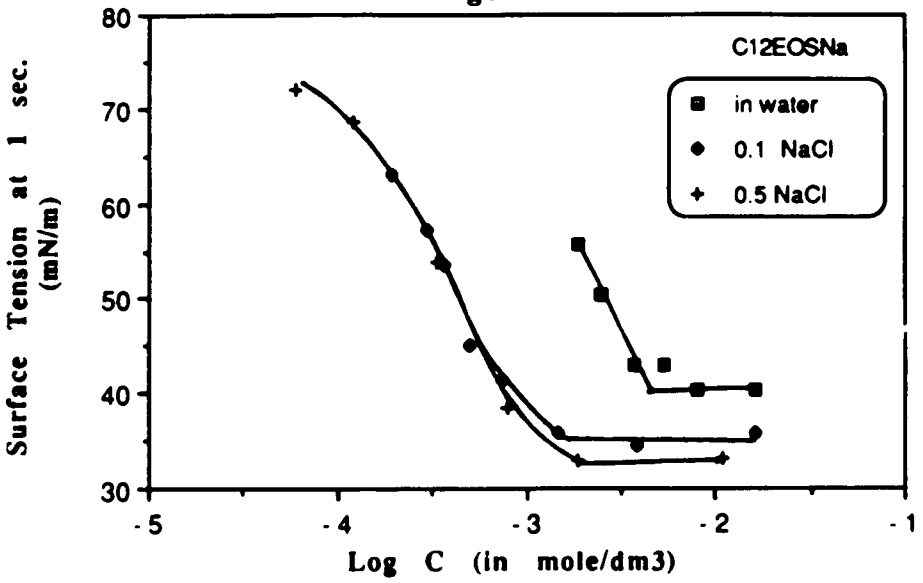

Figure 41

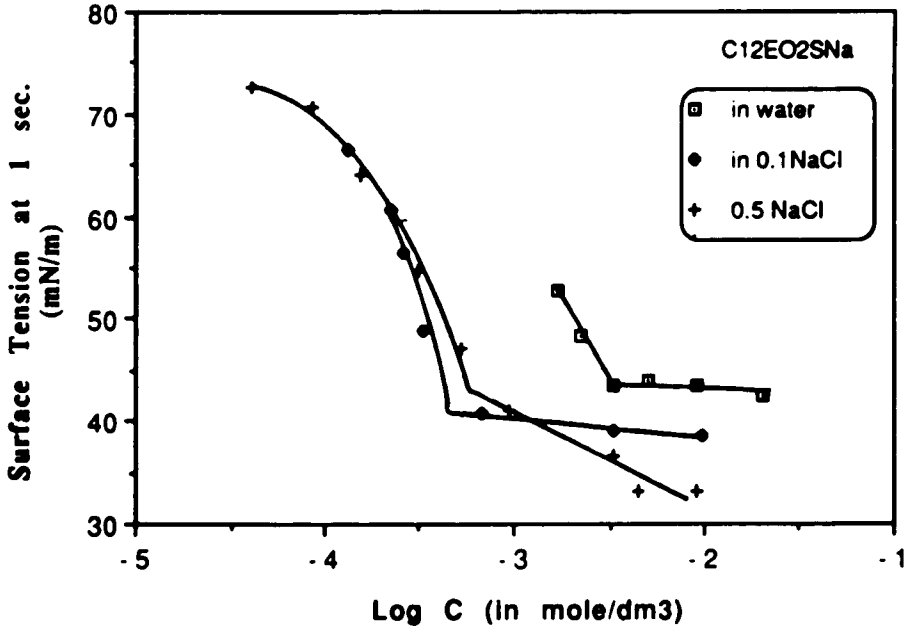

Figure 42 (a)

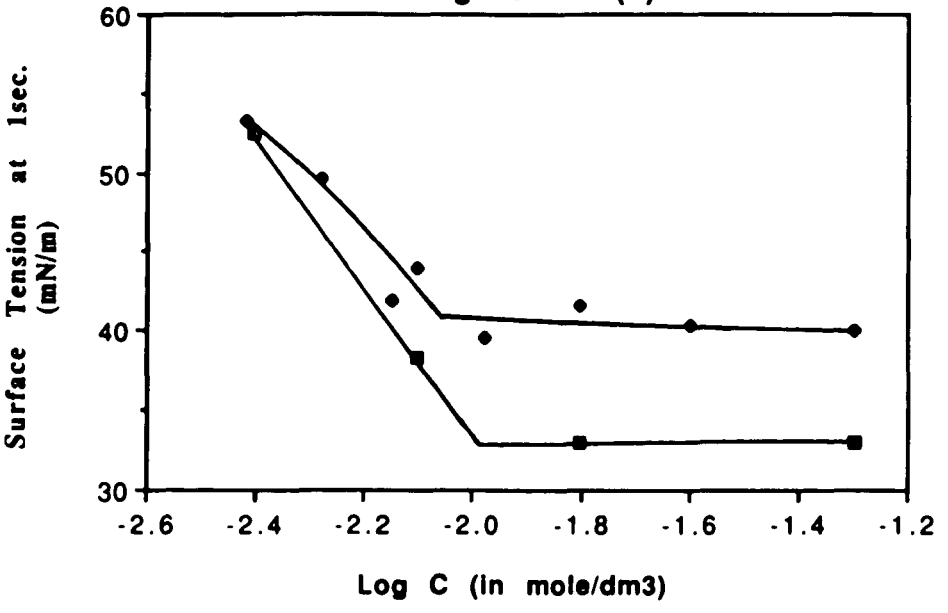

Figure 42 (b)

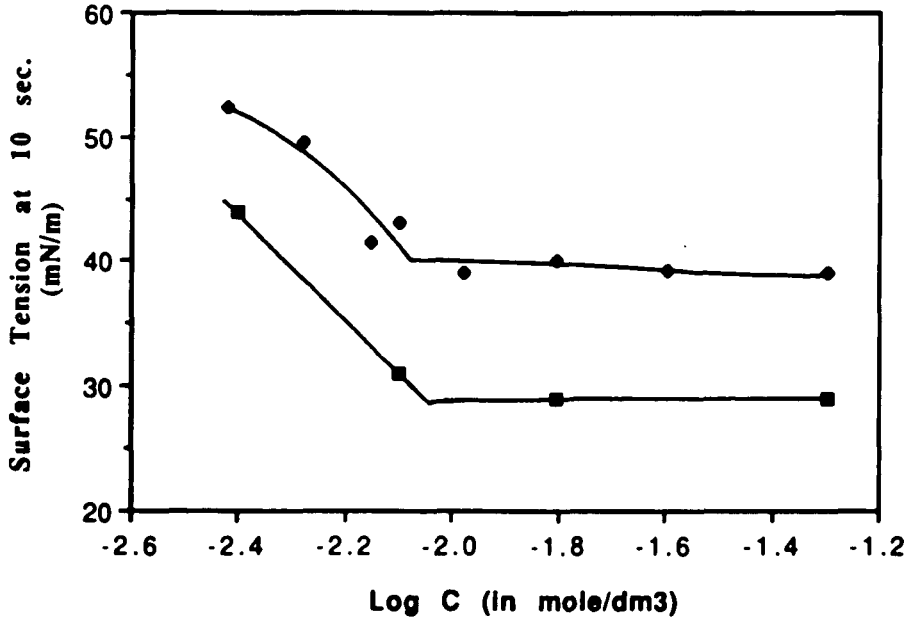

Figure 43

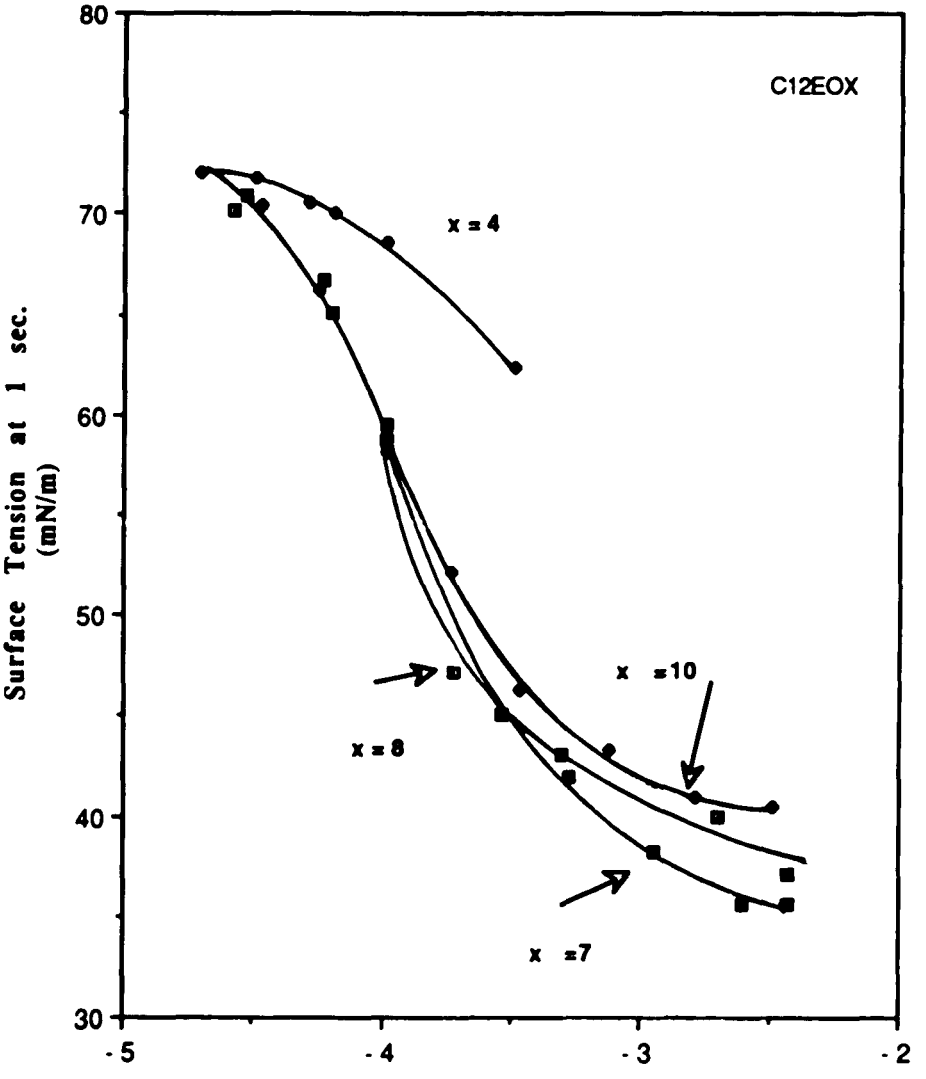
C12EOX
x = 4
x = 8
x =10
x =7
Surface Tension at 1 sec. (mN/m)
80
70
60
50
40
30
-5
-4
-3
-2
Log C (in mole/dm3)

Figure 44

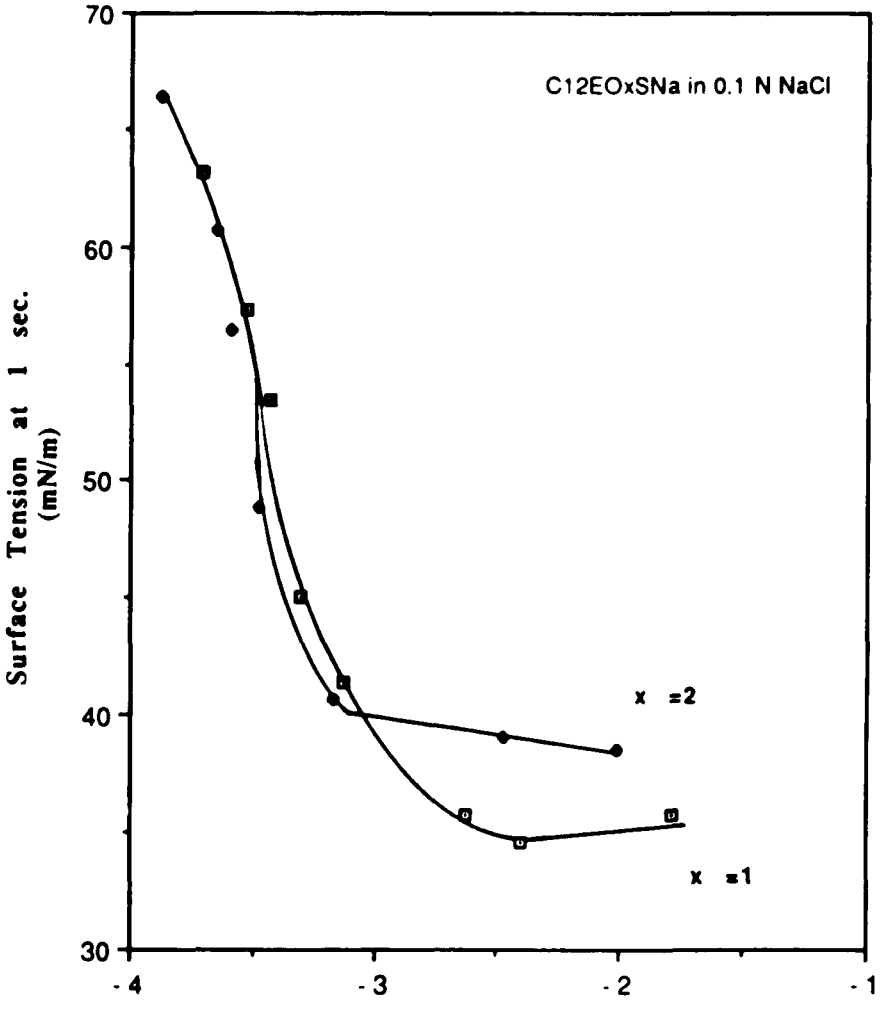
C12EOxSNa in 0.1 N NaCl
x =2
x =1
Surface Tension at 1 sec. (mN/m)
70
60
50
40
30
-4
-3
-2
-1
Log C (in mole/dm3)

Figure 45 (a)

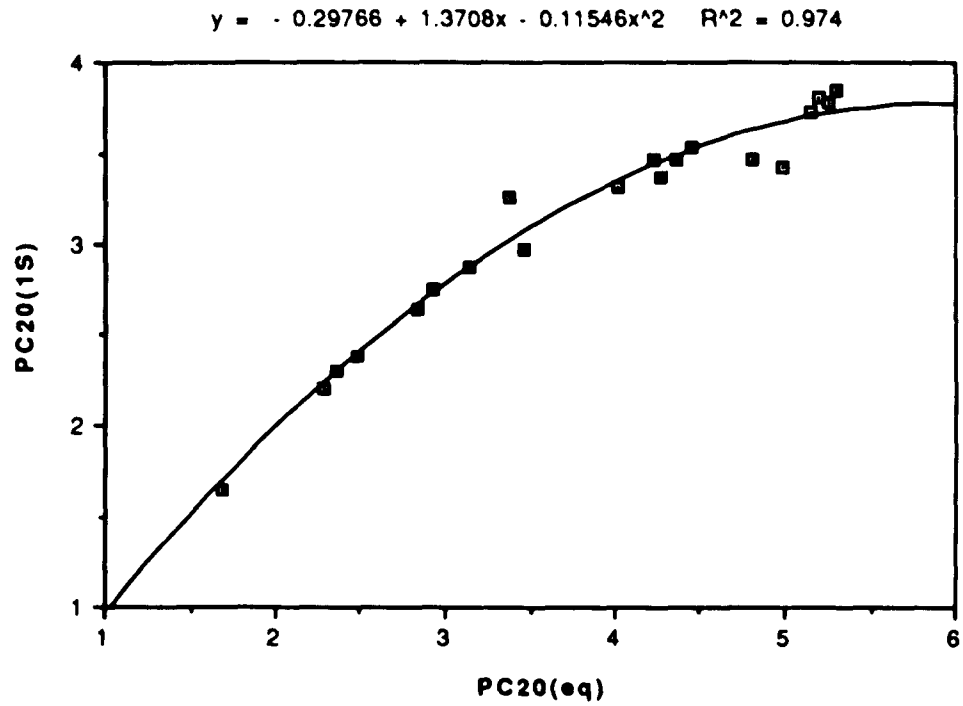

Figure 45 (b)

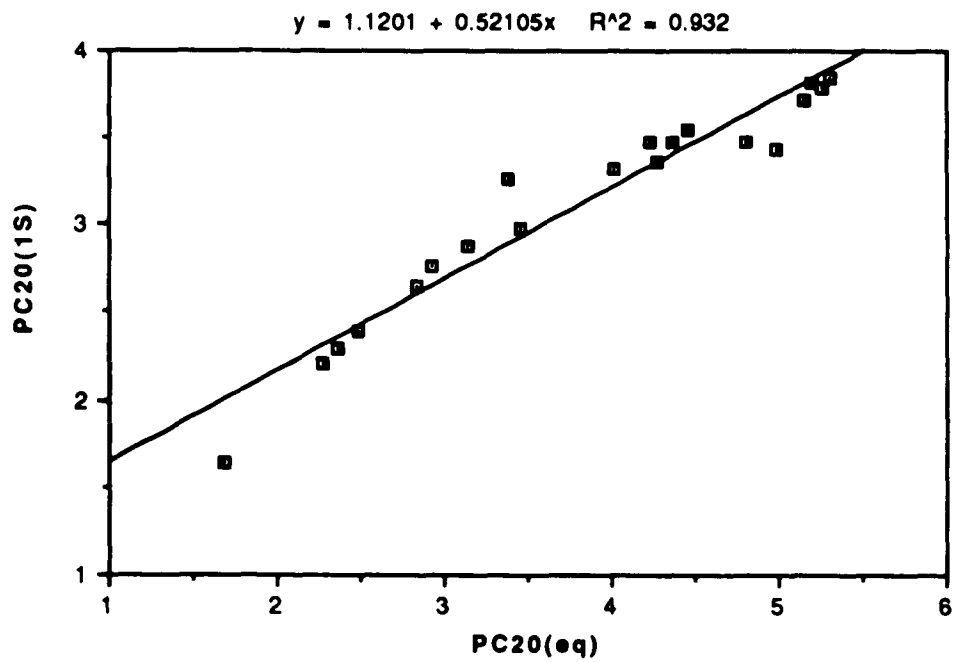

Figure 46

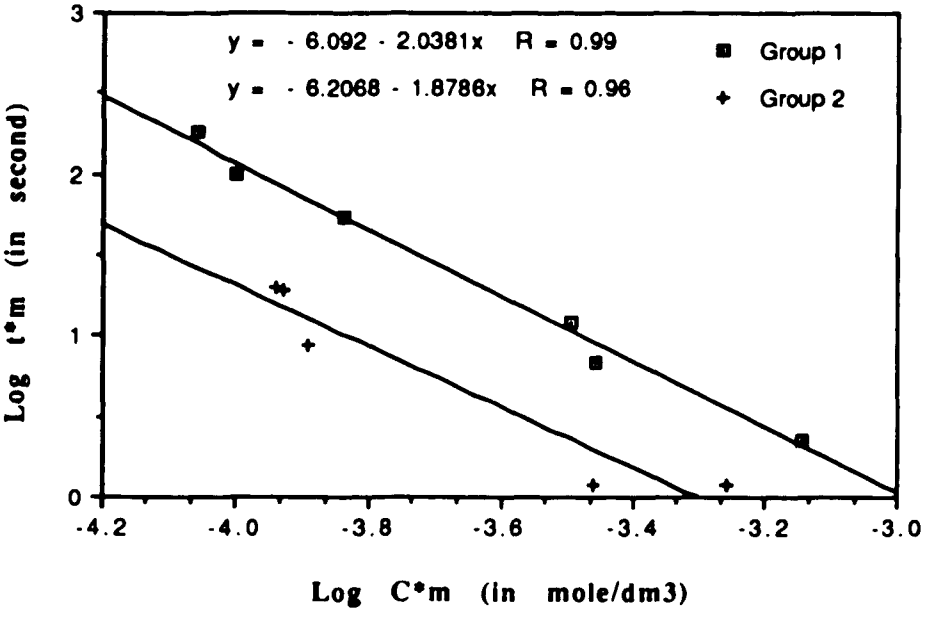

Figure 47

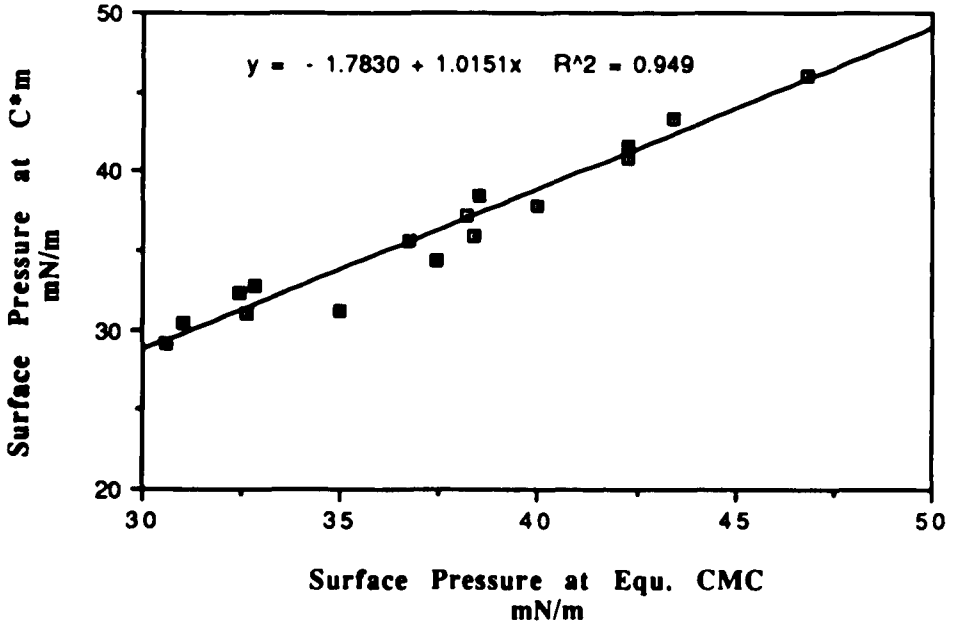

Figure 48

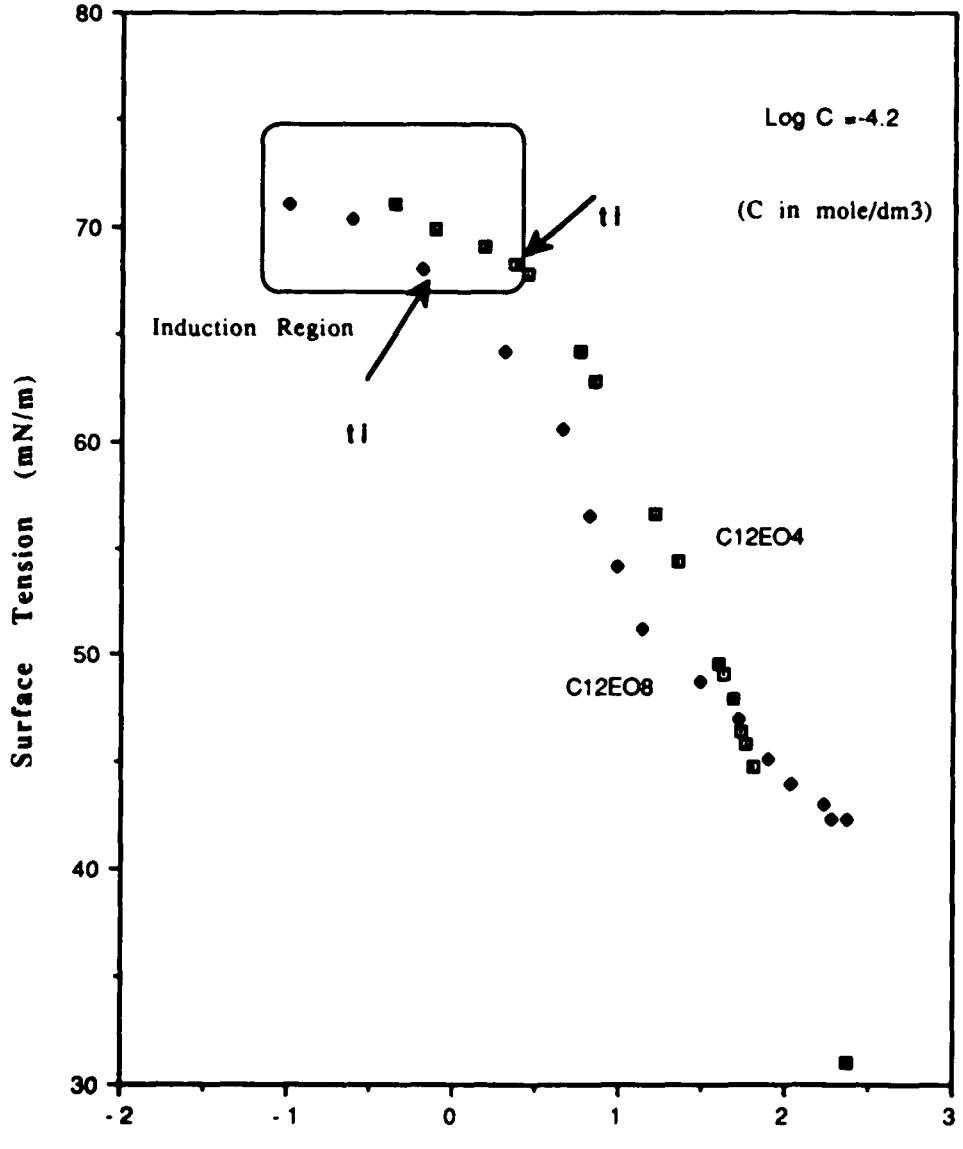
80
70
60
50
40
30
-2
-1
0
1
2
3
Surface Tension (mN/m)
Log t (in second)
Log C =-4.2
(C in mole/dm3)
Induction Region
t1
t1
C12EO4
C12EO8

Figire 49

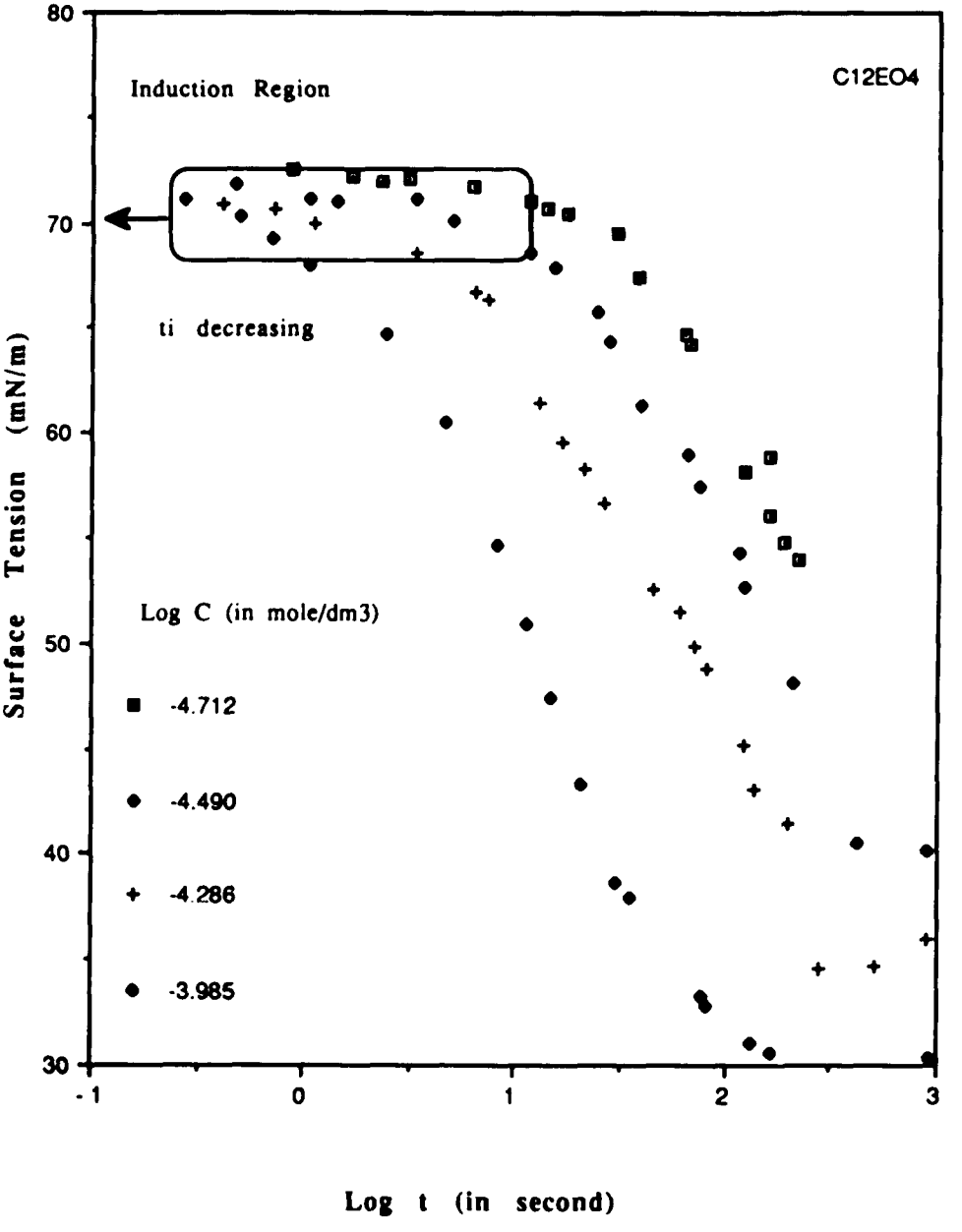
Induction Region
C12EO4
ti decreasing
Log C (in mole/dm3)
-4.712
-4.490
-4.286
-3.985
Surface Tension (mN/m)
Log t (in second)
80
70
60
50
40
30
-1
0
1
2
3

Figure 50

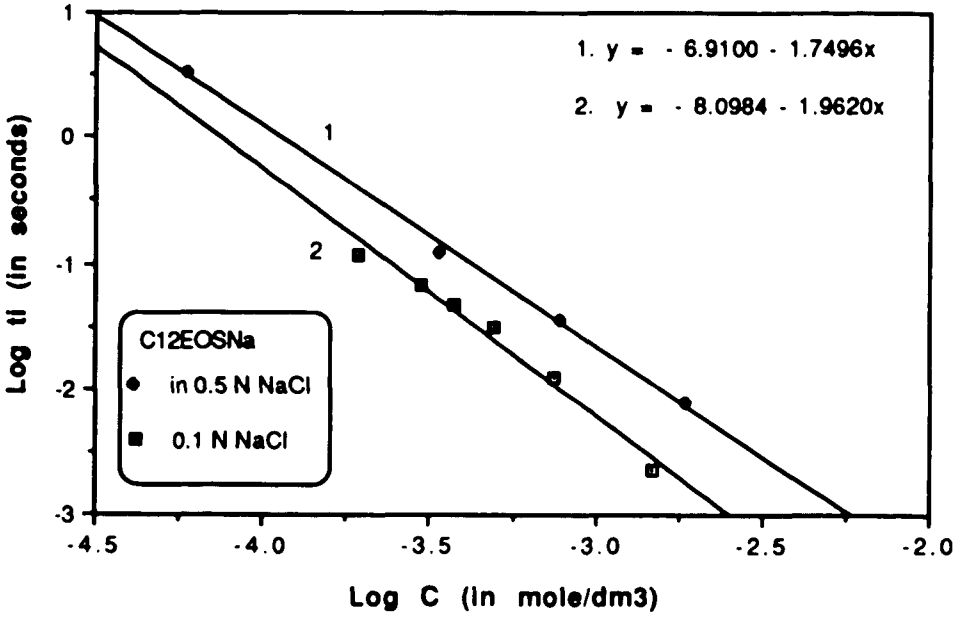

Figure 51

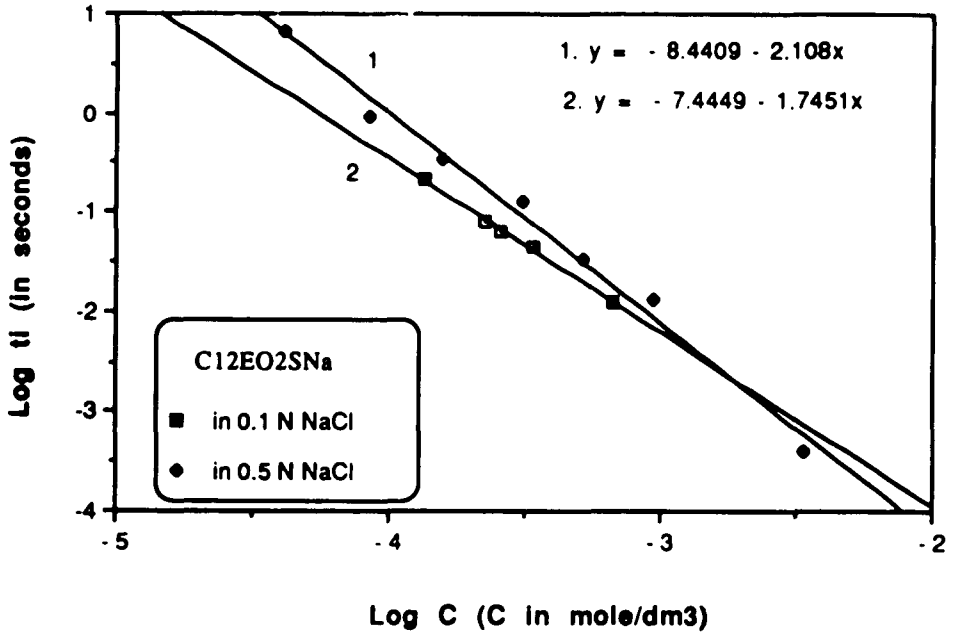

Figure 52

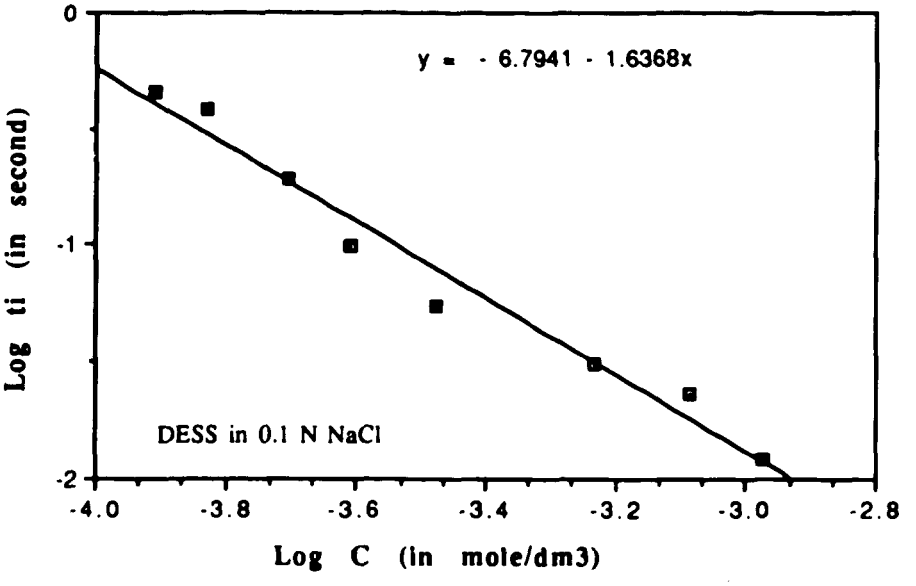

Figure 53

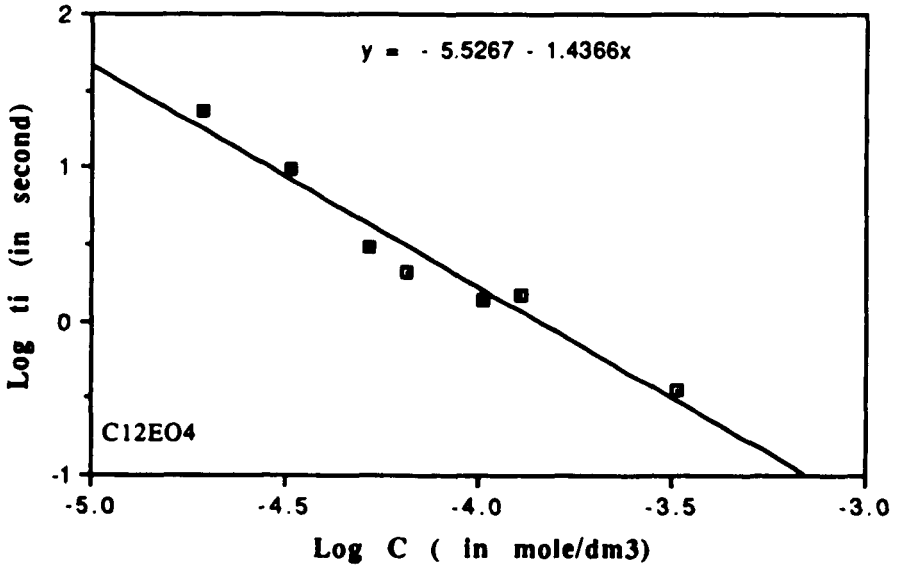

Figure 54

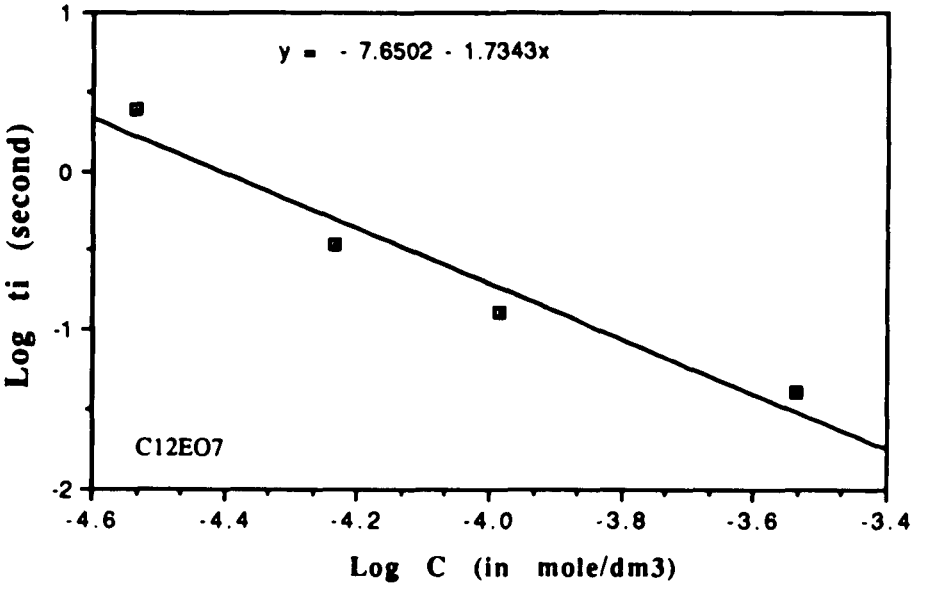

Figure 55

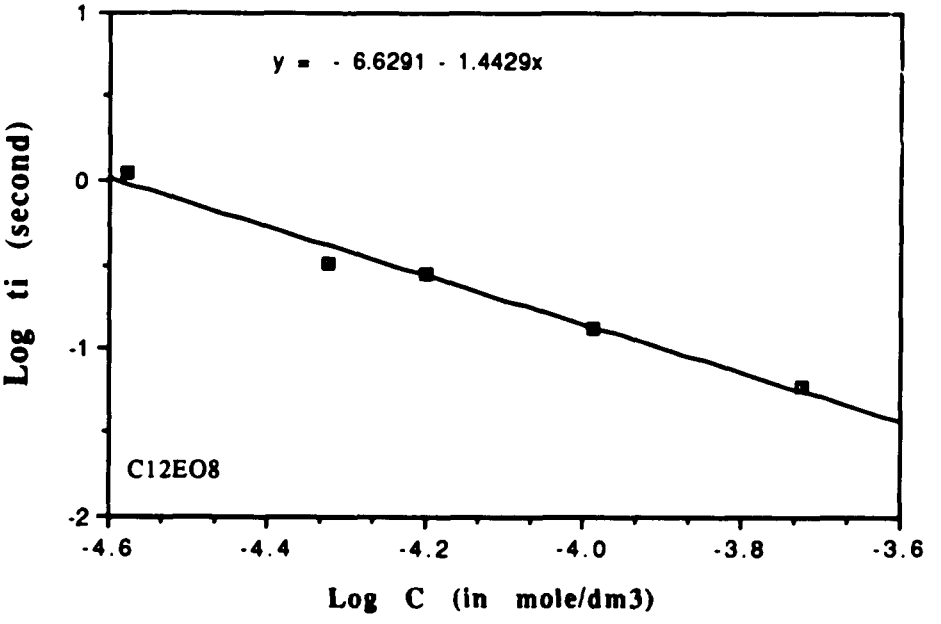

Figure 56

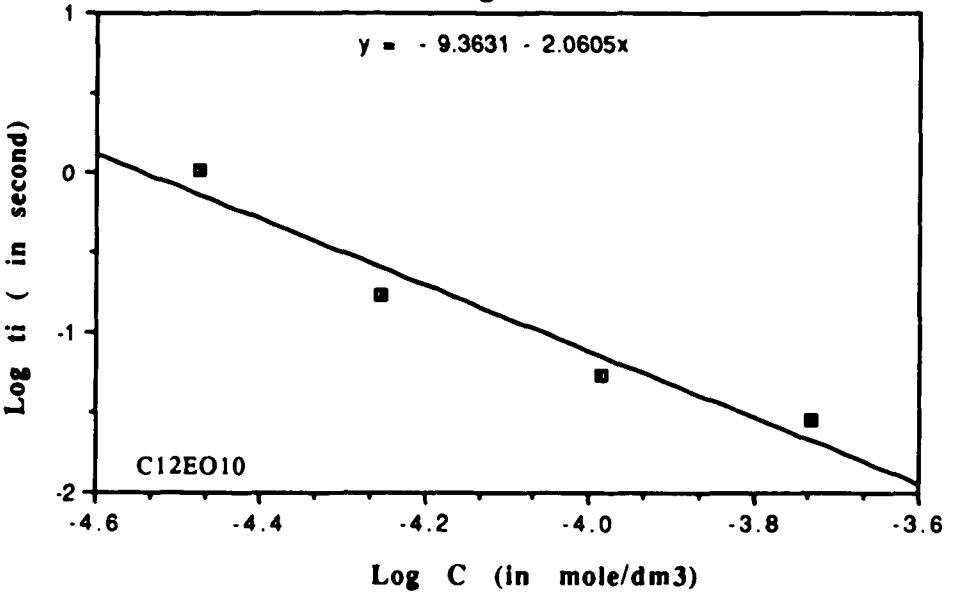

Figure 57

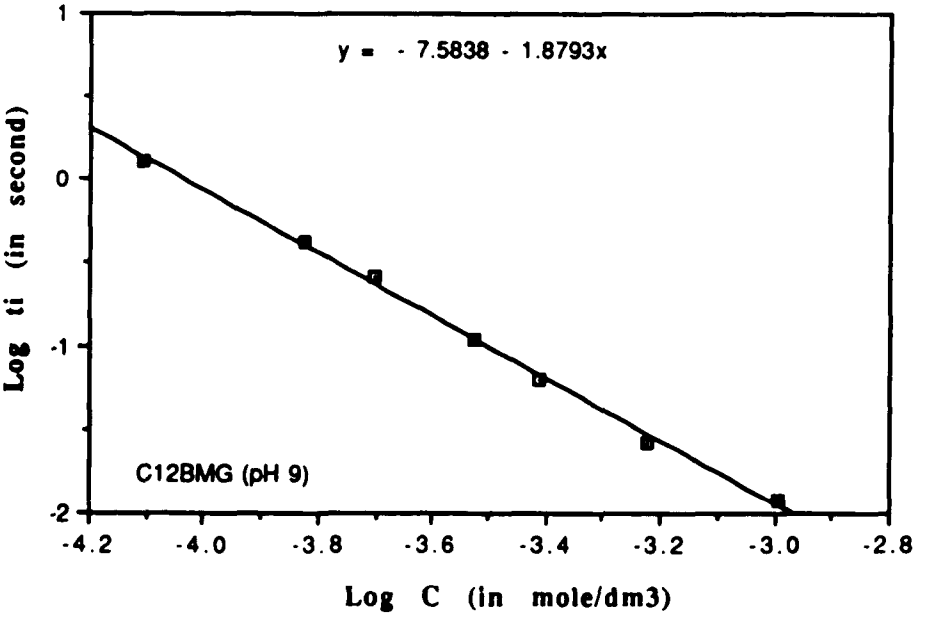

Figure 58

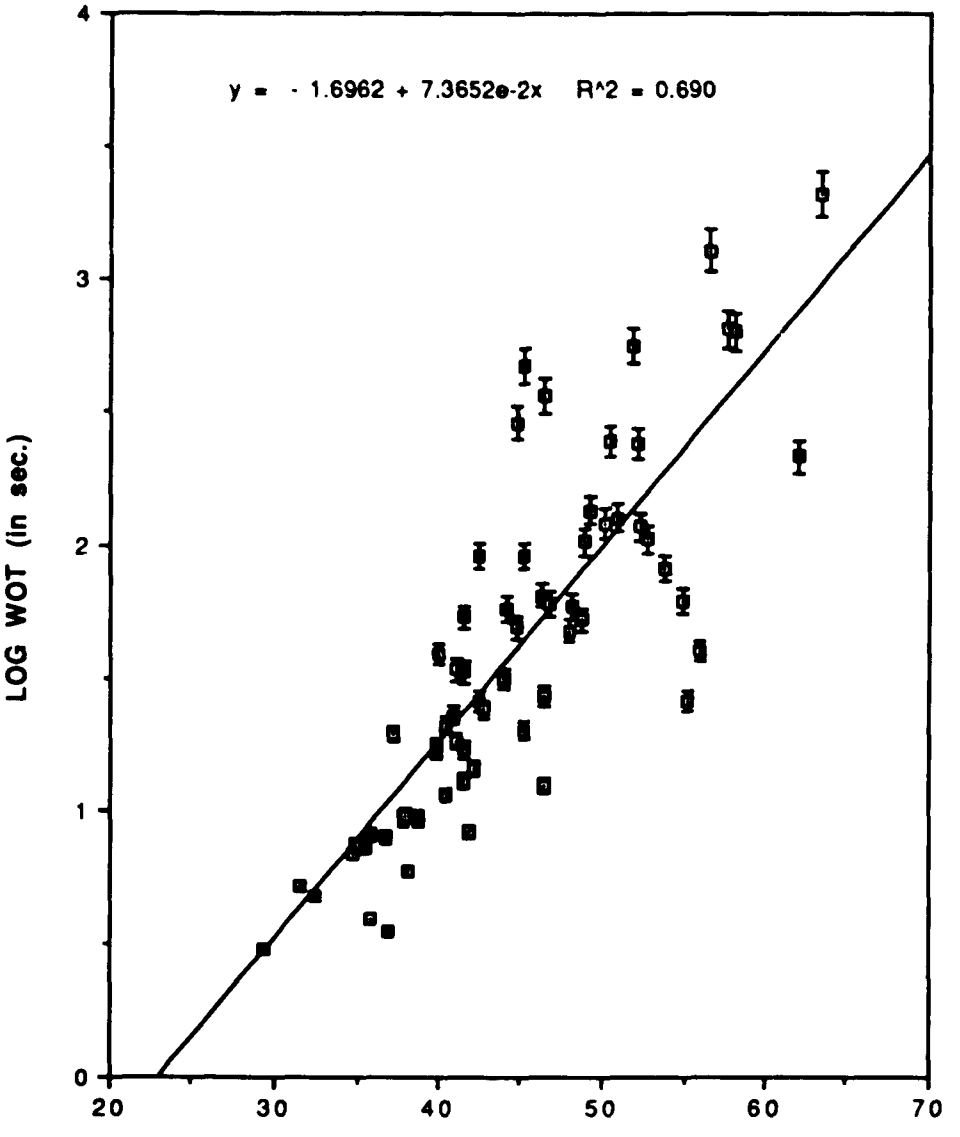
y = - 1.6962 + 7.3652e-2x R^2 = 0.690
LOG WOT (in sec.)
0
1
2
3
4
20
30
40
50
60
70
Surface Tension at 0.4 Sec.
(mN/m)

Figure 59

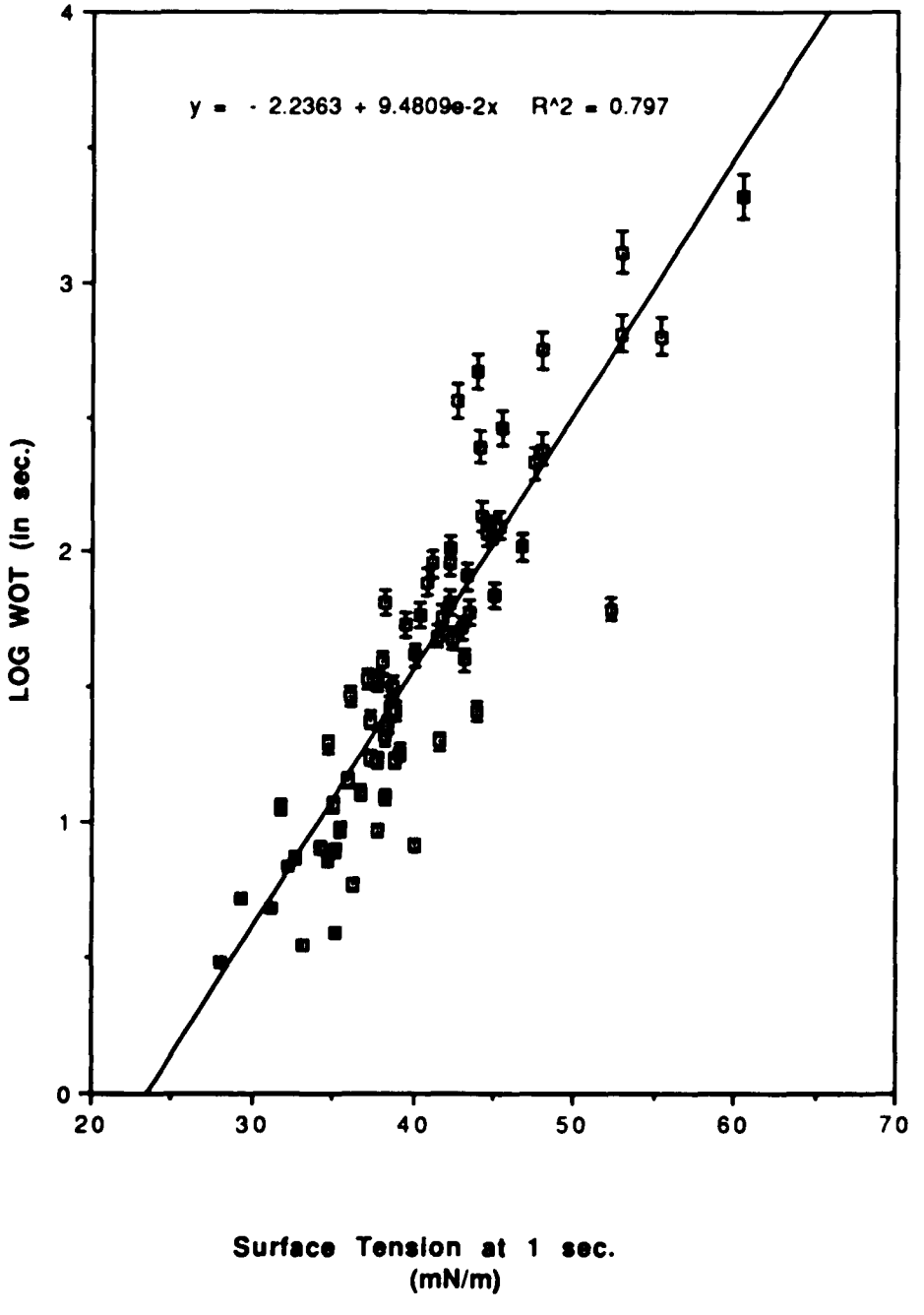
y = - 2.2363 + 9.4809e-2x R^2 = 0.797
LOG WOT (in sec.)
0
1
2
3
4
20
30
40
50
60
70
Surface Tension at 1 sec.
(mN/m)

Figure 60

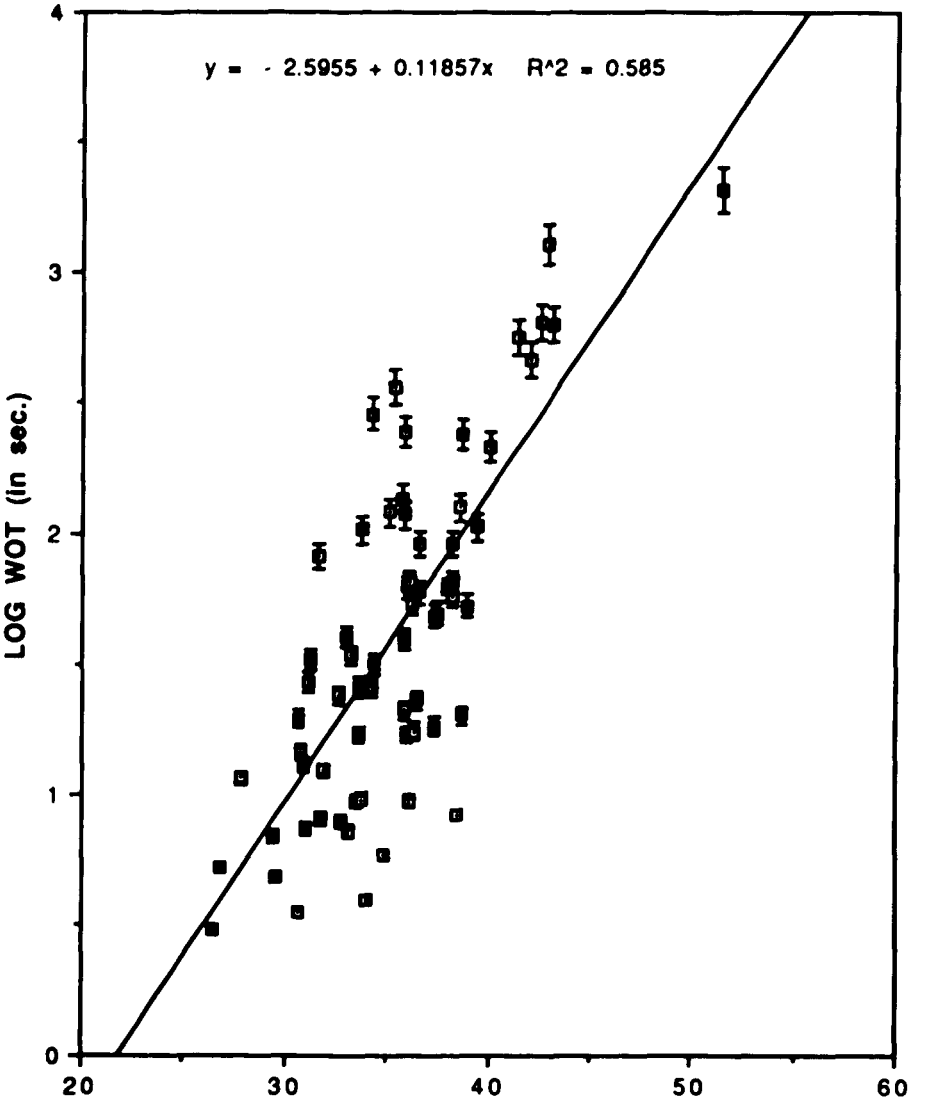
y = - 2.5955 + 0.11857x R^2 = 0.585
LOG WOT (in sec.)
0
1
2
3
4
20
30
40
50
60
Surface Tension at 10 Sec.
(mN/m)

Figure 61

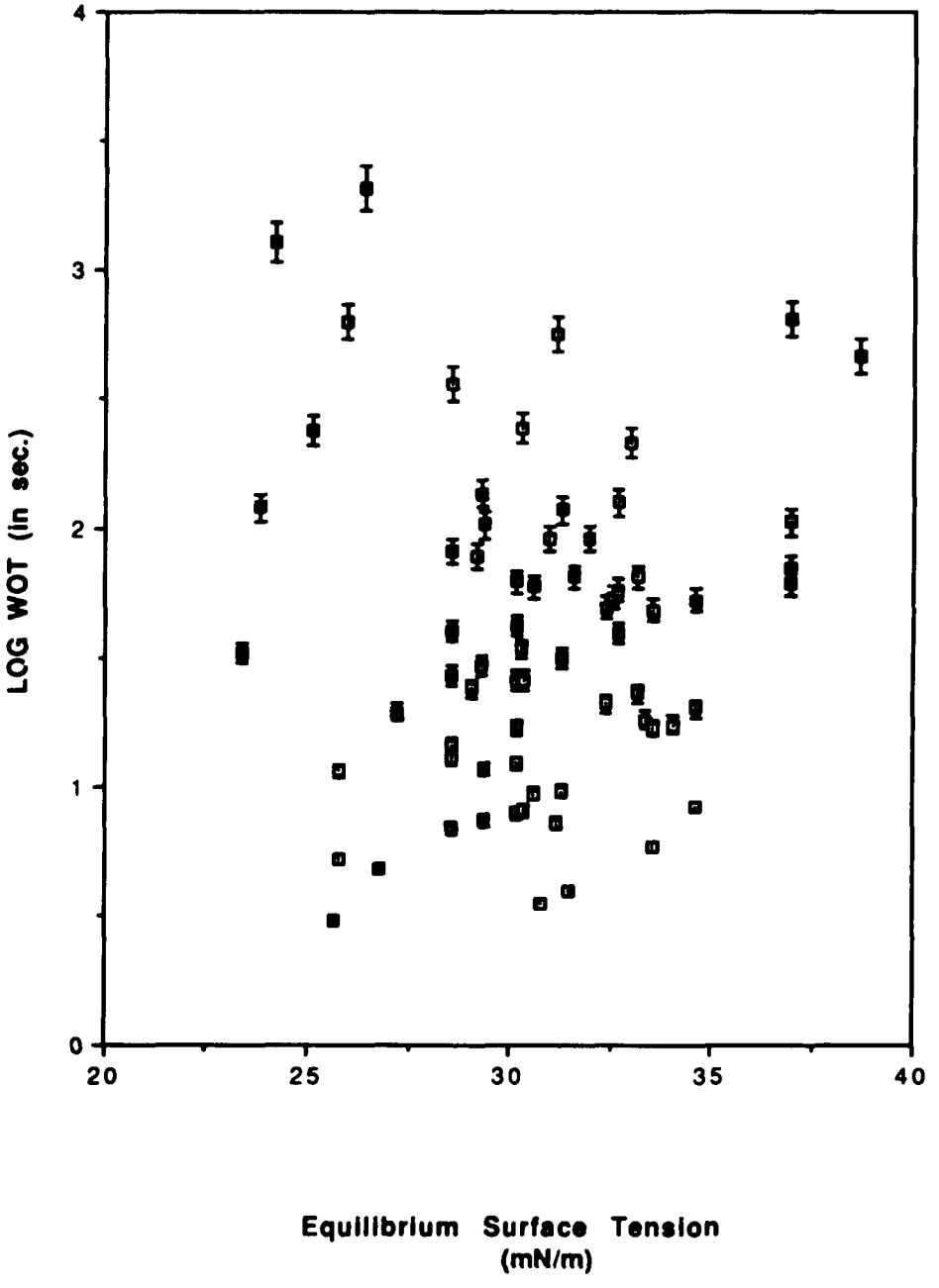
LOG WOT (in sec.)
4
3
2
1
0
20
25
30
35
40
Equilibrium Surface Tension
(mN/m)

Appendix 1

Calculation of Apparent Diffusion Coefficient

The simplified Ward and Tordai equation was used for calculation of the apparent diffusion coefficient at the induction time:

$$\Gamma_t = 2\ (D_{ap}/\pi^{1/2})(C\ t^{1/2}) \qquad [A-1]$$

where Γ_t is the surface concentration at time t, D_{ap} is the diffusion coefficient, C is the concentration in the bulk phase of the solution, π is 3.1416.

The Langmuir equation was used in the calculation of Γ_t in the equation 1, based on the assumption that the sub-surface and adsorbed film is in equilibrium.

$$\Gamma_t = \frac{\Gamma_{max}\ (b\ C_s)}{(1 + b\ C_s)} \qquad [A-2]$$

where Γ_{max} is maximum adsorption in static condition, which can be obtained from equilibrium surface tension data, b is a constant, which can be obtained from the equilibrium surface tension data by the Szyszkowski equation, C_s is the concentration of a surfactant in the sub-surface at time t, which can be obtained from the dynamic surface tension data by use of the Szyskowski equation.

The Szyskowski equation describes the relationship of equilibrium surface tension and the surfactant concentration:

$$\gamma_0 - \gamma_{eq} = \Gamma_{max} RT \ln (1 + b\ C) \qquad [A-3]$$

where γ_0 is the surface tension of solvent.

When the Szyskowski equation is used for calculation of C_s , it becomes

$$\gamma_0 - \gamma_t = \Gamma_{max} RT \ln (1 + b C_s) \qquad [A\text{-}3']$$

The assumption implied in this equation is that the equilibrium is instantaneously established between sub-surface and adsorbed film.

Appendix 2

Determining the Radius of the Capillary For Use in the Maximum Bubble Pressure Apparatus

One method to determine the radius of a capillary is by measuring the response of the transducer to pure water for a certain capillary at 25 ^{0}C. To avoid the correction for the immersion of the capillary under the liquid surface, the tip of the capillary is placed just at the water surface. The reading in voltage is convered to dyne/cm by use of the transducer constant, supplied by the manufacturer. The Laplace equation is used in the calculation:

$$\Delta p = \frac{2\gamma}{r} \qquad [1]$$

where γ is the surface tension, r the radius of a capillary, Δp the maximum pressure difference between the bubble and the atmosphere. When the surface tension of pure water is known, the radius of a capillary can be calculated simply by measuring Δp, which can be obtained from the response of the transducer. Thus,

$$r = \frac{2 \times 72.0 \text{ dyne/cm}}{\text{reading (v)} \times 2.999 \text{ (W.H.in IN/ v)} \times 2.4908 \times 10^3 \text{ dyne/cm}^2 \cdot \text{IN}}$$

----------[2]

where W.H. is the water column height in inch, IN is inch, V is voltage, r is the radius of the capillary. Multiplying the reading in voltage by the transducer constant, 2.999 W.H. in IN per voltage, converts its unit to W.H. in IN; multiplying the factor, 2.4908×10^3 dyne/cm^2. IN, converts the unit to dyne/cm. Thus, the denominator in equation 2 is Δp in dyne/cm^2, the surface tension of pure water at 25 ^{0}C is 72.0 dyne/cm.

Appendix 3: Data Tables

Data in Appendix 3 were measured at 25 ^{0}C. The symbols are: γ_{1s}, surface tension at 1 second; γ_m, surface tension at meso-equilibrium; γ_{eq}, surface tension at equilibrium; C, surfactant concentration in mole/dm^3.

Table A-I
Dynamic and Equilibrium Surface Tension of $C_{12}EO4$ in Water

Log C	γ_{1s} mN/m	γ_m mN/m	γ_{eq} mN/m
-4.712	72.0	47.0	39.2
-4.490	71.8	40.3	34.8
-4.286	70.6	34.6	30.7
-4.189	70.0	31.3	28.6
-3.985	69.5	28.8	28.6
-3.888	69.5	28.8	28.6
-3.490	62.3	27.7	28.6

Table A- II

Dynamic and Equilibrium Surface Tension of $C_{12}EO7$ in Water

Log C	γ_{1s} mN/m	γ_m mN/m	γ_{eq} mN/m
-4.536	70.9	45.1	41.0
-4.235	66.7	39.3	36.0
-3.986	59.5	36.9	33.6
-3.536	45.1	36.1	33.6
-3.277	42.0	35.7	33.6
-2.944	38.2	35.0	33.6
-2.608	35.6	34.4	33.6
-2.424	35.6	34.4	33.6

Table A- III

Dynamic and Equilibrium Surface Tension of $C_{12}EO8$ in Water

Log C	γ_{1s} mN/m	γ_m mN/m	γ_{eq} mN/m
-4.577	70.2	51.5	43.3
-4.325	Nb	46.7	39.6
-4.201	65.1	41.3	37.9
-3.986	58.7	39.0	34.9
-3.723	47.2	38.2	34.6
-3.306	43.1	37.6	34.6
-2.704	40.0	37.6	34.6
-2.424	37.1	36.4	34.6

Table A-IV

Dynamic and Equilibrium Surface Tension of $C_{12}EO10$ in Water

Log C	γ_{1s} mN/m	γ_m mN/m	γ_{eq} mN/m
-4.475	70.4	48.1	43.8
-4.253	66.2	45.5	41.0
-3.986	58.1	41.4	37.7
-3.730	52.1	40.8	37.0
-3.475	46.3	40.7	37.0
-3.123	43.3	40.5	37.0
-2.788	41.0	39.0	37.0
-2.487	40.4	39.0	37.0

Table A-V

Dynamic and Equilibrium Surface Tension of C_{12}BMG in Water (pH 9)

Log C	γ_{1s} mN/m	γ_m mN/m	γ_{eq} mN/m
-4.108	70.7	48.4	46.6
-3.826	64.5	44.8	41.9
-3.701	59.0	41.9	39.8
-3.525	48.6	39.9	36.8
-3.410	43.6	37.3	34.9
-3.244	36.7	34.8	32.8
-2.992	36.5	34.6	32.8
-2.792	35.0	33.9	32.8
-2.419	33.9	32.9	32.8

Table A-VI

Dynamic and Equilibrium Surface Tension of C_{14}BMG in Water (pH 9)

Log C	γ_{1s} mN/m	γ_m mN/m	γ_{eq} mN/m
-4.478	Nb	39.5	38.4
-4.294	Nb	36.4	33.9
-4.268	Nb	36.0	33.5
-4.219	Nb	35.4	32.2
-4.127	>71	33.4	31.7
-3.993	71	32.6	31.7

Table A-VII

Dynamic and Equilibrium Surface Tension of $C_{12}SO_4Na$ in water

Log C	γ_{1s} mN/m	γ_m mN/m	γ_{eq} mN/m
-2.419	53.2	52.8	49.8
-2.278	49.6	49.2	45.4
-2.102	44.0	43.0	39.4
-2.152	42.0	42.0	39.4
-1.979	39.6	38.9	39.4
-1.803	41.6	40.1	39.4
-1.597	40.4	39.7	39.4
-1.296	40.0	39.3	39.4

Table A-VIII

Dynamic and Equilibrium Surface Tension of $C_{12}EOSNa$ in water

Log C	γ_{1s} mN/m	γ_m mN/m	γ_{eq} mN/m
-2.731	55.7	54.0	49.4
-2.607	50.5	48.6	45.3
-2.430	43.0	41.5	39.8
-2.270	43.0	41.5	39.2
-2.174	No	39.8	39.2
-2.094	40.4	39.1	39.2
-1.793	40.4	39.1	39.2

Table A-IX

Dynamic and Equilibrium Surface Tension of $C_{12}EOSNa$ in Aqueous 0.1 N NaCl

Log C	γ_{1s} mN/m	γ_m mN/m	γ_{eq} mN/m
-3.713	63.2	46.7	41.8
-3.527	57.3	43.4	37.6
-3.430	53.5	40.9	35.3
-3.305	45.0	35.5	33.7
-3.129	41.4	36.3	33.7
-2.828	35.8	34.2	33.7
-2.420	34.6	34.2	33.7
-1.793	35.8	33.0	33.7

Table A-X

Dynamic and Equilibrium Surface Tension of $C_{12}EOSNa$ in Aqueous 0.5 N NaCl

Log C	γ_{1s} mN/m	γ_m mN/m	γ_{eq} mN/m
-4.223	72.0	45.5	39.0
-3.922	68.5	39.1	30.6
-3.471	53.9	30.9	30.6
-3.107	38.5	31.2	30.6
-2.731	33.0	30.6	30.6
-1.961	33.1	32.0	30.6

Table A-XI

Dynamic and Equilibrium Surface Tension of $C_{12}EO_2SNa$ in water

Log C	γ_{1s} mN/m	γ_m mN/m	γ_{eq} mN/m
-2.777	52.9	51.1	47.9
-2.652	48.5	46.4	44.5
-2.476	43.6	42.9	41.4
-2.294	44.0	43.4	41.4
-2.044	43.5	42.5	41.4
-1.692	42.4	41.2	41.4

Table A-XII

Dynamic and Equilibrium Surface Tension of $C_{12}EO_2SNa$ in Aqueous 0.1 N NaCl

Log C	γ_{1s} mN/m	γ_m mN/m	γ_{eq} mN/m
-3.874	66.4	44.8	42.7
-3.652	60.7	45.3	38.3
-3.590	56.4	41.9	36.9
-3.476	48.9	36.8	35.6
-3.175	40.7	36.2	35.6
-2.476	39.1	36.6	35.6
-2.018	38.5	36.6	35.6

Table A-XIII

Dynamic and Equilibrium Surface Tension of $C_{12}EO_2SNa$ in Aqueous 0.5 N NaCl

Log C	γ_{1s} mN/m	γ_m mN/m	γ_{eq} mN/m
-4.387	72.6	44.5	41.3
-4.070	70.6	40.7	34.9
-3.807	64.0	34.6	32.9
-3.506	54.7	34.9	32.9
-3.284	47.2	34.9	32.9
-3.029	41.1	34.6	32.9
-2.476	36.7	34.4	32.9
-2.347	33.2	34.4	32.9
-2.046	33.2	34.4	32.9

Table A-XIV

Dynamic and Equilibrium Surface Tension of DESS in water

Log C	γ_{1s} mN/m	γ_m mN/m	γ_{eq} mN/m
-3.476	59.5	52.6	45.7
-3.233	49.5	47.1	41.0
-3.044	42.6	40.5	37.3
-2.902	38.7	36.6	34.7
-2.610	31.6	31.0	29.7
-1.941	29.4	29.3	29.7

Table A-XV

Dynamic and Equilibrium Surface Tension of DESS in Aqueous 0.1 N NaCl

Log C	γ_{1s} mN/m	γ_m mN/m	γ_{eq} mN/m
-3.911	60.6	32.1	31.7
-3.832	56.3	31.0	30.6
-3.707	43.0	29.7	28.8
-3.610	36.9	28.0	27.6
-3.476	31.3	26.2	25.9
-3.233	28.2	26.7	25.6
-3.087	27.2	26.2	25.6
-2.973	27.0	26.2	25.6
-2.418	26.5	25.2	25.6
-1.941	25.6	25.6	25.6

Table A-XVI

Dynamic and Equilibrium Surface Tension of $C_{12}SNa$ in Aqueous 0.1 N NaCl

Log C	γ_{1s} mN/m	γ_m mN/m	γ_{eq} mN/m
-3.529	61.9	55.3	55.4
-3.432	56.5	53.0	53.4
-3.277	53.9	50.3	50.4
-3.198	49.7	47.6	48.5
-2.919	46.4	43.3	42.3
-2.773	42.4	40.6	39.0
-2.664	40.8	38.6	36.6

Table A-XVII

Dynamic and Equilibrium Surface Tension of n-C_8PY in Water

Log C	γ_{1s} mN/m	γ_m mN/m	γ_{eq} mN/m
-2.185	29.0	28.8	29.0
-2.301	35.0	34.2	30.8
-2.602	44.0	42.2	38.7
-3.000	54.2	51.8	48.7
-3.363	62.8	56.9	Nb

Table A-XVIII

Dynamic and Equilibrium Surface Tension of n-C_{10}PY in Water

Log C	γ_{1s} mN/m	γ_m mN/m	γ_{eq} mN/m
-4.018	70.8	Nb	45.3
-3.598	67.7	Nb	34.7
-3.496	64.5	Nb	32.2
-3.362	46.3	Nb	28.6

Table A-XIX

Dynamic and Equilibrium Surface Tension of $C_{10}SNa$ in Water

Log C	γ_{1s} mN/m	γ_m mN/m	γ_{eq} mN/m
-1.853	60.2	58.8	57.5
-1.677	54.4	53.2	51.8
-1.500	47.6	46.8	45.5
-1.375	43.6	43.3	41.5
-1.000	41.6	41.0	41.0
-0.523	40.0	39.3	Nb
-0.301	39.2	38.7	Nb

Table A-XX

Dynamic and Equilibrium Surface Tension of $C_{10}SNa$ in Aqueous 0.1 N NaCl

Log C	γ_{1s} mN/m	γ_m mN/m	γ_{eq} mN/m
-2.074	51.3	50.4	47.7
-1.853	46.4	45.7	43.2
-1.677	42.8	42.0	39.6
-1.375	41.8	41.2	39.4
-1.000	41.6	41.0	Nb

Table A-XXI

Dynamic and Equilibrium Surface Tension of C_{10}BMG in Water (pH 9)

Log C	γ_{1s} mN/m	γ_m mN/m	γ_{eq} mN/m
-2.977	52.1	49.5	45.5
-2.579	43.5	42.0	38.0
-2.278	37.6	37.1	33.6
-2.113	36.7	36.3	33.6
-1.702	36.1	36.1	Nb
-1.446	35.7	35.3	Nb

Figure A-1

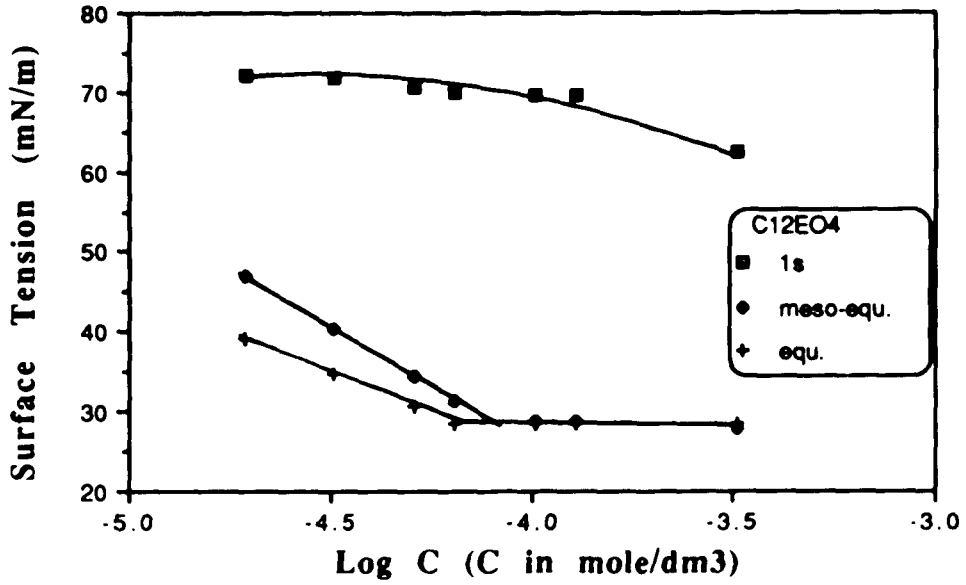

Figure A-2

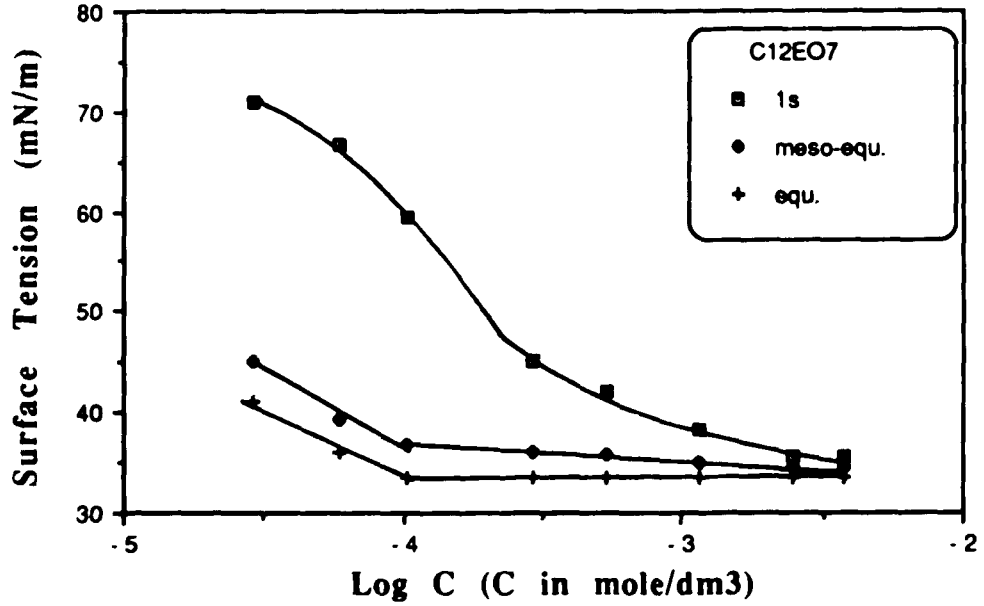

Figure A-3

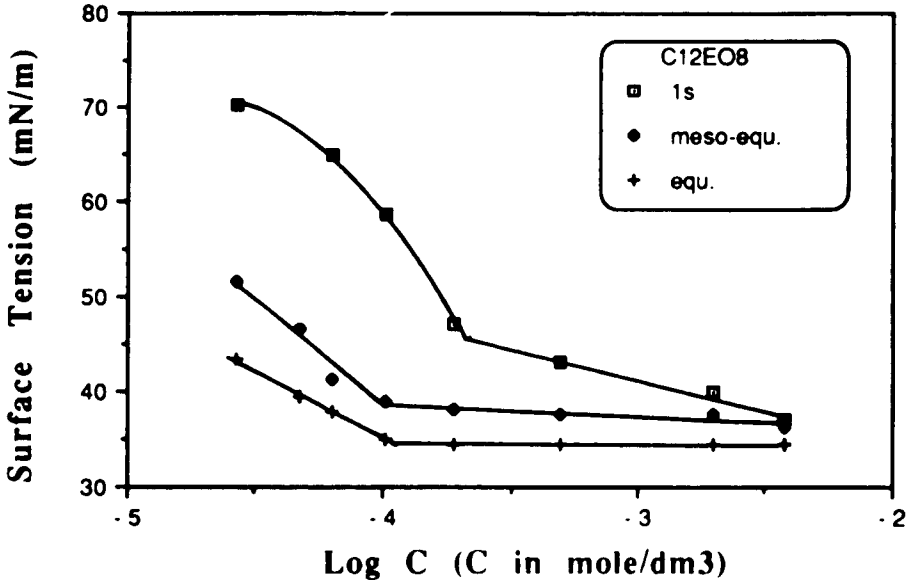

Figure A-4

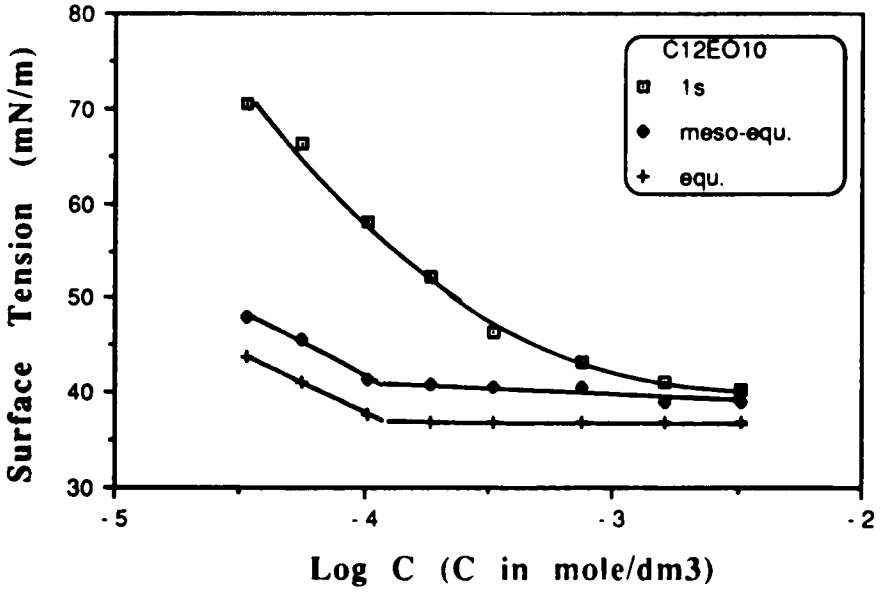

Figure A-5

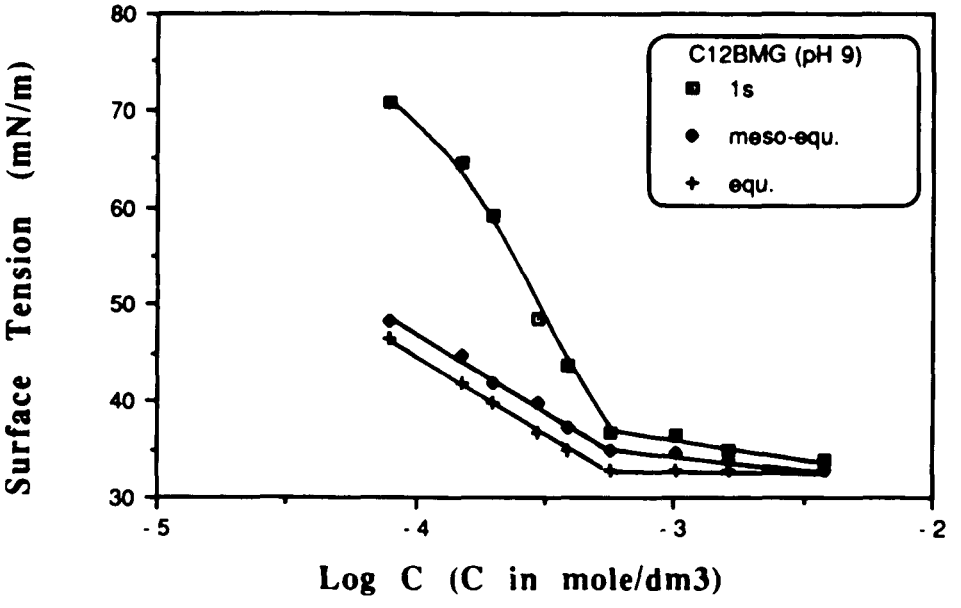

Figure A-6

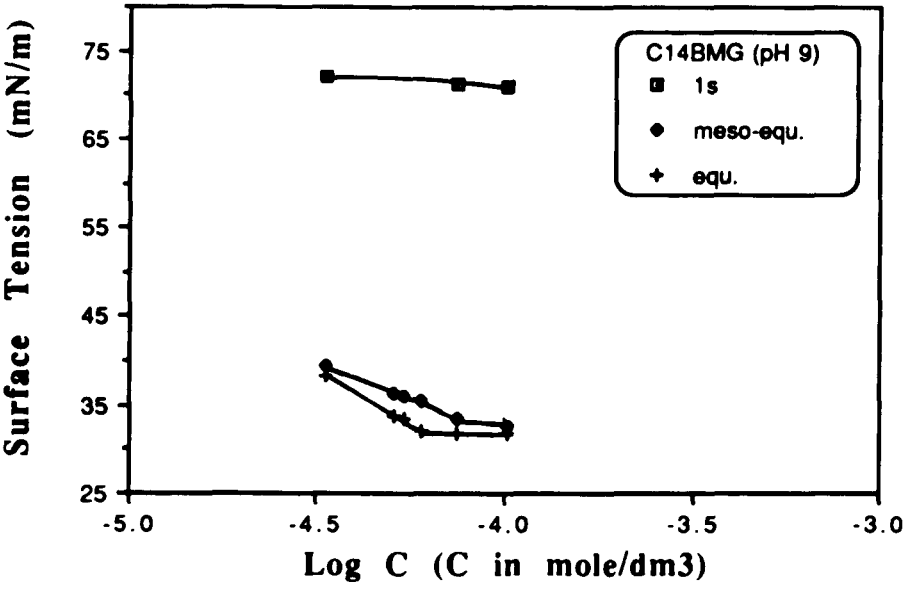

Figure A-7

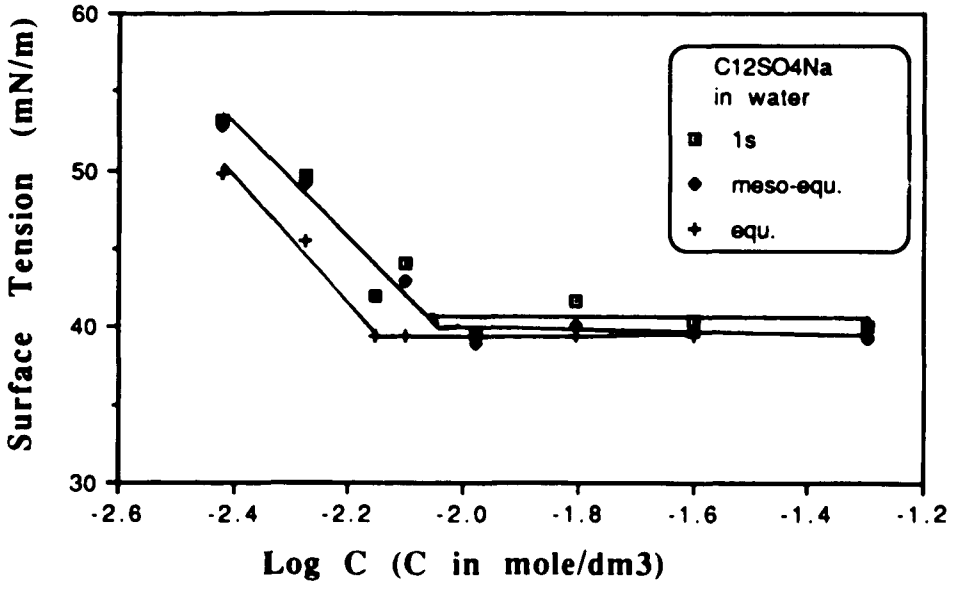

Figure A-8

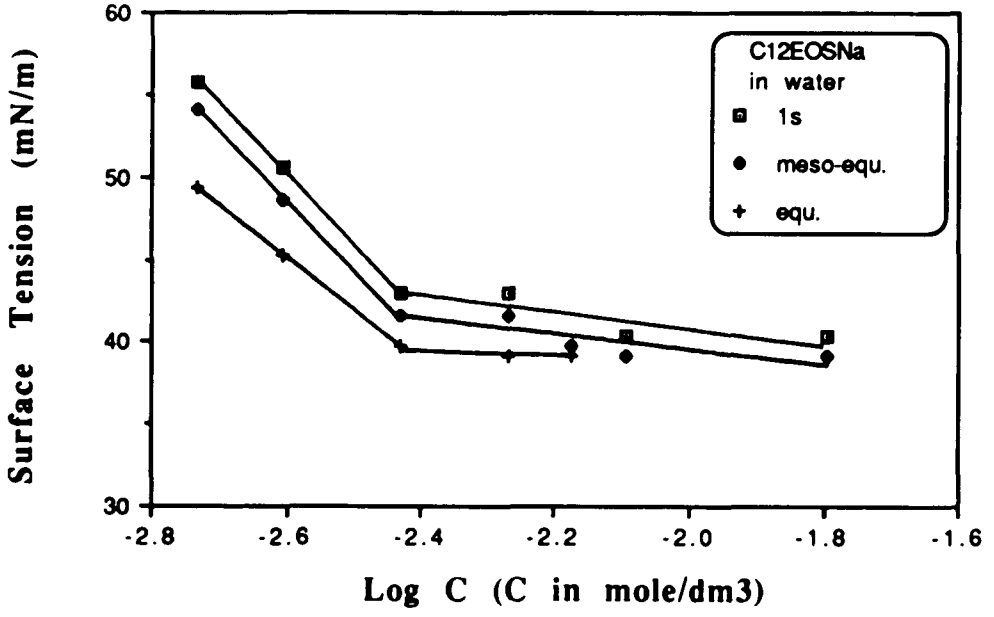

Figure A-9

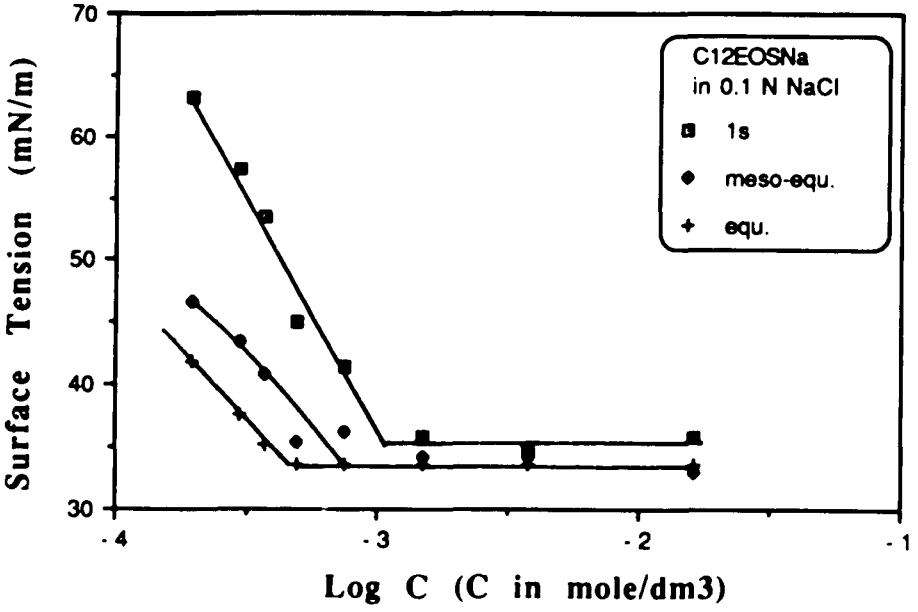

Figure A-10

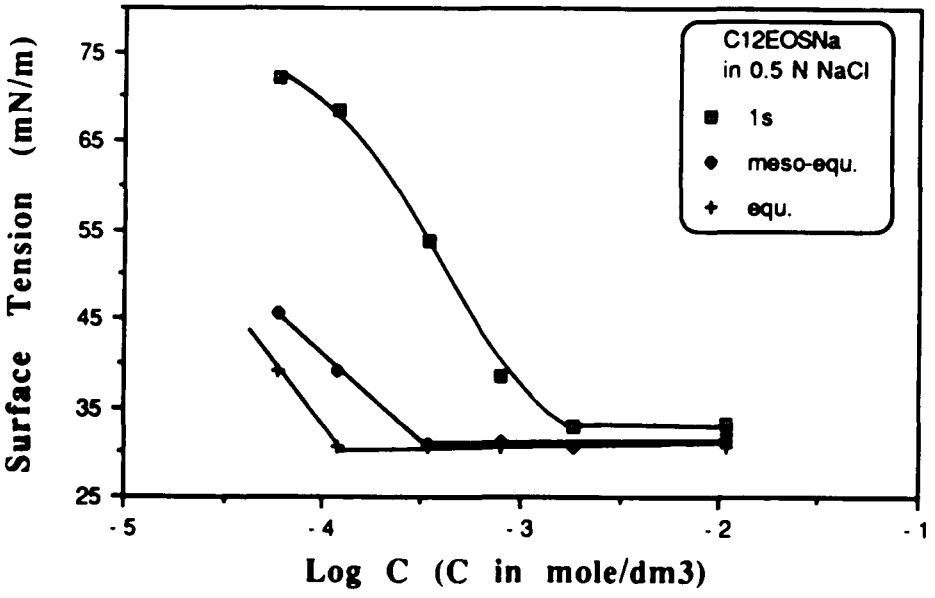

Figure A-11

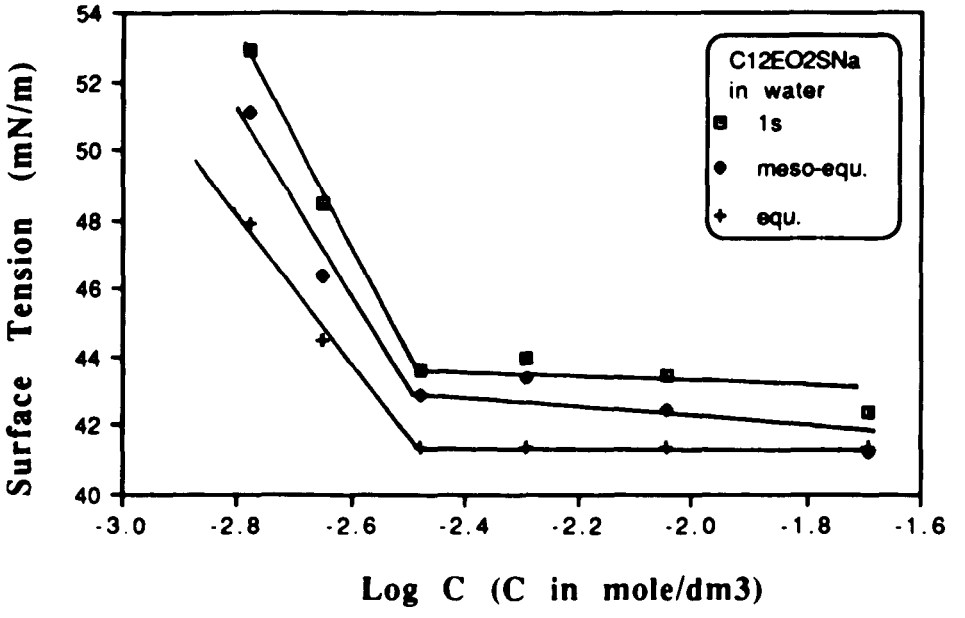

Figure A-12

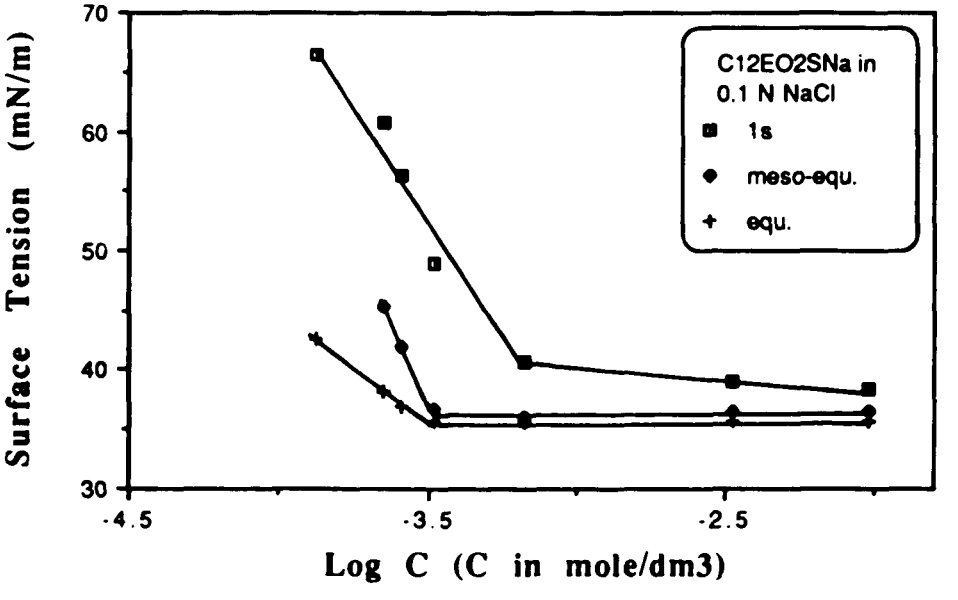

Figure A-13

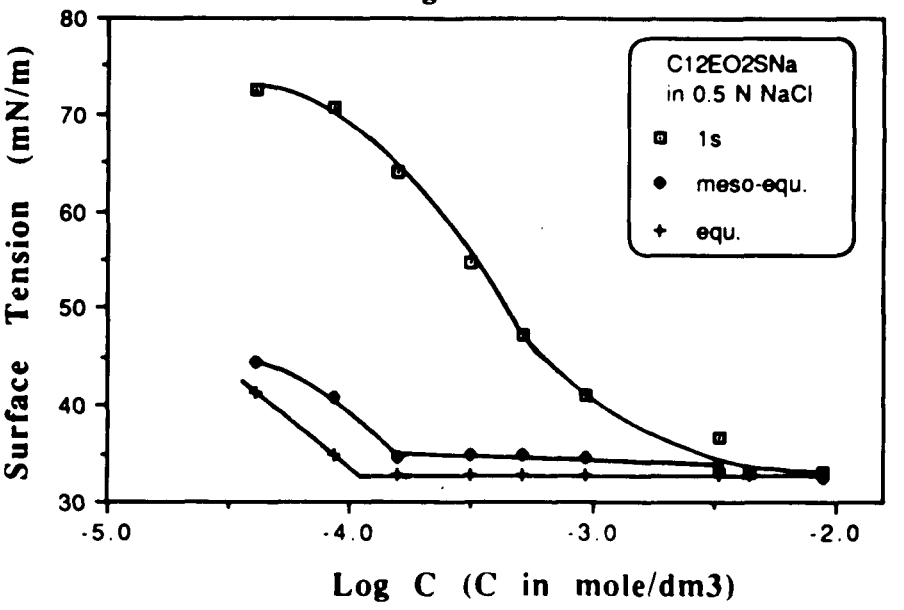

Figure A-14

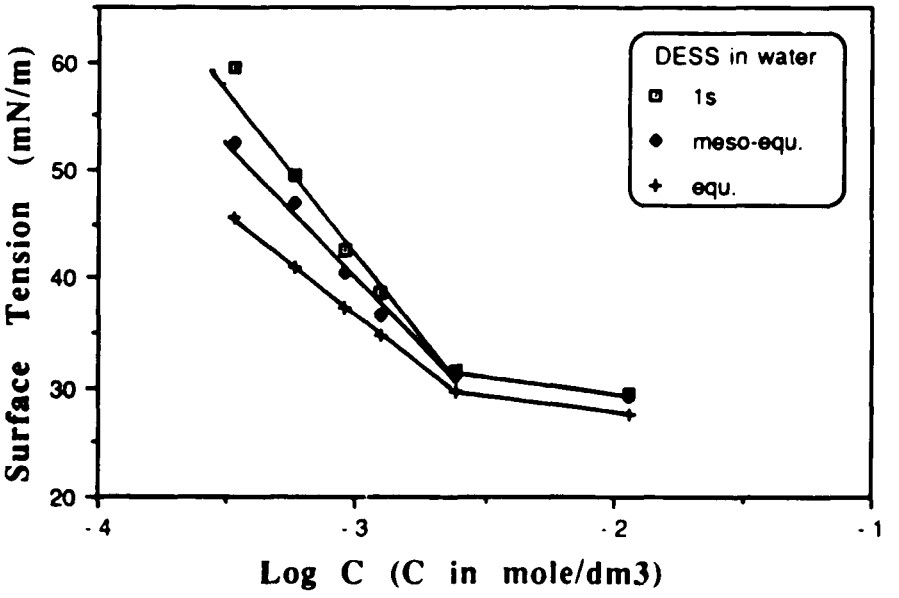

Figure A-15

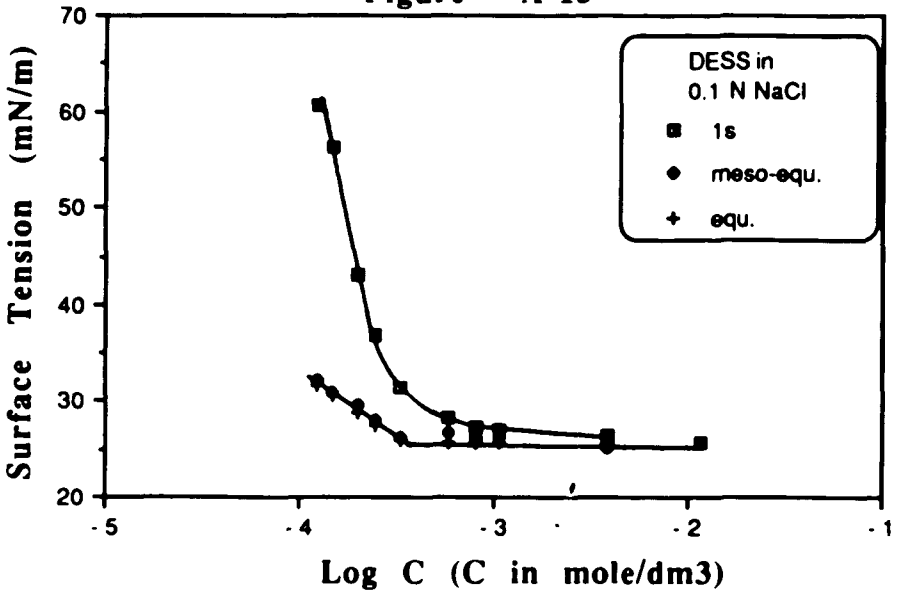

Figure A-16

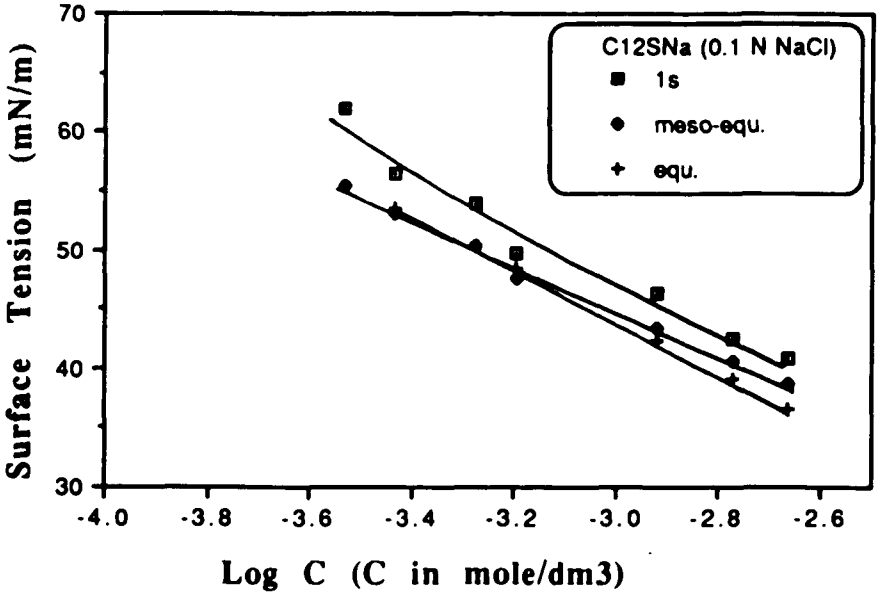

Figure A-17

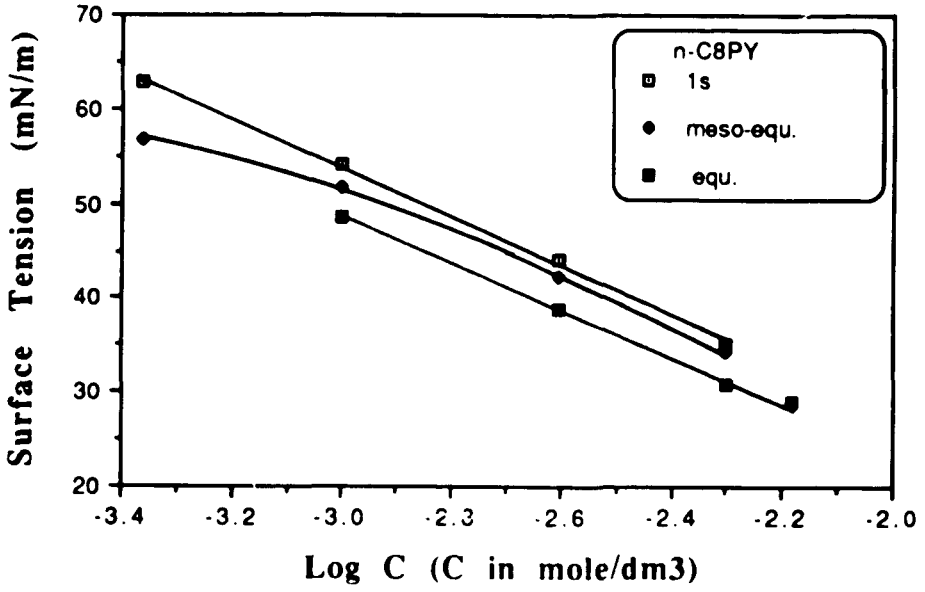

Figure A-18

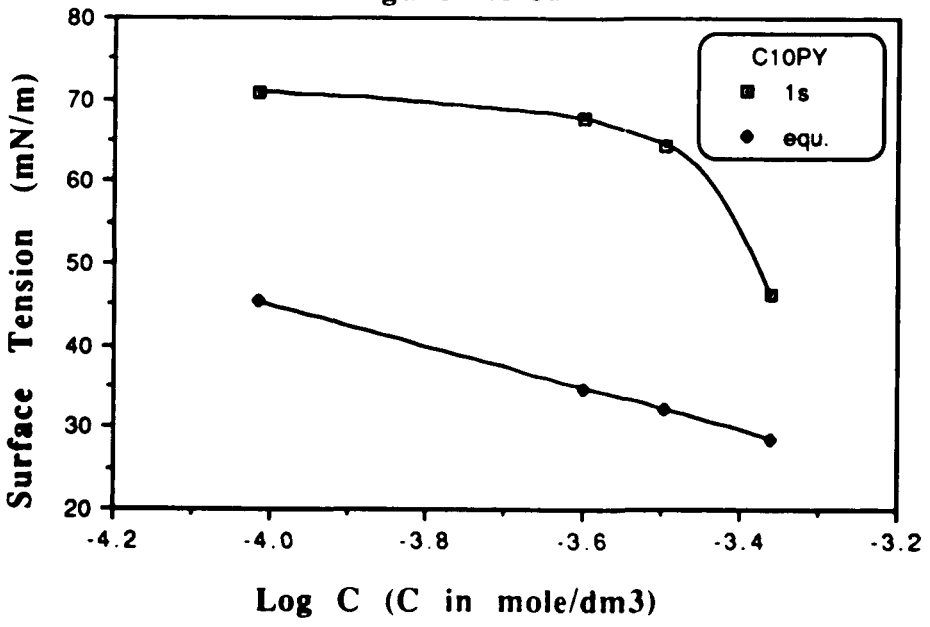

Figure A-19

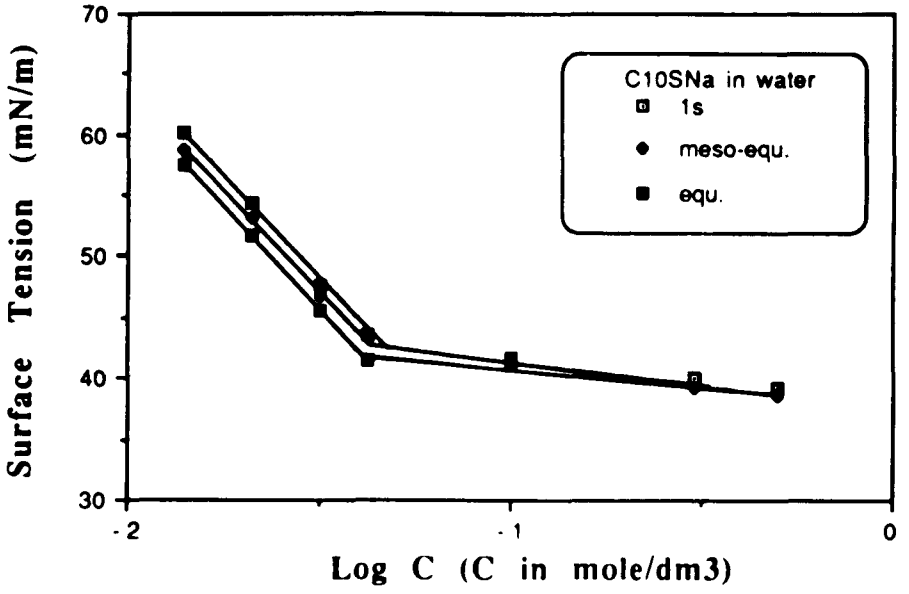

Figure A-20

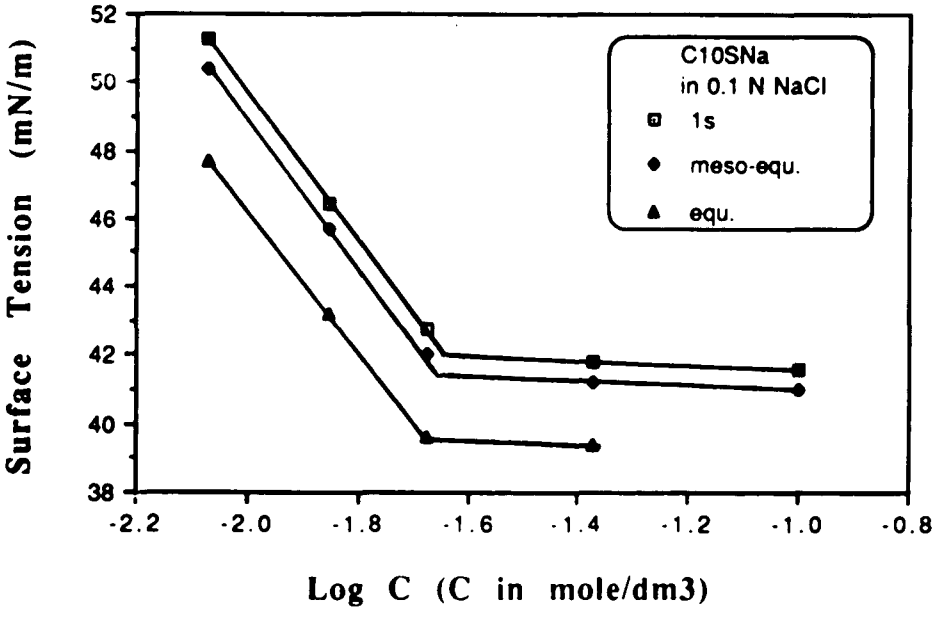

Figure A-21

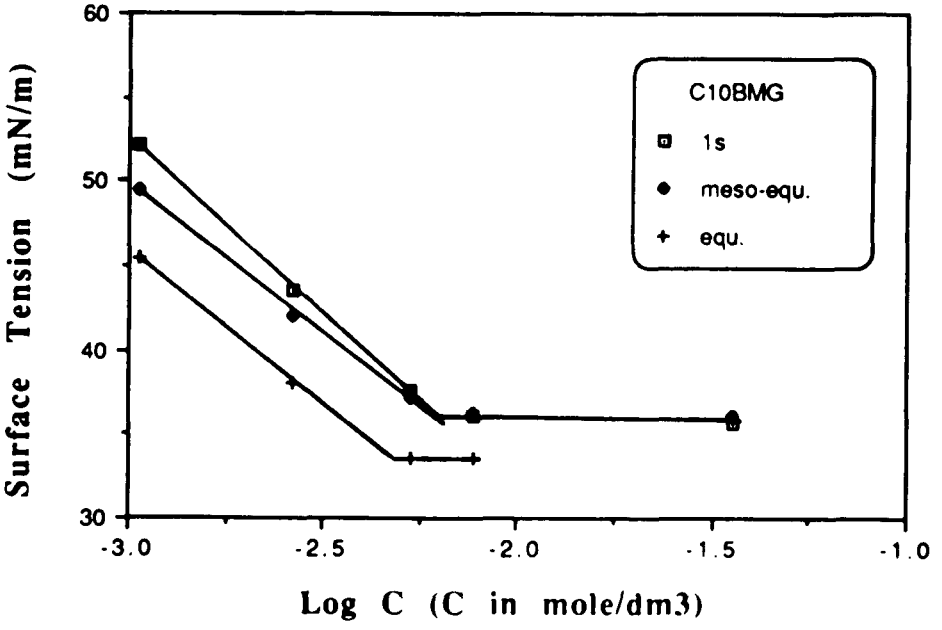
C10BMG
1s
meso-equ.
equ.
Surface Tension (mN/m)
60
50
40
30
-3.0
-2.5
-2.0
-1.5
-1.0
Log C (C in mole/dm3)

References

1. Molliet, J. L.; Collie, B. Surface Activity; D. Van Nostrand: New York, 1951; p 85.
2. Addison, C. C. J. Chem. Soc. 1943, 535.
3. Addison, C. C. J. Chem. Soc. 1944, 252.
4. Adisson, C. C. J. Chem. Soc. 1944, 477.
5. Addison, C. C. J. Chem. Soc. 1945, 98.
6. Addison, C. C. Phil. Mag. 36, 1945, 73.
7. Addison, C. C. J. Chem. Soc. 1945, 354.
8. Addison, C. C. J. Chem. Soc. 1953, 1143, 1151, 1155.
9. Addison, C. C. Nature 1953,171, 393.
10. Ward, A. F. H. Surface Chemistry; Butterworths: London, 1949; p 55.
11. Rayleigh, L. Proc. Roy. Soc. (London). 1879, 29, 71.
12. Pederson, P. O. phil. Trans. 1906-1907, A207, 341.
13. Bohr, N. Phil. trans. 1908-1909, A209, 291.
14. Stocker, H. Z. Physik. Chem. 1920, 94, 149.
15. Sutherland, K. L. Thesis, London,1950; Also see Defey, R.; Hommelen, J. R. J. Colloid Sci. 1959, 13,553.
16. Garner, F. H.; Mina, P. Trans. Farday Sco. 1959, 55, 1607.
17. Van den Bogaert R.; Joos, P. J. Phys. Chem. 1979, 83, 2244.
18. Simon, Ann. Chim. Phys. 1851, 32, 5.
19. Rehbinder, P. Z. Phys. Vhem. 1924, 111, 447.
20. Adam, N. K.; Ahute, H. L. Trans. Faraday Soc. 1938, 34, 758.

21. Kuffer, R. J. J. Colloid Sci. 1961, 16, 497.

22. Kragh, A. M. Trans. Faraday Sco. 1964, 60, 225.

23. Austin, M.; Bright, B. B.; Simpson, E. A. J. Colloid Interface Sci. 1967, 23, 108.

24. Kloubek, J. Tenside 1968, 5, 317.

25. Kloubek, J. J. Colloid Interface Sci. 1972, 41, 1.

26. Kloubek, J. J. Colloid Interface Sci. 1972, 41, 7.

27. Kloubek, J. J. Colloid Interface Sci. 1972, 41, 17.

28. Fainerman, V. B. Colloid J. USSR (Engl. Transl.) 1979, 41, 79.

29. Papeschi, G,; Bordi, S.; Costa, M. Ann. Chim. (Rome) 1981, 71, 407.

30. Fainerman, V. B.; Lylyk, S. V. Colloid J. USSR (Engl. Transl.) 1982, 44, 538.

31. Hu, P. C. SPE-DOE joint Symposium on Energy Recovery, Tulsa, OK 1984.

32. Pugachevich, P. P. Russ. J. Phys. Chem. (Eng. Trans.) 1964, 38, 758.

33. Razouk, R.; Walmsly, D. J. Colloid Interface Sci. 1974, 47, 515.

34. Smirnov, M. V. Chem. Abstr. 1978, 88, 295-55299b.

35. Becht, J.; Lunkenheimer, K. Colloid Polym. Sci. 1982, 260, 234.

36. Wolf, F.; Sauerwald, F. Kolloid Z. 1950, 118, 1.

37. Schrodinger, E. Ann. Phys. (Leibzig) 1915, 46, 413.

38. Sugden, S. J. Chem. Sco. 1922, 121, 858.

39. Sugden, S. J. Chem. Sco. 1924, 125, 27.

40. Cantor, M. Ann. Phys. (Leibzig) 1902, 7, 698.

41. Feustel, R. Ann. Phys. (Leibzig) 1905, 16, 61.

42. Zickendraht, H. Ann. Phys. (Leibzig) 1906, 21, 146.

43. Warren, E. L. Philos. Mag. 1927, 4, 358.

44. Brown, R. C. Philos. Mag. 1932,13, 578.

45. Kuffner, R. J.; Bush, M. T.; Bircher, L. J. J. Am. Chem. Soc. 1957, 79, 1587.

46. Romagosa, E. E.; Gaines, G. L., Jr. J. Phys. Chem. 1969, 73, 3150.

47. Feldman, I. N.; Malkova, I. V.; Sokolovskii, V. I.; Zaturenskii, R. A. J. Appl. Chem. USSR (Engl. Transl.) 1980, 53, 1594.

48. Belov, P. T. Russ. J. Phys. Chem. (Engl. Transl.) 1981, 55, 302.

49. Kisil, I. S.; Malko, A. G.; Dranchuk, M. M. Russ. J. Phys. Chem. (Eng. Trasl.) 1981, 55, 17.

50. Joos, P.; Rillaerts, E. J. Colloid Interface Sci. 1981, 79, 96.

51. Mysels K. J. Langmuir, 1986, 2, 429.

52. Miller, T. E.; Meyer, W. C. American Laboratory, 1984, 16, 91.

53. Cahn # 2670 Dynamic Surface Tension Instrument Manual, 1967, Cahn Instrument Co., Paramount, CA 90723.

54. Neumann, A. W.; tanner, W. Tenside, 1967, 4, 220.

55. Tornberg, E. J. Colloid Interface Sci. 1978, 64, 391.

56. Guyot, Ann. Physique, 1924, 2, 506.

57. Frumkin, Z. Physikal Chem. 1925, 116, 485.

58. Schulman and Rideal, Proc. Roy. Soc. 1931, A130, 259.

59. Posner, A. M.; Alexander, A. E. Trans. Faraday Soc. 1949, 45, 651.

60. Thomas, W. D. E.; Potter, L. J. Colloid Interface Sci. 1975, 50, 397.

61. Finch, J. A. and smith, G. W. J. Colloid Interface Sci. 1973, 45, 81.

62. Davies, J. T.; Collins-Smith, J. A.; Humphreys, D. G. Proc. Intern. Congr. Surface Activity, 2nd London 1951, 1; p 281.

63. Defay, R.; Hommelen, J. R. J. Colloid Interface Sci. 1959, 14, 401.

64. Ward, A. F. H.; Tordai, L. J. Chem. Phys. 1946, 14, 453.

65. Defay, R.; Hommelen, J. R. J. Colloid Interface Sci. 1959,14, 411.

66. Joos, P.; Bley, G. J. De Chimie Physique, 1982, 79, 387.

67. Van Voorst Vader; Erkelens, Th.; Van den Tempel, M. Trans Farad. Sco. 1964, 60, 1170.

68. Hansen, R. S. J. Phys. Chem. 1960, 64, 637.

69. Bendure, R. L. J. Colloid Interface Sci. 1971, 35, 238.

70. Alexander, A. E.; Posner, A. M. Trans. Faraday Soc. 1949, 45, 652.

71. Kimizuka H.; Abood L. G.; Tahara T.; Kaibara, K. J. Colloid Interface Sci. 1972, 40, 27.

72. Sutherland, K. L. Austral. J. Sci. Res. 1952 A-5, 683.

73. Hansen, R. S. J. Colloid Sci. 1961, 16, 549.

74. Tsonopoulos, C.; Newman, J.; Prausnitz, J. M. Chem. Eng. Sci. 1971, 26, 817.

75. Fainerman, V. B. Colloid J. U.S.S.R. 1977, 39, 91.

76. Fainerman, V. B. Colloid J. U. S. S. R. 1978, 40, 437.

77. Miller, R.; Kretzschmar, G. Colloid Polymer Sci. 1980, 258, 85.

78. Borwankar, R. P.; Wasan, D. T. Chem. Eng. Sci. 1983, 38, 1637.

79. Borwankar, R. P.; Wasan, D. T. Chem. Eng. Sci. 1988, 43, 1323.

80. Joos, P.; Bleys, G.; Petre, G. J. Chim. Phys. 1982, 79, 387.

81. Bleys, G.; Joos, P. J. Phys. Chem. 1985, 89, 1027.

82. Bleys, G.; Joos, P. Colloid Polym. Sci. 1983, 261, 1038.

83. Fordham, S. Trans. Faraday Soc. 1954, 50, 593.

84. Hansen, R. S.; Wallace, T. C. J. Phys. Chem. 1959, 63, 1085.

85. Burcik, E. J. J. Colloid Sci. 1950, 5, 421.

86 Burcik, E. J.; Vaughn, C. R. J. Colloid Sci. 1951, 6, 522.

87. Burcik, E. J. J. Colloid Sci. 1953, 8, 520.

88. Burcik, E. J.; Newman, R. C. J. Colloid Sci. 1954, 9, 498.

89. Netzel, D. A.; Hoch, G.; Marx, T. I. J. Colloid Sci. 1964, 19, 774.

90. Mysels, K. J. Langmuir, 1986, 2, 423.

91. Addison, C.C.; Hutchinson, S. K. J. Chem. Soc. 1948, 943.

92. Woolfrey, S. G.; Banzon, G. M.; Groves, M. J. J. Colloid and Interface Science, 1986,112, 583.

93. Petrova, L.; Radkov, I.; Basheva, E.; Nikolov, A. Abh. Akad. Wiss. DDR, Abt. Math Naturwiss Tech. 1987, 12, 4.

94. Durham, k. Surface Activity and detergency, St Martin: New York, 1961; pp 206-207.

95. Goodrich, F. C. J. Phys. Chem. 1962, 66,1858.

96. Mysels, K. J. J. Phys. Chem. 1962, 66,1862.

97. Hansen, R. S. and Mann, J. A. J. Appl. Phys. 1964,35,152.

98. Levich, V. G. Physicochemical Hydrodynamics, Prentice-Hall,

Englewood Cliffs, N. J., 1962.

99. Van Den Tempel, M. and Van De Riet, R. P. J. Chem. Phys. 1965,42, 2769.

100. Stuke, B. Chem. Eng. Tech. 1961, 33, 173.

101. Lucassen-Reynders, E. H. and Lucassen, J. Advan. Colloid Interface. sci. 1969, 2, 347.

102. Rusanov, A. I. and Krotov, V.V. in Cadenhead, D. A. and Danielli, J. F. (Eds.), Progress in Surface and Membrance Science, Academic Press, New York, 1979; pp 418-524.

103. Lucassen-Reynders, E. H. in "Anionic Surfactants", Marcel Dekker, Inc., New York and Basel, 1981; pp 179-189.

104. Kretzschmar, G. and Lunkenheimer, K. Ber. Bunsenges. Phys. Chem. 1970, 74, 1064.

105. Lunkenheimer, K. and Kretzschmar, G. Z. Phys. Chem. (Leipzig). 1975, 256, 593.

106. Wantke, K. D.; Miller, R. and Lunkenheimer, K. Z. Phys. Chem. (Leipzig). 1980, 261, 1177.

107. Clint, J. H.; Neustadter, E. L. and Jones, T. J. Developments in Petroleum Science. 1981, 13, 135.

108. Miller, T. E. and Meyer, W. C. American Laboratory. 1984, 16, 91.

109. Dahanayake, M.; Cohen, A. W.; Rosen, M. J. American Chemical Society. 1986, 90, 2413.

110. Dehanayake, M. and Rosen, M. J. in "Structure/ Performance

Relationship in Surfactants" ACS Symp. Ser. 253, Amer Chem. Sco., Washington, DC, 1984; P 49.

111. Rosen, M. J. J. Colloid Interface Sci. 1981, 79, 587.

112. Hua, X. Y. and Rosen, M. J. J. Colloid Interface Sci. 1988, 124, 652.

113. Reid, V. W. and Alston, T.; Heinerth, E. Tenside, 1968, 5, 90.

114. Li, Z. P. and Rosen, M. J. Anal Chem. 1981, 53, 1516.

115. Rosen, M. J.; Cohen, A. W.; Dahanayake, M.; Hua, X. Y. J. Phys. Chem. 1982, 86, 541.

116. O'Connell, A. W. Anal Chem. 1986, 58, 669.

117. Rosen, M. J.; Zhu, Z. H.; Gu, B.; Murphy, D. S. Langmuir, 1988,4, 1273.

118. Rosen, M. J. and Yang, D. unpublished data.

119. Draves, C. Z. and Clarkson, R. G. Am. Dystuff Rep. 1931, 20, 201.

120. Atherton, N. M. "Electron Spin Resonance Theory and Applications", Halsted Press, New York, 1973; p 260.

121. Lucassen, J.; Giles, D. J. Chem. Soc. Faraday Trans. I, 1975, 71, 217.

122. Lucassen-Reynders, E. H. in "Anionic Surfactants", Marcel Dekker, New York and Basel, 1981; pp 229-231.

123. Carrington, A.; Mclachlan, A. D. "Introduction to Magnetic Resonance", Harper & Row, New York, 1967; pp 9-10.

124. Shive, J. N.; Weber, R. L. "Similarities in Physics", John Wiley & Sons, New York,1982.

125. Prigogine, I. "Introduction to Thermodynamics of Irreversible

Processes", second edition,Interscience, a division of John & Sons, New York and London,

126. Shinoda, K."Principle of Solution and Solubility", Marcel dekker, New York and Basel, 1978; p160.

127. Rosen, M.J., Surfactants and Interfacial Phenomena, Second Ed., John Wiley & Sons, New York, 1989; pp. 84-90.